EUROPEAN SPALLATION SOURCE

2014/2015 Round Instrument Construction Proposal
Revision Date 15/01/2015

ESS Instrument Construction Proposal

T-REX: A Time-of-flight Reciprocal space Explorer

A bispectral chopper spectrometer for magnetism and material science

	Name	Affiliation
Main proposer	Thomas Brückel Prof. Dr. t.brueckel@fz-juelich.de	Jülich Centre for Neutron science Forschungszentrum Jülich GmbH 52425 Jülich (D)
Co-proposers	Jörg Voigt Nicolò Violini Andrea Orecchini Alessandro Paciaroni Francesco Sacchetti Marco Zanatta	Jülich Centre for Neutron science Forschungszentrum Jülich GmbH 52425 Jülich (D) Department of Physics and Geology, Università di Perugia, 06100 Perugia (I)
With contributions from	Margarita Krutyeva, Yixi Su and Earl Babcock, JCNS (DE); Raphael Hermann, U. Liège, (BE); Stewart Parker, Rutherford Appleton Lab. (UK); Paul Freeman, EPFL Lausanne (CH); Martin Rotter, MPI Dresden (DE); Kasper Steen Pedersen, U. Copenhagen (DK); János Füzi, György Káli, Márton Markó, Ferenc Mezei and László Rosta, Wigner Research Centre for Physics (HU)	
ESS coordinator	P.P. Deen	ESS

The following table is used to track the ESS internal distribution of the submitted proposal.

	Name	Affiliation
Document reviewer	Ken Andersen	ESS
Distribution	Dimitri Argyriou, Oliver Kirstein, Arno Hiess, Robert Connatser, Sindra Petersson Årsköld, Richard Hall-Wilton, Phillip Bentley, Iain Sutton, Thomas Gahl, relevant STAP	

European Spallation Source ESS AB
Visiting address: ESS, Tunavägen 24
P.O. Box 176
SE-221 00 Lund
SWEDEN

www.esss.se

EXECUTIVE SUMMARY

We propose a bispectral direct-geometry time-of-flight chopper spectrometer with Repetition Rate Multiplication (RRM) and polarization analysis (PA) for the European Spallation Source ESS. The instrument is optimized for mapping excitations and fluctuations in the four dimensional reciprocal scattering vector and energy space $(\mathbf{Q}, \hbar\omega)$ over up to four decades in energy, thus justifying the name **T-REX** for **T**ime-of-flight **R**eciprocal space **EX**plorer. The additional neutron polarization degree of freedom allows one to distinguish magnetic from nuclear scattering and to determine the polarization and eigenvectors of magnetic excitations. It also permits the separation of coherent and nuclear spin incoherent scattering functions, $S_{\mathrm{coh}}(\mathbf{Q}, \hbar\omega)$ and $S_{\mathrm{inc}}(\mathbf{Q}, \hbar\omega)$, respectively, which is of particular importance for hydrogen containing samples in soft matter and life sciences.

The scientific mission of the proposed instrument has been worked out in several science case workshops and from written input by distinguished colleagues. Quite general, knowledge of the dynamics of condensed matter systems provides the most stringent approach to a fundamental understanding of the properties of materials on microscopic length- and time-scales. With the ability for 4D reciprocal space mapping combined with full PA, the instrument is optimized for the study of coherent excitations, spin correlations and fluctuations in e.g. (i) novel phases appearing in low dimensional, topological and frustrated materials, (ii) systems tuned near quantum criticality or quantum magnets, (iii) high temperature superconductors with their interplay with magnetism, (iv) multifunctional oxides with strong electronic correlations and competing degrees of freedom, (v) molecular magnets. Given the rapid development in the field of sample preparation for nanomagnetic systems (multilayers with negligible interface roughness, 3d ordered assemblies of magnetic nanoparticles etc.) the proposed instrument promises for the first time the access to magnetic excitations in these fascinating materials, where the physical properties are dominated by interface effects. The instrument length is a key parameter as the narrow bandwidth results in all RRM pulses falling into a narrow dynamic range of interest, PA distinguishes the magnetic scattering and the large reciprocal space coverage enables efficient mapping of the excitation landscape. Hence it is fair to state that T-REX combines the best of both worlds, namely the high usable peak flux from spallation sources with the high repetition rates and adaptable resolution of reactor based chopper spectrometers.

With the scattering vector and energy range of T-REX, combined with the high count rate capability, the other focus of the instrument lies in the study of functional materials, in particular for energy research, e.g. (i) catalysis metals and support, (ii) nanomaterials such as nanoporous or metal-organic frameworks for hydrogen storage, (iii) thermoelectrics and magnetocalorics, (iv) ion transport *in-operando* (batteries etc.).

Finally, with its PA option, T-REX will enable unique experiments in soft matter and life sciences complementary to CSPEC: e.g. (i) dynamics in polymers and bio-molecular materials, (ii) bio-catalysts and bio-sensors, (iii) dynamics of proteins and protein hydration water.

Independent of the specific application, the combination of a high pulse flux and a maximized number of useful pulses makes the instrument a real game changer: it will allow (i) parametric studies with acquisition times below one hour for a full data set from single crystals, (ii) the application of extreme conditions, (iii) *in-situ* or *in-operando* studies on timescales of seconds or (iv) spectroscopy from sub 100 mg single crystals.

The main instrument parameters derived from the science case are as follows:

incident energy:	2 meV < E < 160 meV
energy resolution:	20 μeV < $\Delta\hbar\omega$ < 10 meV
wave vector range:	0.05 $Å^{-1}$ < Q < 17 $Å^{-1}$
wave vector resolution:	0.01 $Å^{-1}$ < ΔQ < 0.1 $Å^{-1}$
sample size:	≤10 x30mm^2
features:	• PA as standard tool • repetition rate multiplication • four dimensional mapping capabilities • low background / high intensity • adjustable resolution, flexible trading of resolution for flux • enabling complex sample environment and *in-situ* / *in-operando* studies

These design parameters are achieved by the following characteristics:

- bispectral beam extraction with optional polarizer to enable the large dynamic range and an ideal transmission for thermal as well as for cold polarized neutrons,
- total instrument length of 169.3 m resulting in a bandwidth of $\Delta\lambda$<1.7Å, perfect for (i) dense coverage of the energy range of interest, (ii) reciprocal space coverage for single crystal studies and (iii) polarization analysis (PA),
- neutron guide system with optimized brilliance transfer of above 85% and homogeneous beam and divergence profile for a 10 mm x 30 mm beam spot,
- no direct line-of-sight by a curved neutron guide and a T_0 chopper installed downstream the curved section,
- versatile chopper system featuring fast counter rotating choppers (maximum frequency 406 Hz, 700 mm diameter) for precise energy definition and the novel Fan chopper to adapt the recording time frames to the different initial wavelengths inherent to RRM,
- a sample-to-detector distance of 3 m required to match the energy resolution of the primary spectrometer of $\Delta E/E$ < 1 % for low energy, and coverage of a huge volume in reciprocal space at reasonable cost
- highly efficient PA over the entire spectral range with a wide angle ^{3}He filter cell with variable pressure in a "magic PASTIS" magnetic system.

The performance of T-REX has been benchmarked against existing state-of-the-art TOF-spectrometers by ray tracing simulations for standard instrument configurations. The flux gain factors for T-REX at comparable energy resolution range between 9 comparing single pulses and 140 for maximal repetition rate multiplication, thus enabling entirely new scientific problems to be tackled:

Instrument	LET	IN5	CNCS	4-SEASONS
Monochromatic gain factor	38	9	9	9
Gain factor single chopper pulse	38	45	9	9
Gain factor including RRM	90	100	140	45

In summary, T-REX will cover a science case, where neutrons excel, namely in the field of quantum phenomena and correlated electron systems, and complement the endorsed chopper spectrometer suite (CSPEC, VOR, CAMEA) by optimization for the thermal energy range and for PA in the entire energy range from thermal to cold. T-REX will feature unprecedented four dimensional reciprocal space coverage, make PA for chopper spectrometer a standard tool and outperform existing instruments by a large margin in signal-to-noise-ratio. This is a safe bet for new scientific breakthroughs.

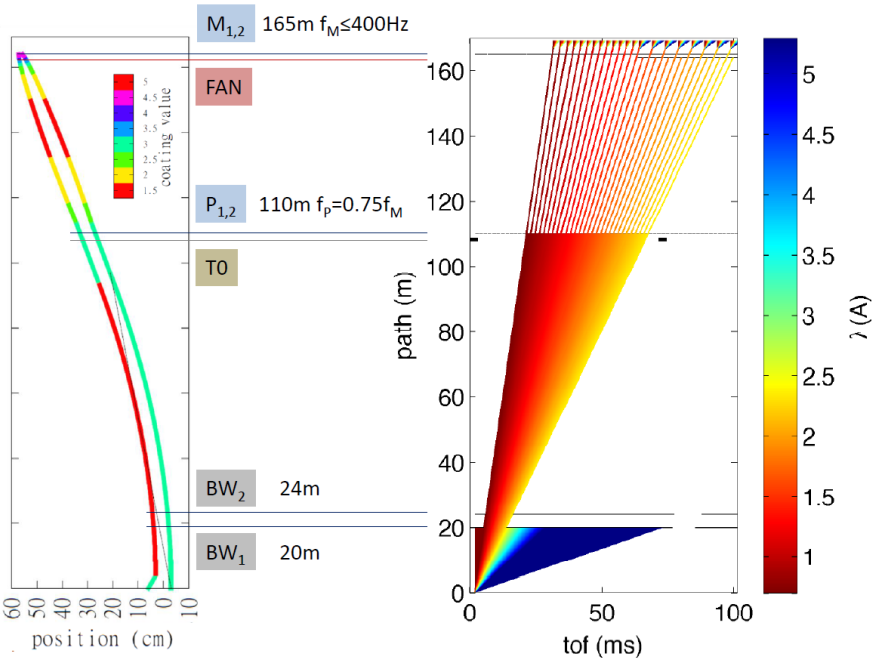

Figure. Schematics of the neutron guide and chopper system together with a time-distance diagram of the proposed instrument T-REX.

Contents

1 Instrument proposal **5**

1.1 Scientific Case . . . 5
1.1.1 User Community . . . 5
1.1.2 Scientific Domains and General Considerations . . . 6
1.1.3 Quantum Phenomena . . . 7
1.1.4 Functional materials . . . 12
1.1.5 Soft Matter and Life Sciences . . . 13
1.1.6 Disordered materials and liquids . . . 17
1.1.7 Instrument design parameters from the science case . . . 19
1.2 Description of Instrument Concept and Performance . . . 21
1.2.1 The chopper system . . . 22
1.2.2 Neutron transport . . . 26
1.2.3 The secondary spectrometer . . . 29
1.2.4 Polarization Analysis . . . 31
1.2.5 Instrument performance and benchmarking . . . 33
1.2.6 Ternary spectrometer . . . 41
1.3 Technical maturity . . . 42
1.3.1 Chopper system . . . 42
1.3.2 Detector . . . 43
1.3.3 Neutron guide and shielding . . . 43
1.3.4 Polarization Analysis . . . 43

2 Costing **44**

3 List of abbreviations **46**

1 Instrument proposal

1.1 Scientific Case

Neutron spectroscopy provides unique information about dynamic properties of condensed matter. Computer modeling of the inelastic neutron scattering cross sections allows one to obtain parameters of model Hamiltonians, such as inter-atomic forces or exchange constants, which enable the prediction of the macroscopic response of a material and thus lead to a microscopic understanding of the relation between structure and function. Neutron spectroscopy gives direct access in absolute units to self-, pair-, and spin-correlation functions, which are the fundamental quantities derived by modern ab-initio theories. Thus, the simplicity of the neutron cross sections and the fact that they can be measured on an absolute scale allows benchmarking of ab-initio theories and computer modeling with huge impact in many different scientific fields. In this important aspect, neutrons are unrivaled, as no other method can provide such stringent test of microscopic theories. It is true that particular problems can nowadays be addressed with modern synchrotron radiation techniques: steep phonon branches can be determined with high resolution ($\sim$ 1 meV) inelastic x-ray spectroscopy; element specific partial phonon density of states can be measured for certain elements by nuclear resonance scattering; slow dynamics in colloids can be followed by coherent x-ray correlation spectroscopy; and high energy magnon dispersions by resonant inelastic x-ray scattering (RIXS). All these x-ray techniques are largely complementary to inelastic neutron scattering, but none of them gives the same direct and universal access to absolute scattering functions as does neutron spectroscopy. To give an example: due to the restricted resolution, RIXS can only be used to determine relatively high energy magnetic excitations. But due to the resonance process involved, with its unknown transition matrix elements, RIXS cannot provide a model-free access to the eigenvectors, which neutrons naturally do. For these quite general arguments, neutron spectroscopy will remain essential and unrivaled for many decades to come. With its pulse structure, ESS is ideally suited for this task employing time-of-flight techniques. Evidently chopper spectrometers are the best suited instruments for ESS, where this new type of source can truly excel.

1.1.1 User Community

The present science case has been compiled with the help and input from many colleagues on the occasion of several focused workshops (Berlin, 12.07.2011; Berlin, 28.11.2011; Bernried, 17.-19.06.2013), but also from written feedback. A complete list of participants in the above workshops is given in [1].

In order to predict the user base we firstly analyzed the past user records of existing direct geometry chopper spectrometer. For this reason we have collected corresponding information from the leading facilities. These statistics show that the existing world class instruments have an over-subscription rate higher than two on a regular basis. For example LET at ISIS has over-subscription rate of 2.4 (average over last 3 years),

CNCS at SNS has 5 (average over last 5 years), IN5 at ILL has 2.3 (in 2012).[1] We have also examined the chosen incident energies for existing instrument suites while in the user program at SNS and ISIS. Interestingly the analysis shows that the thermal energy range, 50 meV $< E_i <$ 200 meV, is commonly chosen by the users in 25% of experiments at the SNS and in the 30% at ISIS[1].

As neutron spectroscopy is a demanding technique, it is less widely spread as e.g. small angle scattering or powder diffraction. However, we could readily identify about 100 prominent groups in Europe, which employ neutron spectroscopy as one main experimental technique. A list is given in the enclosures[1], which is by no way exhaustive. If we assume an average of five scientists working in each group, we can estimate that the present community of professional users is safely above 500 individuals. In addition there are the occasional users. With the new possibilities offered by the future powerful spectrometers at ESS and the increasing use of neutron techniques by the eastern European and Baltic countries, the user community will certainly grow in the future.

1.1.2 Scientific Domains and General Considerations

With its versatility, T-REX will attract users from many different scientific communities: solid state physics, physical chemistry, materials science, soft matter and life sciences. Independent of the specific application, a gain factor of one to two orders of magnitude in flux as compared to some of the best existing instruments is a true game changer. The types of studies that benefit directly from the high flux include:

- parametric studies as function of external variables such as pressure, temperature, magnetic or electric field, humidity, etc. These studies will become routine - comparable to the situation at high flux diffractometers nowadays. We estimate acquisition times well below one hour for a full data set from a single crystal down to a few seconds in favorable cases (e.g. powder)
- studies under extreme conditions, which restrict the sample volume, such as in high pressure cells
- studies of non-equilibrium processes, e.g. kinetic studies of the relaxation of the dynamics of a condensed matter system after a pump pulse (light, pressure, field)
- in-*situ* or in-*operando* studies with adapted sample environment, particular for energy research
- neutron spectroscopy simultaneously with other types of measurements, like light spectroscopic techniques (absorption, Brillouin, Raman, Kerr) or static measurements like calorimetry, AC susceptibility or dilatometry, magnetization
- spectral features from sub 100 mg single crystals or nanostructured materials

[1] Time use on CNCS: Magnons in crystals (46%) and powders (18%), phonons in crystals (6%) and powders (6%), chemistry and protein dynamics (16%) and helium (8%). On IN5: magnetic excitations (40%), non-magnetic excitations (20%), liquids (15%), biology and soft matter (25%).

1.1.3 Quantum Phenomena

With its ability for rapid mapping in four dimensional (Q,ω) space employing RRM and crystal rotation, combined with the PA option, T-REX is optimized for studies of excitations in quantum condensed matter. This includes the determination of coherent excitations, spin correlations and fluctuations in (i) novel phases appearing in low dimensional, topological and frustrated materials, (ii) systems tuned near quantum criticality or quantum magnets, (iii) high temperature superconductors with their interplay with magnetism, (iv) multi-functional oxides with strong electronic correlations and competing degrees of freedom, (v) molecular magnets. The energy scale of interest in these systems ranges from several tenth of μeV for the determination of small energy gaps to several hundreds of meV, for studies of e.g. excitations in the parent compound of high T_c superconductors or excitations into the Stoner continuum. T-REX is designed to provide high E_i to study the excitations in correlated electron system necessary to reach a deeper comprehension of e.g. high temperature superconductivity, charge order or the magneto-caloric effect.

Recent example:[2] M. Loire et al., *'Parity-Broken Chiral Dynamics in* $Ba_3NbFe_3Si_2O_{14}$*'*; PRL 106 (2011), 207201.

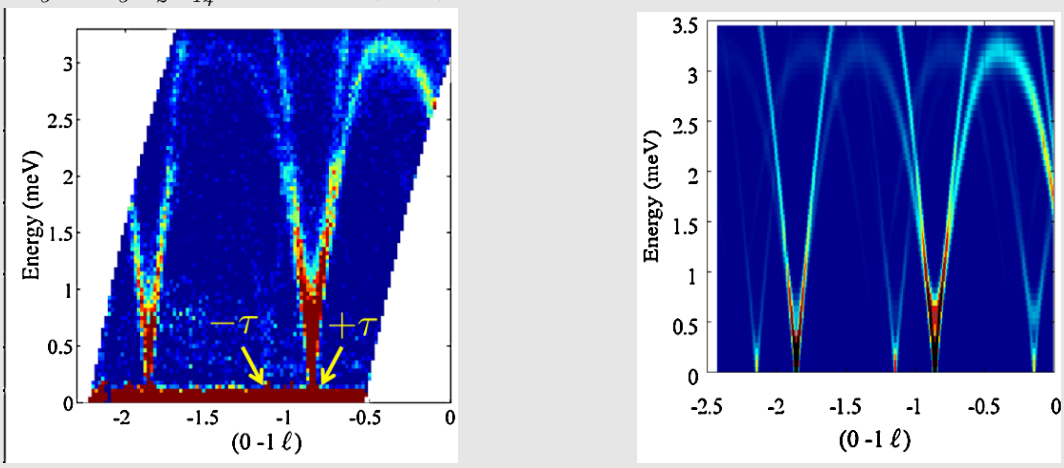

Figure 1: The figure shows inelastic neutron scattering intensities collected on IN5 at ILL compared to the calculated dynamical structure factor. The observed spectra correspond to spin wave excitations emerging from chiral helically modulated 120° magnetic order in an enantiopure crystal. While the TOF data give a nice overview of the dispersion relation, PA on the triple axis spectrometer (TAS) IN20 was needed to prove dynamical spin chirality. With the PA option of T-REX, the entire information could be gained in one experiment.

The highlighted recent example clearly stresses the need for PA on a chopper spectrometer combined with very good energy resolution.

With neutron PA, the magnetic anisotropy of the dynamic susceptibility can be probed, which gives information on the symmetry of the gap function, see e.g.[3] . At

present this can only be done at TAS spectrometers, while in the seminal paper on cuprate superconductors [4] the usefulness of chopper spectroscopy for non-polarized investigations had already been impressively demonstrated. Back then a 58 g sample was needed for the MAPS spectrometer. For the energy range up to 160 meV, T-REX will be largely superior, requiring crystals of well below 0.5 g mass, while giving far more detailed information on the position of the incommensurate peaks, line shapes etc.

Examples for possible highlight experiments:

- Magnetic excitations in novel phases

  Recently the Higgs transition from a magnetic Coulomb liquid to a ferromagnet has been discovered in the quantum spin ice system $Yb_2Ti_2O_7$ [5]. This discovery required PA of diffuse scattering. To elucidate in detail the mechanism of this transition requires the investigation of the change of spin dynamics as function of temperature in the mK range, a task ideally suited to a chopper spectrometer with PA and using thermal neutrons.

- Magnetic excitations in nanomagnetic systems

  Heterostructures of transition metal oxides or ordered assemblies of magnetic nanoparticles in a matrix (metal, ferroelectric, etc.) are fascinating systems, where the physical properties are dominated by interface effects. Due to minute sample quantities, only elastic neutron scattering from such systems is possible at present. The susceptibility of these systems is entirely different from the bulk, which can only be understood from microscopic spin dynamics. Given the rapid progress in sample preparation, combined with the special features of T-REX (coverage of a large section of (Q, ω) space without sample rotation through RRM, high flux, focusing onto a dynamic range of interest and suppression of background with PA), such studies will be within reach in ten years from now.

Frustrated Magnetism: Frustration results in novel phases like spin liquid, spin ice and Higgs condensate. Frustrated spin systems are characterized by a hierarchy of energy scales. T-REX gives access to virtually all of them as it can be operated with high E_i up to 160 meV and in the same experiment with ultimate energy resolution $\Delta E \approx 20\mu$eV at $E_i = 2$ meV. PA is a crucial tool as the suppressed ordering results in diffuse scattering and the broad magnetic signal otherwise risks getting lost in background.

Molecular magnets: In molecular magnets magnetic ions can be arranged in a variety of shapes including rings, chains, horseshoes and many more. Neutron spectroscopy has played a crucial role in revealing the energy levels of the magnetic molecules. Recently Baker et al.[6] investigated a single crystal of Cr_8 rings with high resolution TOF spectroscopy and could determine the spin pair correlations and compare them to model calculations with excellent agreement. While this study is feasible today, chemists would like to screen the magnetic excitation spectrum from synthesis series. Here the high flux

will permit a high throughput to qualify the influence of synthesis parameters on the magnetic properties of the sample and provide fast feedback. A vision is the study of entanglement and stability of the prepared states by an applied magnetic field. Here one could not only probe the typical time scale of a neutron scattering experiment ranging from ps to ns, but could also investigate the relaxation of, for example, optically excited states on the ms time scale using the subsequent pulses in RRM. Hybrid systems of molecular magnets and nano-particles are expected to exhibit novel magnetic properties. To understand their behavior it is crucial to probe the dynamics at the interfaces.

Interactions of spin systems with other degrees of freedom: Correlated electron systems feature a subtle interplay of a multitude of degrees of freedom, leading to emergent behavior such as superconductivity, giant magneto resistance and multiferroicity. The collective excitations of such systems can no longer be described by simple perturbation theory. The energy range of these excitations is very broad, requesting thermal neutrons to study the high energy region and cold neutrons to realize ultimate energy resolution. Studying the line shape of the excitations provides a solid test for theory. Such experiments will be possible using the good energy resolution of T-REX. With increasing materials complexity, the excitation spectra become richer, but less unique. PA allows the distinction not only between lattice and spin excitations, but also between excitations of different origin. We emphasize here in particular multiferroic compounds, where the ferroelectric order originates from a chiral magnetic structure or exchange striction.

High temperature superconductivity: The excitation spectra of the high temperature superconductors extend over a large energy range: from the formation of the spin gap to the high energy part of the hour glass shaped magnetic excitation spectrum. Furthermore spin-phonon or electron-phonon coupling results in life time effects altering the line shape of spin or lattice excitations. With the high flux and the good energy and momentum resolution of T-REX it will be possible to study the evolution of such features depending on external parameters such as magnetic field or pressure. The RRM will be particularly powerful for parametric studies, because the response can be probed on the different energy scales simultaneously.

Quite general it is crucial for any of the correlated electron systems to provide a high flux at high E_i. Thanks to the narrow bandwidth of T-REX, high energy excitations are sampled by numerous neutron pulses yielding additional information, which is not available today. This is illustrated by the following example:

Recent example:[7] Y. Drees, D. Lamago, A. Piovano & A.C. Komarek; *'Hour-glass magnetic spectrum in a stripeless insulating transition metal oxide'*, Nature Communication 4 (2013), 2449

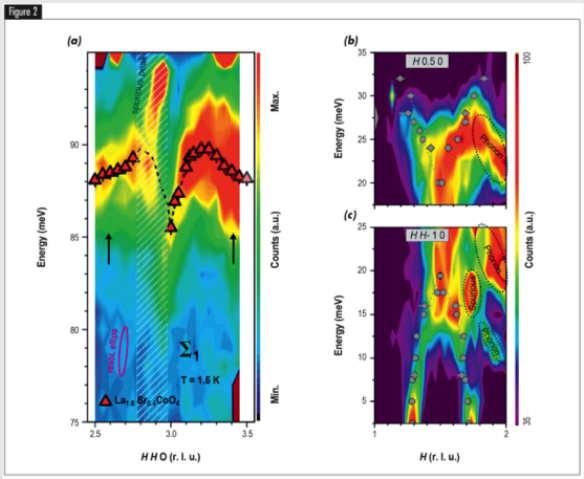

Taken from [2]. **(a)** Neutron scattering intensity as a function of energy and momentum transfer obtained at the spectrometer IN8. Red triangles denote the high-frequency Co-O bond-stretching phonon dispersion. A distinct softening at Q = (2.5 2.5 0) becomes apparent. **(b,c)** Inelastic neutron scattering intensities obtained from constant-energy scans across the planar antiferromagnetic wavevector in **(b)** the [100]-direction and **(c)** the [110]-direction. All basic features of a so-called "hour-glass" dispersion are visible: the inward-dispersing branches that merge with increased intensity ("neck" of the hour-glass) and the outward-dispersing branches at higher energies.

Figure 2: Excerpt from Abstract: An hour-glass-shaped magnetic excitation spectrum appears to be a universal characteristic of the high-temperature superconducting cuprates. Fluctuating charge stripes or alternative band structure approaches are able to explain the origin of these spectra. Recently, an hourglass spectrum has been observed in an insulating cobaltate, thus favoring the charge stripe scenario. Here we show that neither charge stripes nor band structure effects are responsible for the hour-glass dispersion in a cobaltate within the checkerboard charge-ordered regime of $La_{2x}Sr_xCoO_4$. (Figure taken from ILL annual report 2013).

Data have been measured on IN8 at ILL. The shown example can be used to demonstrate the unique strengths of T-REX, which are not provided by any other of the proposed spectrometers for ESS:

- Coverage of the needed energy transfer range in one go (only one frame, i.e. one setting of the spectrometer); only T-REX gives access to the required high E_i up to 160 meV.
- In contrast to the triple axis instrument used, T-REX would give full information on scattering events in four dimensional reciprocal space (Q, E). Spurious events visible in the above data could be readily identified and the corresponding region in reciprocal space can be excluded from the analysis.
- Moreover due to RRM, the data are taken with a redundancy, which further helps eliminating any spurious scattering.
- The authors claim that scattering at higher Q and around 12 and 25 meV is due to phonons. Using PA, this assumption could be directly verified at T-REX allowing one to obtain a very clean spectrum. This in turn would make it possible to identify any possible magnon-phonon coupling, which can play an important role in correlated electron systems.

Quantum phase transitions: Many of the system exhibiting quantum phase transitions exist only as small single crystals. Furthermore, the complex sample environment, such as high pressure apparatus or cryomagnets, limits the sample volume. While devoted instruments aiming for ultimate parameter values are planned for ESS (CAMEA), measurements at modest parameter values can be combined with the complete reciprocal space coverage provided by T-REX. The unique identification of an excitation character with PA will provide a solid test for theoretical models.

Low dimensional quantum magnets: Recent investigations reveal often only the onset of the excitation continuum where the intensity is high. The structure deep in the continuum is hidden as the scattered intensity fades out. With a signal-to-noise gain by up to 2 orders of magnitude new facets of the excitation spectrum become accessible, also considering that investigations are often limited by small single crystalline samples.

1.1.4 Functional materials

With the scattering vector and energy range of T-REX, combined with the high count rate capability, the other focus of the instrument lies in the study of functional materials, in particular for energy research, e.g. (i) catalysis metals and support, (ii) nanomaterials such as nanoporous or metal-organic frameworks for hydrogen storage, (iii) thermo-electrics and magneto-calorics, (iv) ion transport in-*operando* (batteries etc.). Also here the instrument benefits strongly from the combination of thermal and cold neutrons. Experiments that are nowadays performed at different instruments in different beam-times to cover e.g. the quasielastic response and the phonon spectrum can be performed in a single experiment with identical conditions on T-REX.

Recent example: W. Paulus et al, *Lattice Dynamics To Trigger Low Temperature Oxygen Mobility in Solid Oxide Ion Conductors*, JACS 130 (2008) 16080.[8]

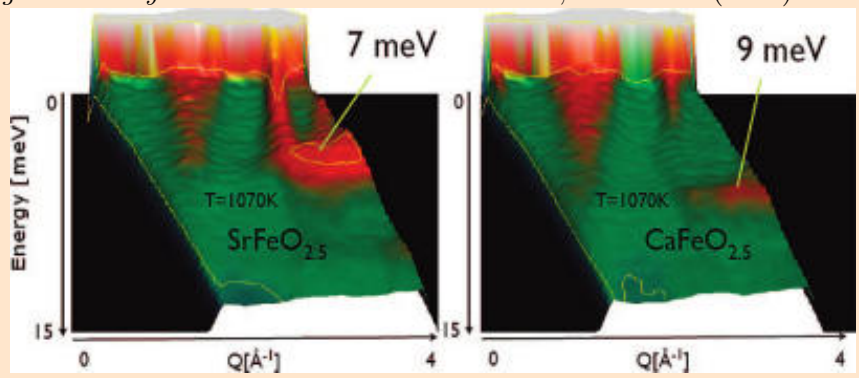

Figure 3: The figure shows the scattering function S(Q, ω) for two solid oxide ion conductors collected on IN6. In both cases, the acoustic phonons emerging from the Bragg peaks and the dominating low frequency band of optic vibrations become evident. While in the case of $CaFeO_{2.5}$ the optic band is nicely separated from the acoustic phonon intensities, it merges with those in the case of $CaFeO_{2.5}$. Such studies reveal the microscopic origin of the significant difference in low temperature oxygen mobility of the two compounds. Good energy resolution is required to resolve the atomic hopping processes.

Understanding materials for energy research: One of the grand challenges for mankind is the development of a sustainable energy supply for an increasing world population. The solution requests novel sources for energy, the harvest of wasted energy from todays devices and the improvement of the efficiency of the state-of-the-art technology. Inelastic neutron scattering provides a microscopic insight into the dynamic processes, which are involved in the transformation of energy.

Thermo-electrics: Improving thermo-electrics often means reducing the phononic heat transport while keeping it a reasonably good conductor. As a result the phonon spectra are highly anharmonic. Here line shape investigations in a wide range of reciprocal space can contribute a better understanding of the lattice dynamics and ultimately to a

tailored design of novel materials.

Magneto-caloric effect: Domestic refrigeration contributes significantly to the worlds primary energy consumption. Using a magnetic refrigeration cycle holds the promise to increase the efficiency significantly. While applications in the low temperature region are well established, close to room temperature devices exist only as prototypes. Good existing materials are rare, expensive (e.g. Gd or $Gd_5Si_2Ge_2$) and sometimes ecologically problematic (e.g. FeMn(P,As)). The search for new materials requests a deep understanding of the underlying principles. The complete information about the scattering function S(Q, ω) reveals the interplay between the lattice and spin degrees of freedom, which are at the origin of the magneto-caloric effect.

Ion transport: High ion mobility is crucial for the performance of many energy related devices such as membranes in fuel cells, hydrogen storage materials or electrolytes in batteries. Particularly the hydrogen motion can be studied perfectly, as the large incoherent scattering cross section yields mainly information about the self-correlation. An element, which is getting into the focus for battery research recently, is Na. Here PA is a promising tool to distinguish the spin incoherent scattering to achieve reliable information about the diffusion process in novel materials under in-*operando* conditions. Such experiments require the access to the typical time scale of the diffusion process, which is in the order of several ns, but also to the respective Q range up to at least 2 $Å^{-1}$.

Nanomaterials: Nanoporous materials represent a broad class of the materials that require high resolution, low background measurements in combination with PA. A typical neutron application is the investigation of the dynamical features of liquids and gases infiltrated in nanoporous solid materials. Metal-organic frameworks represent promising systems for hydrogen storage. In these systems the hydrogen uptake is mostly dependent on the chemical environment of adsorbed H_2. High resolution inelastic scattering experiments are employed to gain information on the specifics of H_2 binding in this class of adsorbents.[9]

1.1.5 Soft Matter and Life Sciences

Although optimized mainly for quantum and functional materials studies, T-REX will enable unique experiments in soft-matter and life sciences thanks to (i) high intensity, allowing for the use of small samples and the identification of small signals; (ii) wide dynamic range, which allows for investigating low- and high-energy features in a single experiment while keeping the sample in well controlled conditions; (iii) PA, which will give the opportunity to separate coherent and incoherent signals on hydrogenated samples, thus avoiding the use of the expensive and in some cases doubtful H-D isotope substitution, a practice which can affect the dynamics in a subtle way. In this chapter we emphasize the novel possibilities offered by T-REX in the field of Life Sciences, as studies of soft-matter systems are already very wide-spread on present day TOF-spectrometers.

Proteins, DNA, RNA and lipidic membranes are central to cellular function. Although the static structures of these biomolecules are often known in great detail, their functions are ultimately governed by their dynamical character [11]. For instance, well-known bi-

ological processes rely on structural changes of proteins. The opening and closing of ion channels for signaling currents, involved for example in neuron signal transmission, depend on the conformational changes of the transmembrane protein forming the pore [12]. Global structural changes in haemoglobin, the oxygen-transporting protein in blood, are at the basis of the initial binding of oxygen in a single domain and bias the structure towards binding in additional domains to increase delivery efficiency [13]. Protein structural changes critical to biological functionality, such as enzyme efficiency and electron transfer, are supposed to be mediated by long-range vibrational motions involving dynamical networks that extend throughout the protein [14, 15].

In such a general context, picosecond diffusional and relaxational dynamics of biosystems are obviously of paramount importance with respect to functionality. These kinds of motions are indeed already widely studied with present-day spectrometers, by means of quasielastic neutron measurements in the cold region between few μeV and few meV. With its high flux and energy resolution down to 20 μeV, T-REX is clearly an excellent tool to pursue such kind of "traditional" investigations, whose importance does not need to be further stressed. On the other hand, diffusional and relaxational motions in such complex systems cannot be disentangled from their vibrational counterpart. With this respect, some newly emerging experimental results appear particularly promising and can strongly benefit from the purely inelastic capabilities and the thermal dynamical range of a highly-efficient spectrometer like T-REX. Few such examples are suggested in the following.

Functionally-relevant underdamped delocalized vibrational modes in proteins. Very recently, femtosecond optical Kerr effect (OKE) spectroscopy was exploited to study the depolarized Raman spectra of lysozyme and its complex with the inhibitor triacetylchitotriose in solution. Underdamped delocalized vibrational modes in the THz frequency domain are identified and shown to blue-shift and strengthen upon inhibitor binding (see Fig. 4) [16]. These functionally related vibrational motions take place in the range from about 1 meV up to 50 meV. This result opens up new scientific opportunities in the key field of inelastic neutron scattering (INS) applied to biological systems. Indeed, T-REX will be perfectly suited to investigate the functional vibrational motions of proteins: the high flux and low background, combined with the large accessible dynamic range, will allow to reveal the finer details of these inelastic features, also thanks to the high energy resolution allowed by the flexible instrumental design. As a whole, the top-level performances of T-REX will make possible high-throughput inelastic measurements on protein-substrate complexes, to highlight the nature of functionally relevant vibrational modes in different systems and possibly find a relationship between characteristic internal modes and biodiversity. In addition, by exploiting the energy-loss spectral side available at T-REX, this kind of studies will also be possible at low temperatures, where protein dynamics and functionality are usually affected by the interaction with cryoprotectant moieties (e.g. glycerol, trehalose, etc.). This is a subject of strongly growing interest in the field of pharmaceuticals, particularly concerning new drugs design, drug delivery efficiency and drugs shelf-life [17]. Compared to other spectroscopic techniques, such as the OKE spectroscopy, INS will also allow one to use contrast matching methods to single out the signal either from the protein or the environment (solvent). Among

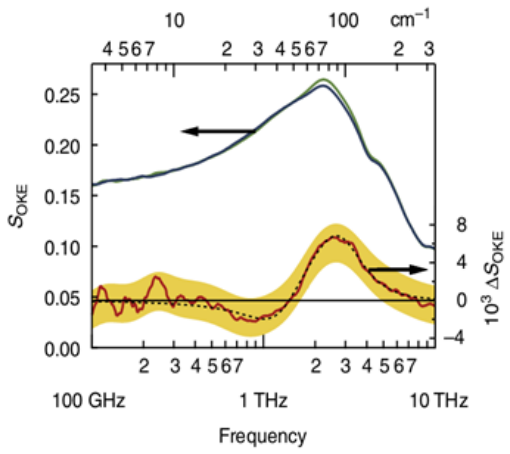

Figure 4: Terahertz region of the OKE (solvent-subtracted) spectra for lysozyme alone (blue), complexed with triacetylchitotriose (green) and the difference between the two spectra (red).

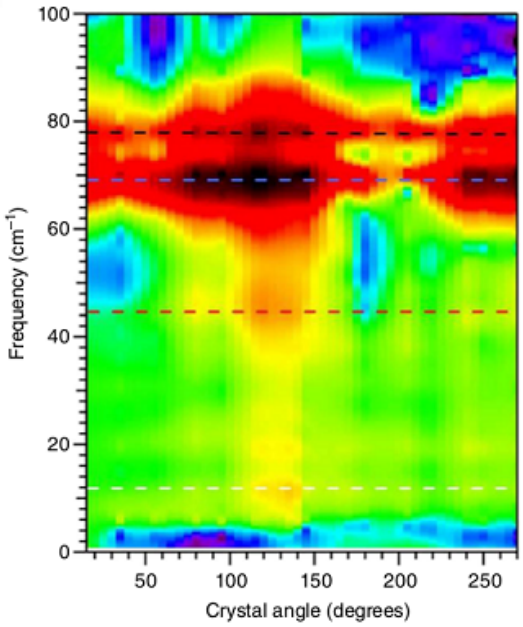

Figure 5: Absorption relative to a single reference direction for lysozyme single crystal as a function of energy and crystal orientation.

such applications, a remarkable specific case encompasses the long-standing and still on-going studies on the dynamical behavior of protein hydration water, the archetype of all biological solvents. For instance, the appearance of the well-known boson peak in the spectrum of protein hydration water has been recently connected with the crossing of the so-called Widom line [18]. Some of the key features available on T-REX (PA, thermal neutrons and high neutron flux) will make it possible to carefully investigate the inelastic behaviour of protein hydration water in an extended range of the (P-T) phase diagram.

Underdamped anisotropic vibrational modes in protein crystals. Another key element of functionally relevant underdamped vibrations in proteins is their anisotropic character, which has been revealed by orientation-sensitive THz near-field microscopy on lysozyme single crystals (see Fig. 5) [19]. A careful characterization of this anisotropic character is needed to understand the role of underdamped vibrational modes for biological functionality. The high flux and PSDs available on T-REX will allow these investigations on a routinely basis, even on small protein crystals (few μl). Even more importantly, PA will allow to measure coherent and incoherent signals in a direct way.

Functionally relevant underdamped delocalized vibrational modes in DNA and membranes. Anisotropic collective vibrational motions were observed by NS and inelastic X-ray scattering also in DNA [20], lipid membranes [21] and chromatin [22]. Interest

on collective vibrational modes in biological systems is therefore steadily increasing and widening to a larger category of samples. In the past, it has been clearly limited by the intrinsic difficulty of experimentally accessing and discerning such a complex phenomenon and thus the growing interest is in part certainly connected to the fact that new or enhanced experimental techniques became available. T-REX will have a similar role in the field of INS.

Functionally relevant vibrational modes in polymers at the interface with biomolecules. One of the most promising ways to control and modify the function of biomolecules is through the interaction with *ad-hoc* functionalized polymers. Quite recently solvent-free myoglobin liquids, with near-native structure and reversible dioxygen binding ability equivalent to the haemprotein under physiological conditions, have been prepared by using polymer surfactant nanohybrids [23]. Elastic neutron scattering was used to show that the relaxational dynamics of the protein interacting with polymer surfactant nanohybrids is quite similar to that of hydrated proteins [24]. The already mentioned T-REX characteristics will allow to single out the incoherent and coherent vibrational contribution from protein and polymer components (by using both isotope labeling and PA), and to understand the mechanisms through which function can be tuned. This would offer new opportunities in protein-based nanoscience and bionanotechnology.

Recent example:[10] A.Stadler et al., *Cytoplasmic Water and Hydration Layer Dynamics in Human Red Blood Cells*, JACS 130 (2008), 16852.

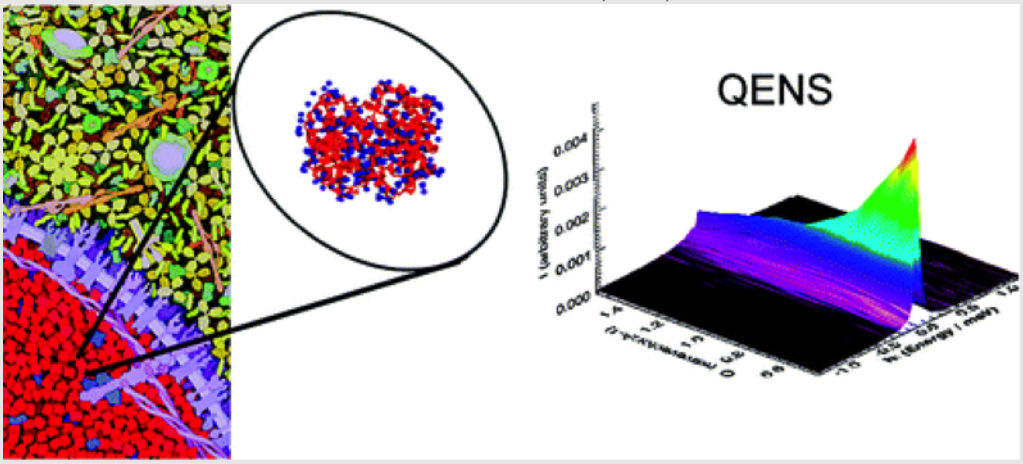

Figure 6: Water is essential to life, and a major scientific interest lies in a detailed understanding of how it interacts with biological macromolecules in cells. The dynamics of water in human red blood cells was measured with quasi-elastic incoherent neutron scattering in vivo in the temperature range typical for living organisms. Neutron spectrometers with several different time resolutions were combined to cover time scales of bulk water dynamics to dramatically reduced mobility of interfacial water. It emphasizes the importance of bi-spectral chopper spectrometer providing a large variety of options combined in one instrument.

1.1.6 Disordered materials and liquids

Disordered materials constitute a wide class of systems that range from glasses and super-cooled liquids to polymers and colloids. Biological systems – such as proteins, DNA, cells and even tissues – belong to the same class of systems, although they are often composites. T-REX would prove as a real game-changer for studying the dynamics of this wide class of systems, thanks to (i) the wide dynamic range offered by the thermal neutron energy range, (ii) the simultaneous acquisition of multi-energy spectra in RRM, (iii) the high intensity needed to study small samples and small signals and (iv) the use of PA for separation of coherent and incoherent scattering signals.

Collective dynamics of disordered systems and liquids.

The study of the collective dynamics in disordered and liquid systems requires measurements of the $S(Q,\omega)$ in an ω range up to several meV and in a Q range between 0.1 Å^{-1} and about 1.5 Å^{-1}. Access to this dynamical range needs the combination of incident thermal energies with small-angle detection. Such requisites are well matched by the incident energies available on T-REX and by its highly pixelled detector, which provides a good coverage of the forward scattering region. Access to low-Q might be further improved by the possible insertion of a bi-dimensional collimator (see [25] for details).

Very recent results have revealed that disordered systems can display dispersion curves of much higher complexity than previously expected [26, 27, 28, 30, 29]. Thanks to the straightforward implementation of RRM, T-REX can significantly ease the study of collective excitations, well beyond today's capabilities that require to combine data from different spectrometers (see boxed text below).

Recent example:[30] M. Zanatta et al., *Inelastic Neutron Scattering investigation in glassy $SiSe_2$: complex dynamics at the atomic scale*, J. Phys. Chem. Lett. 4, 1143 (2013).

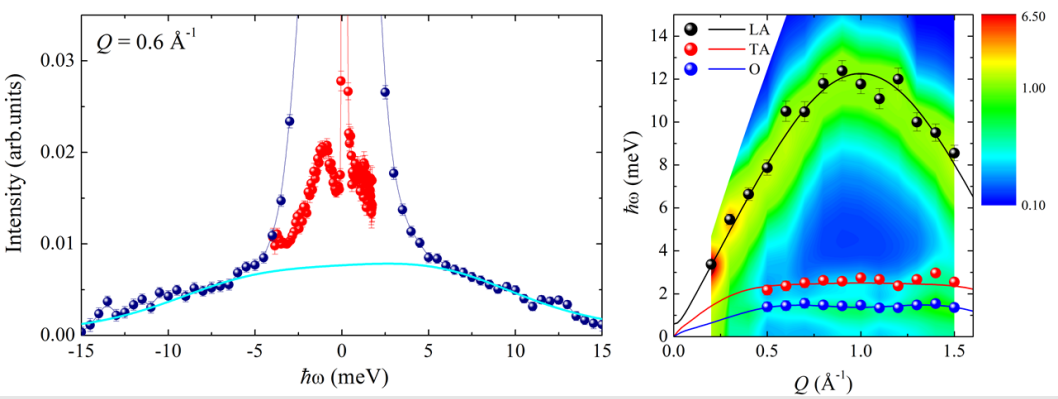

Figure 7: LEFT: $S(Q,\omega)$ of v-$SiSe_2$ measured on BRISP @ ILL (blue dots, E_i = 83.6 meV, δE = 3.1 meV) and TOFTOF @ FRMII (red dots, E_i = 3.27 meV, δE = 0.15 meV). RIGHT: Corresponding dispersion curves, revealing a complex pattern of three interacting excitations.

The unexpected complexity of the dispersion curves was observed only with a combined use of different instruments with complementary resolutions and kinematic ranges. The RRM of T-REX eliminates any need of using different instruments.

The scattering signal from collective modes is always weak. Even on dedicated instruments, measuring times of days are needed for a single thermodynamic point. T-REX will provide a more than tenfold increase of incoming intensity, even using a collimated beam to address science that cannot be done today. Indeed, the high single-wavelength flux of T-REX will allow the investigations of collective modes to be routinely performed in much shorter times, even on smaller samples and under variable thermodynamic conditions. A typical longstanding example is liquid Rb, where the high temperatures and pressures necessary to keep the liquid metal in the thermodynamic conditions of interest are technically incompatible with long acquisition times.

Vibrational dynamics of disordered materials.

Despite a large spectrum of different chemical and physical properties, disordered systems exhibit a universal vibrational feature named boson peak. This is a broad peak visible in the low-energy region (a few meV) of the reduced vibrational density of states $g(\omega)/\omega^2$.

The wide E_i and Q ranges available on T-REX will allow thorough measurements of the $g(\omega)$ for both coherent and incoherent scatterers, respectively requiring access to high- and low-Q regions. In addition, the RRM will enable to use the best resolution to zoom in on specific energy regions and highlight peculiar spectral features.

An effective approach to gather information on the nature of the boson peak relies on the study of its evolution as a function of pressure and temperature. Here the high flux of T-REX is again necessary for parametric studies, even on small samples [31, 32, 33].

This kind of investigations is also relevant to tackle geophysical problems related to the glassy state. An example is the eruptive style of volcanoes, which is closely related to the microscopic properties of magmatic melts and glasses. T-REX will enable extensive studies of magmas under real thermodynamic conditions (up to 0.6 GPa and up to 1200 K) to decipher the process of composition mixing. This is fundamental for a quantitative understanding of eruption dynamics [34].

1.1.7 Instrument design parameters from the science case

- The bispectral beam is needed to provide initial neutron energies $2 < E_i < 160$ meV to explore a huge dynamic range spanned by excitations in condensed matter research:
  - up to 140 meV energy transfer to investigate excitations in correlated electron systems at the fore front of current research,
  - down to 20 μeV energy resolution to investigate frustrated magnetism and quantum phase transitions,
  - combined investigations of lattice dynamics and diffusive motions in materials science,
  - wide incident-energy flexibility, to tackle the relationship between dynamics and functionality of biological systems, in the whole dynamical range from quasielastic relaxational motions to inelastic vibrational modes.
- The narrow bandwidth $\Delta\lambda < 1.7$Å and a wavelength step $\delta\lambda \geq 0.07$ Å concentrates the intensity in a narrow range of E_i whereas the excellent energy resolution gives access to details of the excitation spectra:
  - More than 20 pulses in the thermal band matching the repetition rate of a continuous source with the peak brightness of a spallation source.
  - Efficient PA for an entire band, in the thermal as well as in the cold spectrum.
- Sufficient space and horizontal access is foreseen for complex sample environment, needed for in-*operando* studies on energy materials or for simultaneous measurements with complementary techniques.
- A maximal size of up to 10 mm x 30 mm allows one to benefit from a large scattering volume e.g. for single crystal samples as at present-day, the high flux and a focusing nose piece permits also experiments with tiny samples and still reasonable Q-resolution.
- The detector voxel of 25 mm $\times$ 25 mm$\times$ 25 mm and the distance of 3 m provide an energy resolution of 20 μeV already at $E_i = 2$ meV and hence closes the gap between backscattering and direct geometry ToF spectrometers. The huge solid angle coverage allows the efficient mapping of dispersive excitations in the whole energy range.

Hence T-REX intends to be the spectrometer for high energy transfer, single crystal investigations and polarized neutrons. The requested dynamical range shown in Fig. 8 can be covered by 4 different bands to fulfill its scientific mission.

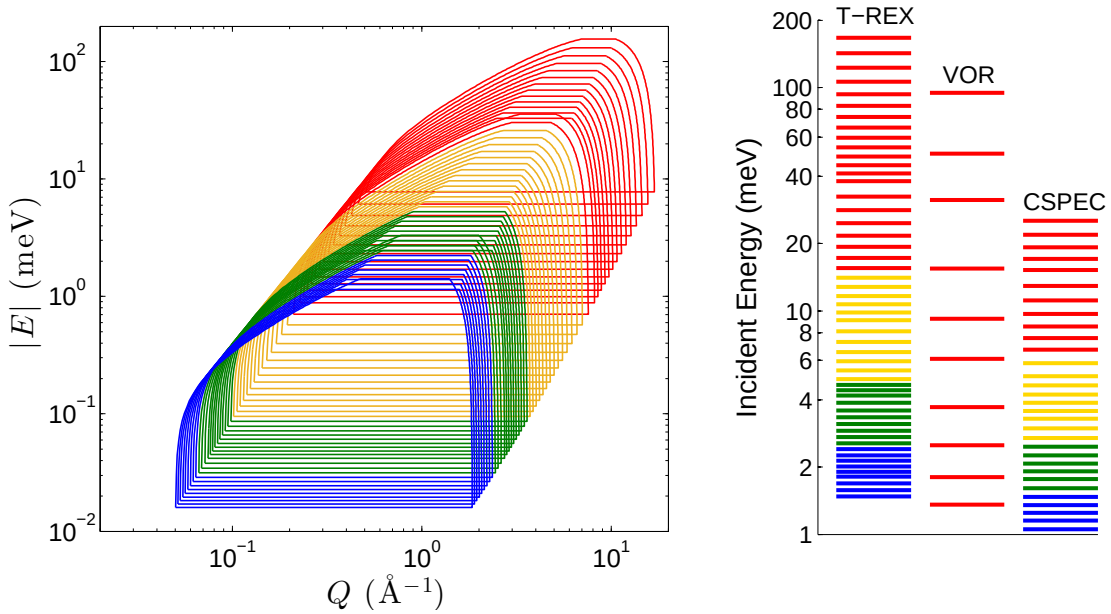

Figure 8: Left: Dynamical range accessible with T-REX using 4 different bands: Each closed line represents the range covered by a single pulse. Right: Initial energy provided by the direct geometry spectrometers proposed for the ESS in 4 bands (T-REX, CSPEC) and in one band (VOR). For T-REX and CSPEC bands can be combined by pulse skipping to enlarge the dynamic range. Please note the logarithmic scales.

Table 1: The relevant parameters of T-REX.

Moderator		Bi-spectral
Flight path length	Moderator-Sample	166.3 m
	Sample-Detector	3 m
Incident Energy E_i	source frame	
≥ 16 meV	1^{st}	
$5-16$ meV	2^{nd}	
$3-6$ meV	3^{rd}	
$2-3$ meV	4^{th}	
Energy resolution	$1\% < \Delta E/E_i < 4\%$ at $E_i = 2$ meV	
	$3\% < \Delta E/E_i < 10\%$ at $E_i = 100$ meV	
Scattering Angle	Horizontal	-30° +150°
	Vertical	-15° +25°
wavevector	range	$0.05\text{Å}^{-1} < Q < 17\text{Å}^{-1}$
	resolution	$0.01\text{Å}^{-1} < \Delta Q < 0.1\text{Å}^{-1}$

1.2 Description of Instrument Concept and Performance

The T-REX spectrometer is specifically designed to benefit from the unique ESS source characteristics:

- The high peak brightness provides monochromatic neutron pulses more intense and resolved than at any existing neutron source thanks to the use of a very efficient guide concept.
- The evolution of the RRM concept increases the duty cycle at the detector to nearly 100% by the use of multiple incoming energies.
- The chopper system offers a wide flexibility to trade resolution for flux with a quantized variation of the spinning frequencies, thus making efficient use of the long pulse structure of the source, which guarantees a long plateau at the highest peak brilliance. The spectrometer can be tuned from high energy resolution, to e.g. analyze excitations beyond the harmonic approximation, to very high flux to investigate minute amounts of sample or very weak signals.
- The bi-spectral extraction allows the sampling of a huge dynamical range in one instrument.

The overall instrument length, which is 169.3m, provides a *natural* incident bandwidth of nearly 1.7Å. For RRM, the step between adjacent incident wavelengths within this band is defined by the M chopper frequencies and amounts to 0.07Åat the maximum speed (336 Hz). The benefits of a long instrument are:

- One can choose the narrow bandwidth of incoming energies freely within the thermal or cold energy range to address a specific scientific question.

- The dynamic range is probed many times with comparable energy resolution, so that all the collected spectra contain useful information.
- The initial wavelength can be used as an additional degree of freedom to map out reciprocal space thanks to the narrow wavelength steps (see Fig. 19).
- Efficient PA is possible for any band, choosing between polarizing supermirror devices and ^{3}He spin filter cells in the region where they work best.
- The entire thermal spectrum 16 meV$< E_i <$160 meV is contained in one band. Hence a removable bispectral extraction system is placed outside the target monolith to enable unperturbed thermal performance. Exchanging the extraction bender with a polarizing bender the cold beam can be polarized without additional transmission losses.

The instrument is designed to map a wide volume of reciprocal space, which is suited to investigate the excitation landscape in novel materials with a focus in magnetism, thanks to the extensive use RRM and to the large area secondary spectrometer characterized by a position-sensitive detector at 3 m distance from the sample, which covers 21 m^2 area. The sample-to-detector distance enables an ultimate energy resolution of 1% at $E_i = 2$ meV, provided that the detector can detect scattered neutrons with radial uncertainty better than 20 mm. The expected high neutron flux allows the application of PA as a standard tool in investigations of quantum phenomena in condensed matter. To fulfill this mission at the best, we favor polarized ^{3}He spin filter cells to analyze the neutron spin because this technique enables large solid angle coverage of the analyzer and independent x-y-z analysis of the spin direction. Furthermore the ^{3}He spin filter cells can be operated with good efficiency for thermal and cold neutrons, by adapting the gas pressure. For a given ^{3}He pressure a good efficiency is reached in a bandwidth $\Delta\lambda < 2$Å. Therefore the instrument offers a fully polarized band for PA that is proposed as a day-one option.

1.2.1 The chopper system

The chopper system of T-REX consists of 6 disks choppers, a T0 chopper and a specifically designed Fan chopper[35]. Details are listed in Table 2. The different tasks are decoupled:

- the pulse shaping ($P_{1,2}$) and monochromating ($M_{1,2}$) disk pairs prepare monochromatic neutron pulses with the requested resolution,
- the bandwidth defining ($BW_{1,2}$) disks select the incident energy band requested for the experiment,
- the fan chopper (Fan) suppresses neutron bunches generated by the M choppers just as needed, in order to have sufficient recording time according to the excitation spectrum of the sample under study,

Table 2: Chopper specifications. The dimensions are subject to review according to the final guide design. The P and M chopper discs are equipped with different windows to provide different resolution configurations. (*) For the M chopper the maximum frequency aimed at is 406 Hz, but the calculations presented assumed 336 Hz, state-of-the-art today.

	Distance from moderator (m)	Diameter (mm)	Frequency (Hz)	Window position (°)	Window width (°)	Guide size (mm x mm)
BW_1	20	1000	14	0	32	60x179
BW_2	24			0	40	60x190
T0	99	600	14	180	18	60x90
P_1	109.9	700	<304.5	0/180	22	60x90
				45/225	36	
P_2	110.1		<304.5	0/180	22	
				90/270	36	
Fan	164	1000	14		15	28x53
M_1	164.99	700	<406(*)	0	2.5	22x46
				90	4.3	
M_2	165.01		<406(*)	180	2.5	
				270	4.3	

- the T0 chopper (T0), is commonly used at spallation sources [36, 37] to suppress the prompt pulse of high energy neutrons by blocking off the beamline around the time of neutron production. At the Japan Proton Accelerator Research Complex (JPARC) tests performed on High Resolution Chopper Spectrometer (HRC) [38] show a reduction of two orders of magnitude in the background noise detected for monochromatic beams of energy above 100 meV [39].

1.2.1.1 Resolution defining choppers

The energy resolution of the proposed instrument is controlled and varied by the two pairs of fast spinning P and M choppers, placed at a distance L_P=110 m and L_M=165 m from the moderator, respectively, and separated by a distance L_{PM}=55 m. The choice of L_P and L_M is not constrained by resolution requirements as the energy resolution improves only marginally increasing the distance beyond 20 m, for the assumed flight path uncertainties of 20 mm [35]. L_P and L_M are instead chosen to fulfill the link to the repetition rates of the P and M choppers (f_P and f_M, respectively) in order to transmit the same wavelength periodically with the source frequency:

$$\frac{f_P}{f_M} = \frac{L_M}{L_P}. \tag{1}$$

The wavelength difference between subsequent pulses is hence given by

$$\delta\lambda = \frac{\hbar}{m_n} \left(L_M f_M\right)^{-1} \tag{2}$$

We have chosen the ratio 165m/110m = 1.5 and double the repetition rate of the P chopper by placing 2 windows on the P chopper disks. If this condition is fulfilled, the cross talk between different openings of the choppers is prevented by the finite pulse length of the source and the overall system is characterized by a fixed extraction time from the moderator for all wavelengths. The resulting acceptance diagram shown in Fig. 9 not only confirms the common time origin of pulses passing through openings of the P and M chopper pairs, but also that the preceding and subsequent common acceptance areas fall into a time, when the source does not produce neutrons. The M choppers have to be placed as close to the sample position as possible not to deteriorate the energy resolution, but far enough to leave the space for complex sample environments including the magic PASTIS setup for wide angle PA. Therefore the distance from the chopper to the sample position L_{MS} is fixed to 1.3 m. The choppers are realized by pairs of counter rotating disk choppers, see Table 2. We have investigated different means to provide very short burst times, see enclosures [40, 41]. As the latest guide design is only 22 mm wide at the position of the M-chopper we opt for the pure disk chopper solution, as the large window with an opening of 4.3° can be used to achieve a very good elastic energy resolution over the widest part of the neutron spectrum. If a high elastic energy resolution is requested, the chopper is equipped with an optional narrow window with 2.5° opening, which can achieve burst times $\tau_M < 10\mu$s. We note here that typically high E_i is used to probe large energy transfer to the sample slowing down the neutron. The reduced E_f makes it most efficient to increase τ_M and to decrease τ_P to best match the uncertainty contributions from the P- and M-chopper pairs. Therefore we consider also the use of the 4-chopper optically blind concept presented by the VOR team with one counter rotating pair to open the beam and a second counter rotating pair to close the beam. It provides not only a wavelength dependent burst time as a function of the distance between the pairs, but also an arbitrary τ_P by control of the phase of the pairs. As some of the features are already provided with two co-rotating choppers (the P-chopper windows are significantly wider than the neutron beam cross section), the installation of two additional P-choppers is planned as an update option.

1.2.1.2 Bandwidth choppers

The chopper system is completed by two disk choppers that select the incident wavelength band useful for the experiment and restrict the time at which the resolution chopper system is fed with neutrons. The two disks are placed at 20 and 24 m from the moderator surface and spin with the source frequency 14 Hz. As evident from the acceptance diagram in Fig. 9, this layout excludes cross talk from earlier source pulses for neutrons with a wavelength λ <75Å. The details of the chopper layout depend on the design of the neutron guide system, as the burst time depends also on the angular width of the neutron guide window. The choppers will be realized as individual disks with a comparably large diameter to optimize the transmission. To change the used band, it is sufficient to shift the relative phase of the bandwidth choppers, while the energy resolution choppers can continue with the same phase. There is also the flexibility to select only every second source pulse to cover a larger dynamical range at the cost of

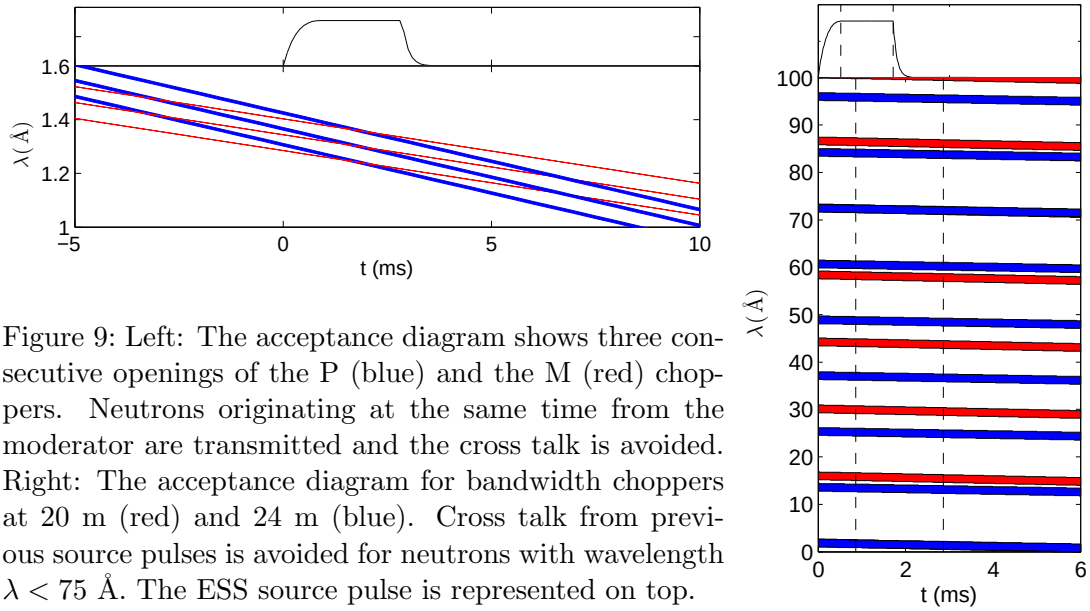

Figure 9: Left: The acceptance diagram shows three consecutive openings of the P (blue) and the M (red) choppers. Neutrons originating at the same time from the moderator are transmitted and the cross talk is avoided. Right: The acceptance diagram for bandwidth choppers at 20 m (red) and 24 m (blue). Cross talk from previous source pulses is avoided for neutrons with wavelength $\lambda < 75$ Å. The ESS source pulse is represented on top.

reduced single pulse intensity.

1.2.1.3 Time frame selection chopper

The use of RRM methods imposes a careful consideration of frame overlap issues. Thanks to a specifically designed Fan chopper [35], T-REX is able to adapt the acquisition time frame necessary to collect the spectra up to the same relative energy transfer. The single acquisition time frame depends on the initial neutron wavelength and the maximum energy transfer to be recorded without frame overlap:

$$T\left(\lambda_i, \hbar\omega\right) = \frac{m_n}{\hbar} \frac{\lambda_i L_{SD}}{\sqrt{1 - \frac{\hbar\omega_{max}}{E_i}}}. \tag{3}$$

We have developed a prototype to proof the principle of operation. It consists of ten chopper blades that spin on a common axle with a common frequency of 14 Hz. This low frequency and the low masses involved pose no particular challenge to the bearings and drive systems. The phase of an individual blade can be set independently to block a single neutron pulse and each blade is connected on a hollow shaft to its own torque drive. The prototype gives the possibility to suppress up to 10 bunches for any frequency of the M chopper within one period of the source. The dimensions of the blades are constrained by the following conditions:

- the blades have to block the beam off for a time shorter than 2 periods of the M chopper, taking into account the opening time of the M chopper, $2\tau_{FAN} = \frac{\alpha+\beta}{\omega} < \frac{2}{f_M}$
- the neutron guide window must be fully blocked when the M chopper transmits neutrons $\frac{\beta-\alpha}{\omega} > 2\tau_M$,

where $f_M = n \times 14$Hz, α is the angular width of the neutron guide at the chopper position, β is the angular width of the blade, $\omega = 2\pi \times 14$Hz. Here, the narrow beam cross section leaves some freedom for the layout of the Fan chopper blade. In Table 2 we have chosen an angular blade width, which leaves also some margin, if higher repetition rates should become feasible at a later stage.

1.2.1.4 T_0 chopper

The background conditions determine crucially the performance of a spectrometer. The optimization of the beam transport for thermal neutrons shows the best performance for a neutron guide that curves only once out of sight [42]. Therefore a $T0$ chopper is foreseen downstream the curved guide section as an additional mean to suppress fast prompt radiation. The $T0$ chopper must be fully opaque for at least the duration of the proton beam hitting the target. As a consequence the chopper blocks fixed energy windows of the neutron spectrum, which are narrow because of the large distance from the moderator. Due to this, also the high energy limit of the transmitted band is well above the highest energies transported by the neutron guide. Hence the full intensity is transmitted for each pulse within the thermal band. For details see [43]. Finally the chopper position is far from any experimental hall. Hence it provides sufficient space also for massive shielding and does not disturb any neighboring instruments.

1.2.2 Neutron transport

1.2.2.1 Cold neutron extraction with polarization option

Thanks to the narrow bandwidth $\Delta\lambda \approx 1.7$ Å measurements using the thermal part of the spectrum 16 meV $< E_i <$ 160 meV can be distinct from measurements using cold neutrons. Therefore the neutron guide is placed to face the thermal moderator surface, see Fig. 10. A solid state bender is placed outside the monolith of the spallation target to feed the neutrons from the cold moderator into the neutron guide, when using bands with $E_i < 16$ meV. It is installed on a lift and can be replaced with a neutron guide to have an unperturbed performance when using the thermal energy band. To improve the illumination of the bender/guide, horizontal mirrors with $m = 3$ coating are used inside the monolith. The bender consists of Si wafers with a thickness of 150μm coated on one side with $m = 2$ Ni−Ti supermirrors. When in place the system is able to reflect neutrons originating from the cold moderator into the beam-line, with an efficiency in between 80% and 90% for neutrons with energy below 16 meV [42], as shown in Fig. 10. It is seen, moreover, that the transmission of thermal neutrons gets lower with increasing the energy, because it is not needed to transmit thermal neutrons, as the experiments with thermal E_i will be made removing the bender from the beam. We propose to use a similar device for the polarization of cold neutrons, see sec. 1.2.4. The polarizing system has identical geometrical parameters, but is coated with m=2 Fe-Si supermirror. As detailed later in section.1.2.4 the polarization by this bender reaches 95%. The simulations of the polarizing efficiency use experimental reflectivity curves for spin-up and down provided by Ken Andersen [44].

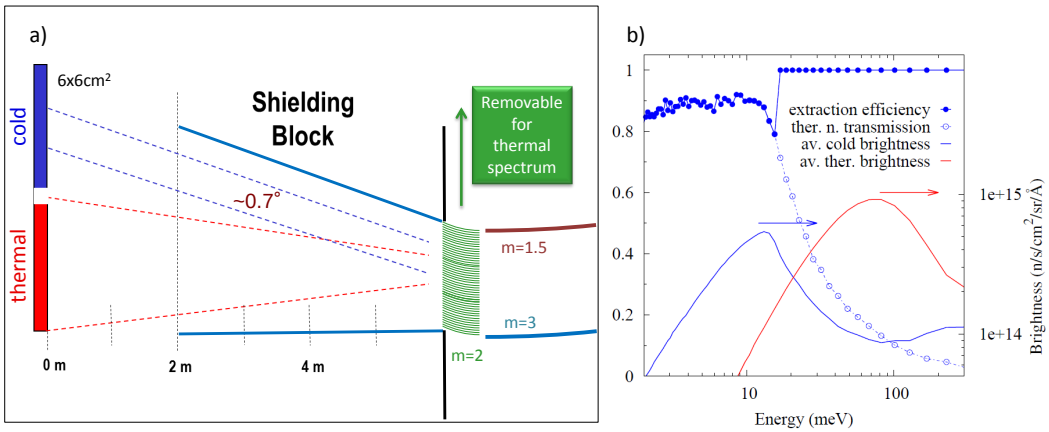

Figure 10: a) Sketch of the extraction system outside the target monolith. b) Efficiency of the cold beam extraction together with the average brightness from the cold and thermal optimized thermal moderators. Note that the efficiency for thermal neutrons is 1, as the bender is removed from the beam if the thermal band is selected for experiment.

1.2.2.2 Avoiding the line-of-sight

The original guide concept of T-REX was based on stacked ellipses, which provided good brilliance transfer in the thermal range and excellent brilliance transfer in the cold range. The drawback of this concepts is the direct view from the sample area into the moderator. With the selection of instruments in the last proposal round, which perform best in the cold spectral range we revised our neutron guide concept to improve the brilliance transfer for the thermal to epithermal spectral range on the cost of a modest reduction of the cold performance. The first step towards a better thermal performance is a less stringent compression of the neutron guide in the vicinity of the P chopper. The burst time requirements allow for a guide cross section up to 60 mm×100 mm.

Several guide geometries have been investigated for T-REX to avoid the direct line-of-sight, which is a potential origin for background, and requires a heavier shielding along the entire neutron guide. The transport needs small reflection angles at the guide walls and also the total number of reflections must be low, as the high energy neutrons are reflected at comparably large momentum transfer and hence reduced reflectivity. We investigated three solutions that fulfill these criteria (see also for more details [42]) :

- a double elliptic shape with a kink across the P-chopper position, following the concept proposed in Ref.s [45, 46], where the line-of-sight is broken once.
- the same double elliptic shape with the kink at the same position and the kink angle increased twice, such that the line-of-sight is broken at 30 m from the moderator. In this layout the T0 chopper might be placed upstream this position (30 m), to allow breaking the line-of-sight twice, by combination of the two measures,
- a curved shape followed by straight and elliptic sections, depicted in Fig. 11a).

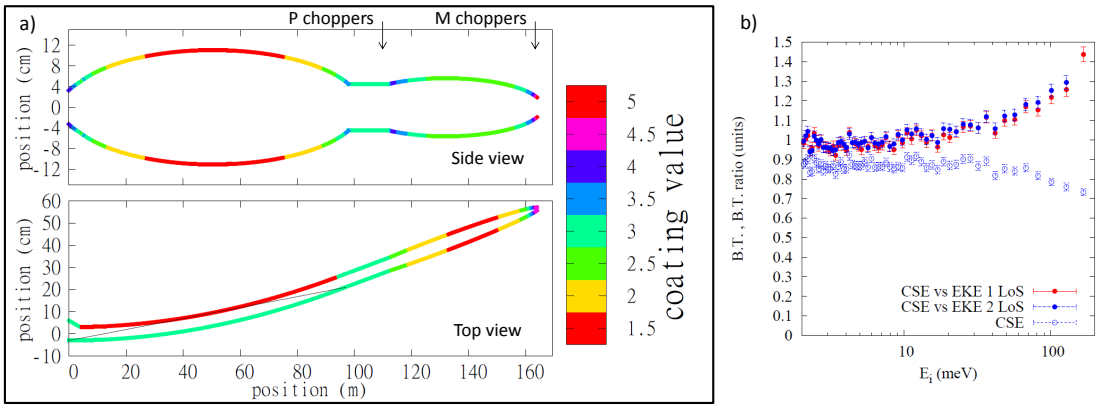

Figure 11: a) Schematic rendering of the vertical (top) and horizontal (bottom) shapes of the neutron guide of T-REX. The value of the supermirror m index is represented in color scale. b) The brilliance transfer at the sample after the curved shape (empty circles) and the comparison to the double ellipse connected with the kink (filled circles).

The curved section transports a wide beam with a narrow divergence and breaks the line-of-sight upstream (before) the P and T0 choppers. The straight section homogenizes the divergence distribution and the final focusing section tailors the phase space.

The transport system was optimized with the highest priority on an efficient transport of high energy neutrons $E_i > 50$ meV within a divergence region of $\pm 0.25°$ to provide a reasonable Q-resolution, followed by the request of a wider divergence transported efficiently for lower energy. In Fig. 11b) we compare the brilliance transfer at the sample for the three options within the region of interest identified by a sample size 10x30 mm^2 within a divergence of $\pm 0.25°$. The curved solution performs better than the others, with a maximum gain of 50% and it reaches high values of the brilliance transfer, for instance the 70% is reached already at around 200 meV. As can be seen in the enclosure [42] the brilliance transfer is very high also for a divergence region of interest $\pm 0.5°$ over the entire cold and thermal spectrum, but is reduced to 60% in the cold spectrum for a divergence region of interest $\pm 1°$. Considering the fact that a reduction of the divergence might be necessary for single crystal studies, we consider this solution best for our science case. The *vertical* shape proposed is a double ellipse with a straight section in the center of the two ellipses. The shape is constrained by the requirements for short burst times at the position of the resolution defining choppers. The rather long burst time required at the P-chopper allows a neutron guide cross section up to 60 mm $\times$ 100 mm, which is well below the width of the chopper disk windows, yielding a trapezoidal pulse shape.

1.2.3 The secondary spectrometer

The spectrometer vessel houses the sample area and the detectors. In operation the whole flight path will be evacuated to a cryogenic vacuum, in order to avoid the use of windows inside the spectrometer chamber, which are a potential origin of background.

1.2.3.1 The detectors

T-REX aims to achieve 1% elastic energy resolution at 2 meV incoming neutron energy. A sample-to-detector distance L_{SD} of 3 m enables this goal assuming the detector contribution to the total flight path uncertainty is below 20 mm. It matches also the resolution requirements for thermal neutrons imposed by the shortest opening times of the M-chopper pair and request reasonably short time frames to maximize the use of RRM. To achieve comprehensive solid angle coverage the horizontal scattering angle ranges from -30° to 150°. The vertical scattering angle ranging from -15° to 25° requires 2.2 m detector height. The total area is 21 m^2, which also reduces the cost compared to the former larger detector. For the given area, the asymmetric layout of the detector is good for maximising the Q range, while reducing cross talk effects from opposite detectors. However, for the small angles equivalent regions of reciprocal space can be mapped to add some redundancy to the data. Due to the use of thermal neutrons the requirements on the detection efficiency of the detectors are very challenging. We aim for a detection efficiency of 70% for neutrons with wavelength $\lambda = 1$ Å averaged over the whole detector area. Furthermore the detectors should have a low susceptibility for background particles, particularly gamma radiation. Here we state a gamma rejection better than 10^{-6}. The tangential position resolution of the instrument is relaxed due to the large incoming divergence and the large sample to detector distance. The radial position resolution is crucial for the energy resolution at the cold end of the neutron spectrum, where the flight path uncertainty is the dominating contribution to the energy uncertainty. Today, most newly built spectrometers employ position sensitive ^{3}He detector tubes as they meet all of the above stated requirements and hence this is the proven technology and must be the benchmark for the T-REX detector. However, the availability of the large amount of ^{3}He is uncertain, despite the fact that several ongoing instrument projects as TOPAS at MLZ, NEAT at BER2 and Fa# at LLB have recently procured large area ^{3}He detectors. We have evaluated alternative detector technologies such as wavelength shifting fibers and a gas detector with thin film solid state converters. The former we have discarded because of background and after-glow issues. The rapid development for the thin film detector technology make it a likely choice for T-REX as the final decision about the detector can be postponed until 2016/17. Considering the targeted price of the ESS development the cost of the detector would be only a fraction of a similar size ^{3}He detector, if this would be procurable at all. Beside the cost argument the novel concepts hold also the potential of new features that are not present in nowadays detectors. E.g. the detection signal contains also the depth information, which increases the information content from the detector. The finite transmission probability results in an exponentially decaying transmission on a line pointing in the direction of the scattered neutron beam with a attenuation coefficient depending on the scattered

Table 3: Typical sample environment and auxiliary equipment to be used on T-REX. Note that the numbers are based on today technology and can change with new developments. This list is not meant to be comprehensive and exclusive.

Sample environment	Parameter range	Remarks
Cryofurnace	1.9 K $< T <$ 650 K	Standard equipment
Furnace	650 K $< T <$ 2000 K	Standard equipment
Polarization analyzer	$B_{Guide} \approx 2$ mT	Can be combined with standard equipment
Cryomagnet	1.9 K $< T <$ 300 K	
	$B < 14$ T, vertical	Only modest limitation of scattering angle
Dilution insert	$T < 50$ mK	Can be combined with standard equipment
Paris-Edinburgh cell	$P < 10$ GPa	Sample size 10 mm^3
Auxiliary equipment:		
Ac- magnetometer		Control of sample state
Dilatometer		Control of sample state
LASER		Pump-probe experiments
Electrometer		Application of electric fields + Control of sample state

neutron wavelength. As the depth information is redundant with the time of flight information, it can be used to distinguish background events. Also signals not originated from scattering at the sample will give an absorption pattern that is not on a radial line and can therefore be identified as spurious. The high energy physics community has many successful strategies to distinguish useful events very fast. The adaption to neutron detection bears the potential to improve the data quality significantly.

1.2.3.2 The sample area

The scientific challenges to be addressed at T-REX often request complex sample environments. As an instrument that focuses on the investigation of quantum phenomena, the most important thermodynamic parameters are temperature, magnetic field and pressure. We aim for state-of-the-art sample environment at the time of the commissioning of the instrument (see Table 3). It is clear that temperatures down to the mK region must be accessible to investigate e.g. quantum critical points or excitations in highly frustrated systems. As for magnetic fields we design the sample area to host compensated vertical field magnets with a form factor as known from today 14 T magnets. This proposal is not opting for the highest magnetic fields that will be available at ESS. Instruments like CAMEA with limited solid angle coverage will be better suited for this. T-REX will provide access to state-of-the-art parameter ranges compatible with the high solid angle coverage, which is the particular strength of direct geometry chopper spectrometers. High-pressure investigations will benefit largely from the increased flux, which allows a reduction of the sample volume in the order of 1 mm^3. The accessible pressure range we aim for is up to 10 GPa,i.e. within reach employing the Paris-Edinburgh cell.

Besides different external parameters, like temperature, pressure, field, an additional degree of freedom is needed to cover $S(Q,\omega)$ in 4D. Today full coverage requires a rotation of the sample by at least 180°. Because of the small step size in incoming wavelength, users of T-REX can also use the initial wavelength to achieve a dense coverage of reciprocal space quickly (see Fig. 19) with the additional option to rotate the sample e.g. to realize identical energy resolution for different Q. More complex studies, e.g. in-*operando* studies, levitation experiments, etc., request an easy access to the sample area and the application of auxiliary characterization tools. For independent control of the sample state we will measure e. g. magnetic AC susceptibility or dilatometry in parallel to the scattering experiment. To study phenomena away from thermal equilibrium we consider the illumination of the sample with laser light. For applications in material science and energy research the possibility of gas loading is essential. Moreover the design of the sample environment area requires special attention. For the TOPAS spectrometer we have recently developed a load lock that enables to vent the volume around the sample while keeping the bulk of the flight volume evacuated, see Fig. 12. We plan to refine the layout to facilitate horizontal access to the sample area for the installation and interaction with complex sample environments. This would allow the flexibility to install complex ancillary equipments for performing, when needed, simultaneous measurements with complementary techniques, such as for instance light spectroscopies.

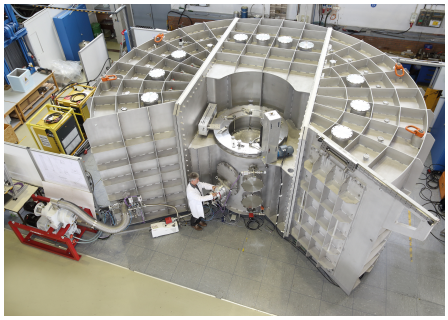

Figure 12: The vacuum vessel of TOPAS

1.2.3.3 The vacuum system

In order to avoid possible background, we intend to reduce the scattering from material in the beam close to the detector. While the largest fraction of the flight volume remains under cryogenic vacuum conditions permanently, the sample area can be separated from the main volume by a gate valve pumped independently. Thus only a small volume needs to be vented and pumped for a change of sample environment. Such a system has already been installed and tested on the TOPAS spectrometer, see Fig. 12. A common vacuum is foreseen for the detector tank and the final neutron guide section including the M chopper pair, which can be separated by valves in case of maintenance. Scattering from neutron guide windows will thus be created at a position far from the detectors.

1.2.4 Polarization Analysis

T-REX is perfectly suited to provide PA in the entire spectral range for novel experimental opportunities in the field of magnetism, but also in the fields of energy materials research or soft matter by the clean separation of spin-incoherent scattering. For the

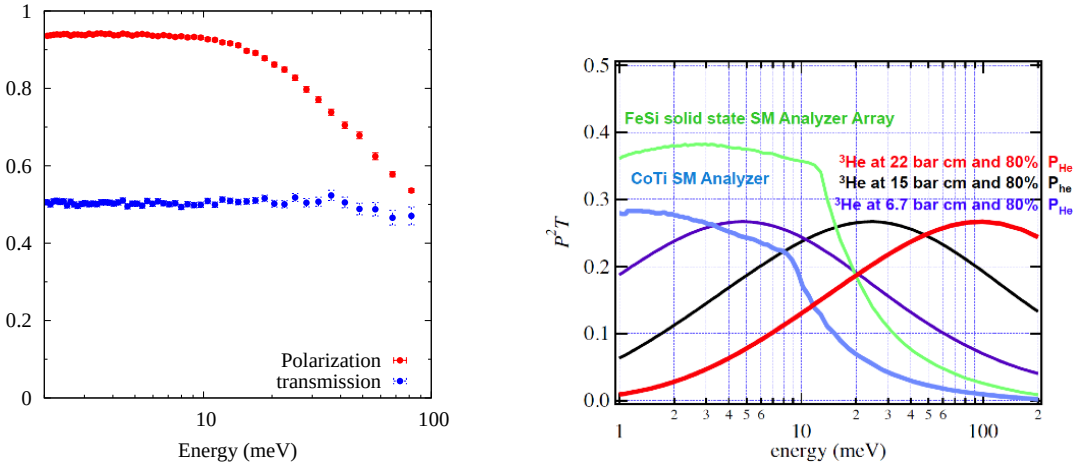

Figure 13: Left: Polarization and transmission of the required spin state passing through the polarizing bender. Note that T=0.5 corresponds to the optimal transmission of all neutrons of the desired spin state. Right: The calculated P^2T for the ^{3}He spin filter cells for an assumed 80% constant polarization of the ^{3}He gas at a given pressure: 6.7 bar cm (violet), 15 bar cm (black) and 22 bar cm (red). The curves for the Fe-Si (green) and Co-Ti (blue) air gap analyzer arrays are included for comparison.

narrow *wavelength* bandwidth all neutrons of an experiment will be polarized with similar efficiency and the combination of cold beam extraction and polarizer in one device optimizes the transport of the requested spin state.

1.2.4.1 Incident neutron polarization

To polarize the cold neutron beam we plan a third stage on the lift for the cold extraction with a polarizing bender. In this case, the transmission for the polarized beam approaches the upper limit of 0.5 as compared to the unpolarized case, see fig. 13. Providing a guide field along the entire neutron guide is technically simple and involves also acceptable costs see tab. 5.

For the use of thermal neutrons ^{3}He spin filter cells provide a better efficiency as seen in fig. 13. By adapting the gas pressure or the cell length, the figure of merit (P^2T) can be optimized for different neutron energies [47]. A guide exchanger will therefore be installed just upstream the M-chopper with a stage for a continuously optically pumped ^{3}He spin filter cell providing the high constant gas polarization and hence constant neutron polarization (Fig. 14). Under realistic experimental conditions we achieve a ^{3}He gas polarization of 80%, constant over several days at our reflectometer at MLZ (MARIA). A simple guide element will be installed on second stage for optimum transport, if the thermal polarizer is not needed. The position of the guide exchanger is chosen to allow for access, when the proton beam is on. At the position of installation the polarizing device can avoid the issues of very high neutron fluxes deteriorating the performance of the spin filter cell [48].

Recently we have also developed a new guide field arrangement to adiabatically rotate a polarized neutron beam in an arbitrary direction even for neutron energies above 100 meV [49] (Fig. 14).

1.2.4.2 Analysis of neutron spin after scattering

PA covering a wide angular range is possible at a few instruments world wide. The D7 at the ILL, the DNS at MLZ and HYSPEC at SNS employ super-mirror arrangements to analyze the neutron spin after scattering. Such a layout works very well for cold neutrons and when the momentum transfer is resolved only horizontally, as the PA affects the divergence distribution. For 2D resolving PSD it is desirable to keep the divergence unaffected. Hence we work on the design of cells, which reduce small angle scattering using single crystal windows.

Wide angle PA using ^{3}He spin filter cells is under development at ILL, ISIS, SNS and J-PARC. For the thermal ToF spectrometer TOPAS, the JCNS is developing an evolution of the original PASTIS set-up developed at the ILL. The design has been refined introducing mu-metal sheets to produce an improved homogeneous magnetic field in a large region and to reduce the blind area due to the support material of the Helmholtz coils (see Fig. 14). The center of the configuration is the sample, placing the ^{3}He cell significantly off center. To accommodate an improved layout at T-REX we increase the space at the sample area by placing the M chopper at 1.3m from the sample. With the new design the potential exists to increase the undisturbed angular range from $\pm 20^\circ$ vertically and 180° horizontally and reduce the blind spot, which is 3° for the present layout. As the optical pumping must be done externally, a filling station is foreseen which is connected to the wide angle spin filter cell to exchange the ^{3}He gas. We expect a daily request for 50 bar l of polarized ^{3}He gas. For the TOPAS spectrometer at the MLZ with similar requirements we are installing a small SEOP facility with a gas recovery system dedicated to exchange the freshly polarized gas with the gas from the wide angle cell.

1.2.5 Instrument performance and benchmarking

T-REX uses the unique features of the ESS source, namely the high peak flux and the long pulse duration, to concentrate the intensity in the narrowest possible spectral range. Even for the long instrument length, the energy resolution is not dictated by the properties of the neutron pulse, but can be controlled by the chopper system. This feature enables a superior performance even in spectral regions, where the short pulse sources provide a significantly higher peak flux. The duty cycle at the detector is optimized by a chopper system, which enables variable time frames particularly for the thermal frame, where the energy changes between subsequent pulses are largest.

1.2.5.1 Analytical calculation of the wavevector-energy transfer resolution

We have developed and described [50] a general method for computing the wavevector-energy transfer covariance matrix, applied to the case of modern neutron time-of-flight

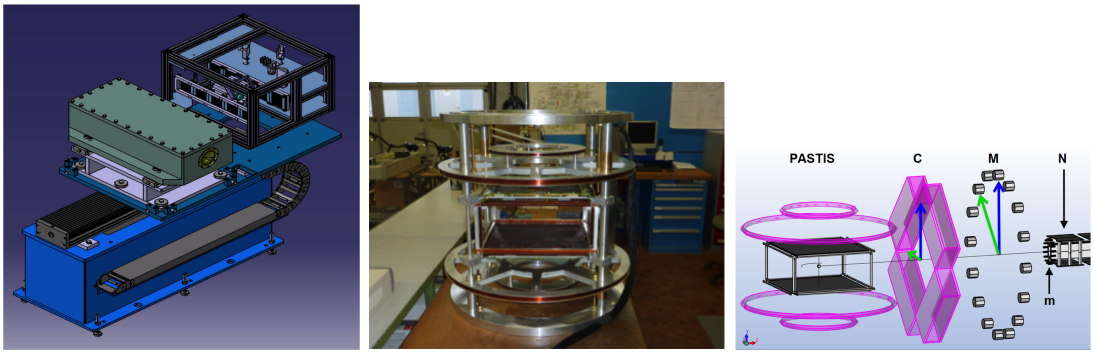

Figure 14: Left: Engineering model for the guide changer with the continuously pumped SEOP polarizer. Center: Coil setup of the 'magic PASTIS' setup. Right: Field layout with permanent magnets and coils for control in the incoming neutron polarization by adiabatic rotation.

spectrometers operating at a spallation source. The method identifies the relevant instrumental parameters and derives the covariance matrix by analyzing the transformation from the control parameters into (Q, ω). The method was applied to an example instrument layout [51] showing an excellent agreement with McStas simulations. The details of the derivation are beyond the scope of this proposal and can be found in the enclosures [50]. Here we present only the expression for the Q resolution limiting the discussion to its broadening around the elastic scattering condition at the scattering angle θ, in the horizontal plane:

$$\sigma_Q^2 = \left(\frac{m}{\hbar}\right)^2 \frac{1}{Q^2} \left\{ (\cos\theta - 1)^2 \left[\left(\frac{v^3}{L_{PM}}\right)^2 \left(1 - \frac{L_{MS}}{L_{SD}}\right)^2 \tau_P^2 + \left(\frac{v^3}{L_{SD}}\right)^2 \tau_D^2 + \right.\right.$$
$$+ \left(\left(\frac{v^3}{L_{PM}}\right)^2 \left(1 - \frac{L_{MS}}{L_{SD}}\right)^2 + \left(\frac{v^3}{L_{SD}}\right)^2 \right) \tau_M^2 + \left(\frac{v^2}{L_{SD}}\right)^2 \left(\sigma_{L_{SD}}^2 + \sigma_{L_{MS}}^2\right) \Bigg] + \tag{4}$$
$$\left. + v^4 \sin^2\theta \left(\sigma_{\theta_i}^2 + \sigma_\theta^2\right) \right\}.$$

The different contributions can be split in two groups: the first contains time and path uncertainties and is multiplied by $(\cos\theta - 1)^2$, whereas the second group is the angular uncertainty and it is multiplied by $\sin^2\theta$. Therefore the weight of the two groups follows a different trend with increasing angle (and increasing Q). The time uncertainty due to choppers openings is relevant at large angles. This enables the capability to trade Q resolution, together with the energy resolution, for flux by control of the choppers. Conversely the divergence of neutrons on the specimen dominates the resolution at small angles. Equation 4 is used to determine the Q broadening around elastic scattering as a function of Q, i.e. of the scattering angle, as shown in Fig.15. The lower transported divergence for thermal neutrons [42] limits the Q broadening to 0.11 Å^{-1} for 100 meV neutrons. Experiments on magnetic dispersions will benefit from this characteristic. The Q-resolution at energies below 20 meV is nearly completely determined by the angular

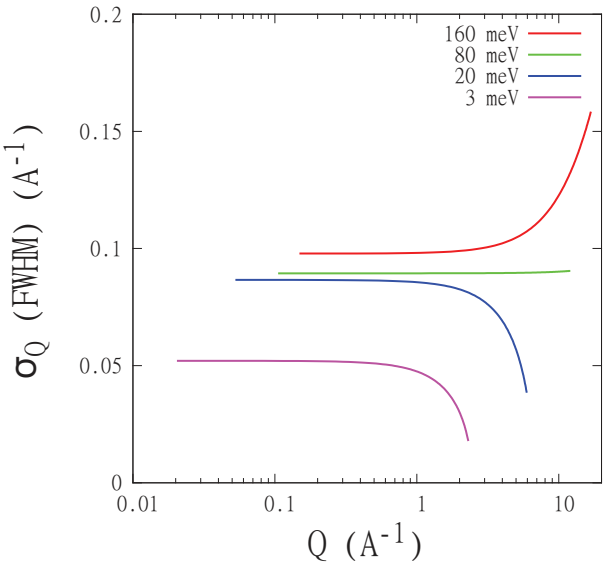

Figure 15: Q broadening (FWHM) as a function of Q, i.e. of the scattering angle for elastic scattering, as the incident energy varies from 3 meV to 160 meV and the scattering angle θ varies between 1° and 150°. The same chopper configuration is assumed, where the M choppers define a burst time of 8 μs.

uncertainties. Therefore we envision also the option to collimate the beam to improve the resolution for the entire energy range in the cold and warmish spectrum. The specimen dimensions and the detector pixel size are chosen to leave some leeway, in case the incoming collimation is improved. In general a rather broad angular divergence of the incoming beam is not a major concern, because a very fine Q resolution is usually not necessary in inelastic scattering experiments. However, in the specific case of disordered systems, the collective dynamics can be observed in the low-Q region only. Even if this is a small portion of the (Q, E) space and the scattering cross sections are fairly small, the information contained in this region is not visible with other approaches. To access this dynamical range, an incoming beam divergence below at least 1° is necessary. Of course, such a fine (two-dimensional) angular divergence has a strong impact on the incoming intensity. Nonetheless, the high intensity available at the ESS will make such experiments possible. To obtain the requested 2D-collimation, an optional short (e.g. 30 cm) honeycomb collimator can be installed just before the sample when needed by the users. Considering the wide sample area, this device has no special impact on the rest of the instrument performance. A set of different honeycomb inserts, having collimations between 0.5° and 1.5°, can be foreseen for the specific needs of different experiments. The collimators can be made of thin Al blades coated with ^{10}B or Gd, depending on the wavelength range.

1.2.5.2 Benchmarking T-REX performance against world-class instruments

The T-REX performance in terms of flux and resolution was characterized by ray tracing Monte Carlo simulations with the Vitess 3.2 package. The simulations are based on a moderator geometry for the optimized thermal moderator of 6x6 cm^2 surface area, as we were actively engaged in the performance comparisons for the different moderator concepts under consideration. The sample flux is determined by 10x30 mm^2 flux monitor at the sample position. To estimate the elastic energy resolution we placed a hypothetical elastic and isotropic scatterer at this position and determined the energy spread at a 3 m distant detector. T-REX allows for many different settings of the resolution at a given E_i, by changing the spinning frequencies of the choppers. We try to set up the simulation to mimic as much as possible the future operation of the instrument. Chopper phases and frequencies are set up for a band and then the intensity of all transmitted bands and the resulting energy resolution is determined without any change. The action of the Fan chopper is taken into account such that a pulse is only accepted, if the resulting time frame is long enough to record inelastic scattering up to $\hbar\omega = 0.8E_i$ before the next pulse arrives at the sample for the thermal band, or if the $\lambda_f = 1.5\lambda_i$ neutrons reach the detector before the next pulse is at the sample for the cold band. These criteria take into account that for cold neutrons the focus is often on the quasielastic response, while thermal neutrons are generally used to explore large energy transfer. Using these criteria for the repetition rate is common practise at continuous sources. In Fig. 16 we compare the flux and the resolution of the individual pulses for different chopper settings in the thermal band and in two different cold bands. For the thermal band, the high resolution setting (HR) is realized by usage of the small neutron windows on the P and M chopper disks (see Table 2), while spinning the choppers at maximum frequency $f_P = 252$ Hz and $f_M = 336$ Hz, respectively. While we expect, that finer energy resolution can be realized by the development of faster choppers than available today, we present the flux and resolution figures for chopper parameters achievable today. The high flux configuration (HF) uses the large windows. The choppers spin at the same frequency. For the cold bands we always employ the large windows on the disks, while in HR setting the choppers spin at 336 Hz and in the HF setting at 140 Hz.

With the present chopper layout the elastic energy resolution is limited to 4.4% at $E_i = 100$ meV and to 5.5% at $E_i = 160$ meV. To improve the energy resolution for this case we investigated different solutions:

- the reduction of the P chopper opening, while using the wide window of the M chopper. In such a setting one balances the tof uncertainty contributions from the P and the M choppers for high energy transfer from neutron to the sample.
- the replacement of the M-chopper disc pair by a Fermi chopper, which can spin with 602 Hz chopper frequency. This requires three equally distibuted disc windows on the P chopper discs to match the increased repetion rate resulting in a frequency ratio $f_P = 0.5f_M$.
- the replacement of the final neutron guide section and the adaption of the M chopper pair for a funnel solution a' la LET. The redesign of the neutron guide

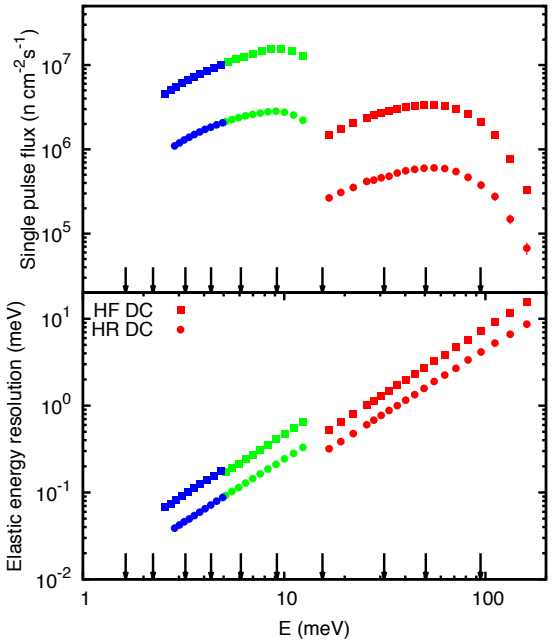

Figure 16: Single pulse flux (top) and elastic energy resolution (bottom) for the thermal band and two cold bands covering 4.8 meV< E_i <15 meV and 2.5 meV< E_i < 5meV. Frame overlap must be considered for $\hbar\omega = 0.8E_i$ for the thermal band and the higher energy cold band and for $\lambda_f = 1.5\lambda_i$ in the case of the lower energy cold band. The arrows indicate the pulse positions for VOR in one band using the same pulse condition. CSPEC can realize a similar pulse density as T-REX in the cold bands. Note the logarithmic energy scale.

was limited to the last 3.6 m and the M-chopper to detector distance was changed to 1.8 m as a result of the optimization.

In Fig. 17 the three solutions are compared to the HR setting as used in Fig 16. For a relative energy transfer larger 0.4 the opt4loss setting provides a better resolution than the high resolution setting with a substantially higher sample flux. For very deep inelastic scattering the resolution even exceeds to Fermi and the funnel case. Considering the fact that the dynamic ranges is sampled with a narrow spacing in initial energy, a large dynamic range 8 meV $< \hbar\omega <$ 150 meV is probed with very good resolution. If better resolution for smaller energy transfer is needed, the two other solutions are viable options As the Fermi chopper solution requires only small changes to the guide layout, it is not surprising that it performs better in terms of flux at the sample. The funnel solution provides an excellent energy resolution. The flux could possibly been improved by reconsidering the entire focusing section of the neutron guide. The first option does not require any modification on the chopper and guide layout. The Fermi chopper setup can be included rather easily by making the M chopper discs and a small section of the neutron guide around the M chopper position removable. The funnel requires the largest adaption but on the other hand it offers the ultimate elastic resolution. At this moment we opt for the first solution, which matches the requirements from the science case, i.e. large energy transfer at large E_i and foresee the other solutions as a potential upgrade path.

In order to estimate the scientific impact of the spectrometer suite at the ESS, the STAP members identified a benchmark suite composed of existing instruments: LET at ISIS (UK) [52], IN5 at ILL (FR) [53], CNCS at SNS (USA) [54], AMATERAS at J-PARC (JPN) [55] and 4SEASONS [56]. We rebuilt the instruments in Vitess 3.2

	τ_P (μs)	τ_M (μs)	Flux $E_i = 100$ meV	Flux Band
HR	130	10	3.7 10^5	7.8 10^6
Opt4loss	80	17	5.8 10^5	1.2 10^7
Fermi	90	11	3.7 10^5	8.9 10^6
Funnel	100	5	1.3 10^5	2.8 10^6

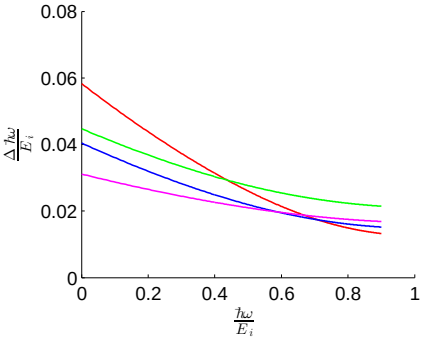

Figure 17: Comparison of the high resolution options. The resolution function is calculated from τ_P, τ_M for $E_i \approx 100$ meV. The shape of the curves remains the same for different E_i, but they are slightly shifted. The elastic resolution matches the results from the virtual experiments.

with the help of the instrument scientists, who provided their simulation models, and reproduced the published simulation results. The J-PARC instruments and LET, which were also built with RRM in mind, have a similar length between 20 and 30 m as for longer instruments at short pulse sources the energy resolution becomes too narrow and the flux too low. Chopper spectrometers are extremely versatile instruments in which energy, flux and resolution can be quite freely tuned. On a long-pulse source, such as the ESS, making the instrument long is a way of maximizing that flexibility. T-REX can be built at a large distance from the moderator increasing the number of pulses per energy interval. In particular in the thermal energy range, which requires comparably short time frames, the intensity is concentrated in a specific spectral range, see Fig. 16. For a comparison with the broad band RRM spectrometers we use the instrument geometry of VOR. The arrows show the pulses generated if the same conditions for the time frame selection as described above are applied. Four pulses out of the large spectral range have E_i above 16 meV. T-REX features 21 pulses in the same range to focus the thermal spectrum. Furthermore it can be tuned to another band to study excitations or quasi-elastic scattering below 100 μeV. The single peak performance is a measure for the quality of the transmission of the optical components including the choppers, see table 4. It shows that T-REX improves the performance already with a single pulse by about an order of magnitude compared to the world best existing instruments. But through the optimization for the RRM, which provides another factor ≥ 10, it can become really a game changer offering novel opportunities for condensed matter research.

[1] Data from CNCS, AMATERAS and 4-SEASONS are normalized to 1 MW source power.

[2] At 20 meV and at 100 meV the peak flux of the J-PARC moderator is significantly larger compared to the ESS moderator. The pulse duration of 12 and 41 μs, respectively, limits the flux at the sample.

Table 4: Comparison of the single pulse performance between T-REX and the reference instruments suggested by the STAP.

				T-REX		
	Incident energy E_i (meV)	Elastic en. res. (μeV)	Flux $(n/s/cm^2)$	Elastic en. res. (μeV)	Flux $(n/s/cm^2)$ single E_i	Flux $(n/s/cm^2)$ full band
LET	5	102	5.6 10^4	88	2.1 10^6	1.6 10^7
IN5	3	104	6.8 10^5	90	6.0 10^6	7.1 10^7
CNCS[1]	3	36	1.6 10^5	42	1.2 10^6	1.6 10^7
AMATERAS[1,2]	3	36	1.5 10^5	42	1.2 10^6	1.6 10^7
	20	200	6.7 10^4	380	3.0 10^5	7.8 10^6
4-SEASONS[1,2]	100	4000	4.0 10^4	4100	3.7 10^5	7.8 10^6

1.2.5.3 T-REX within the ESS Chopper Spectrometer suite

After the last proposal round, the instrument project C-SPEC moved into phase 1 (preliminary design), while VOR and CAMEA moved into phase 0 (preparation for preliminary design). Those instruments address certain aspects of the science case for neutron spectroscopy, but an essential part of it can only be covered by T-REX. This is mainly due to its two unique features: (i) PA over the entire detector area for the entire energy range and (ii) full coverage of the thermal spectrum up to incident energies of 160 meV. C-SPEC has direct view on the cold moderator. The S-shaped guide is used to cut off neutrons of energy above 36 meV, with a reasonable efficiency below 20 meV. The chopper system is adopted from T-REX (published in [35]). No concept for PA is developed. With these specifications, C-SPEC aims at the large user community in soft condensed matter, while T-REX mainly serves the quantum phenomena and materials science community. In particular the strongly correlated electron systems need PA and higher energy transfers than those offered by C-SPEC (see for instance the example on cobaltates, section 1.1.3 of this proposal). But also for the study of magnetic fluctuations of frustrated spin systems in the lower energy range, PA is mostly mandatory (see e.g. the example on the Higgs transition [5]). Moreover, these communities have very different requirements in terms of sample handling, sample environment, data treatment etc., which calls for two instruments to be offered by ESS.

VOR as a rather short chopper spectrometer covers a wavelength band from 1 to 8 Å in RRM. It allows one to perform one shot measurements and is therefore best suited to probe time dependent phenomena, when interesting effects occur over a broad energy band. While VOR offers an overview (typically 10-15 different wavelength pulses over the entire 7Å range), T-REX allows one to focus into certain $(Q, \hbar\omega)$ regions with much enhanced efficiency (up to 23 pulses over the 1.7Å range resolving excitations from 240 μeV to 140 meV using the thermal band). VOR cannot replace a thermal spectrometer, since in RRM only few pulses fall into the thermal energy range (see Fig. 16), while the cold spectrum is somewhat better covered. Since VOR is always working with a very broad wavelength band, it will be extremely difficult to implement PA with all

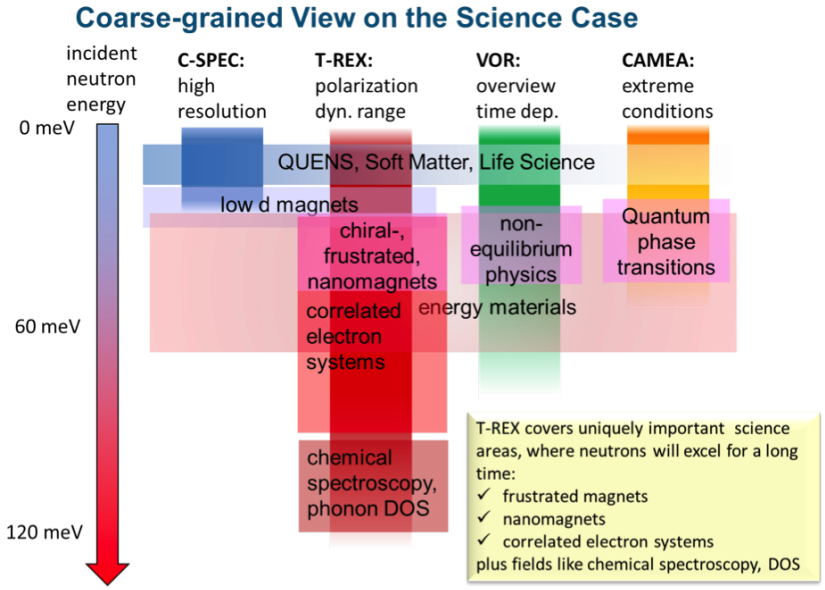

Figure 18: Coarse-graind overview of energy range and scientific applications possible with the different chopper spectrometers proposed for ESS. Naturally this figure cannot capture the full complexity of the respective science cases, but tries to highlight the areas where the different spectrometers do best in a comparison.

techniques known at present.

The comparison between CAMEA and T-REX is the most difficult, as they are different instrument types. Clearly, CAMEA will excel in the intended applications with extreme sample environment. It has limits concerning the coverage of reciprocal space, where the samples have to be realigned to obtain information on the reciprocal space above and below the horizontal plane. Moreover, CAMEA focusses on the cold regime. T-REX will be able to provide much larger Q-space coverage in one go and extend the energy range to higher E_i. Both instruments allow for a PA option, where the one for CAMEA is optimized for the cold neutron regime aimed at.

To summarize, C-SPEC, CAMEA and VOR are good choices for the science cases they were intended for. However, as it is emphasized in Fig. 18, only T-REX can cover efficiently the thermal energy range and provide full PA for the whole detector coverage. The latter is important e.g. (i) to separate magnetic and structural excitations and identify their eigenvectors essential e.g. for frustrated and nanomagnetism, (ii) in research on energy materials to follow the diffusion of light elements other than hydrogen or (iii) in soft matter to separate coherent and incoherent structure factors. The thermal neutron energy range is indispensable for the study of correlated electron materials – a field which regularly produces most visible publications – but also for chemical spectroscopy, phonon density of states etc.

1.2.6 Ternary spectrometer

While the data acquisition, reduction, visualization and analysis are already a considerable task today, it will become even more challenging with the increased data rate of T-REX. The event mode data recording will provide a huge amount of information; we are expecting data rates in the order of hundreds GB per day. Using many different wavelengths can yield either a fast overview of reciprocal space by measuring a few different sample angles, see Fig 19, or provide very redundant data when performing extensive angular scans, which should be used to increase the amount of information extracted from the experiment. Both present now challenges to the data treatment. Linking the data stream to external parameters offers the opportunity to access more

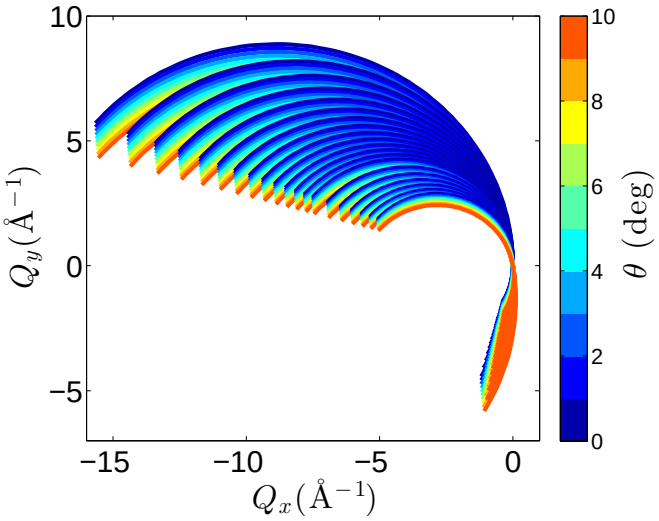

Figure 19: Coverage of the {001} zone in reciprocal space for $\hbar\omega = 0$ meV, when rotating the sample through 10 degrees in 10 steps using the thermal band with a wavelength step $\delta\lambda = 0.07$ Å.

information from the sample, for example using a continuous rotation or pulsed magnetic fields or information from ancillary equipment about the sample state. But it is not only the shear amount of events that has to be treated. Using also the depth information adds another dimension to the data array. Therefore new strategies must be developed, which distinguish detector events that originate from scattering within the sample volume. Furthermore it is important to facilitate the extraction of information from the data. The inclusion of the resolution formalism described in [50] could be used to determine the regions in the recorded reciprocal space, where a dispersion is best resolved in analogy to the planning of experiments at TAS spectrometers. Also the implementation of an UB-matrix formalism for the data space will help to make the data collected at T-REX and the other chopper spectrometers more accessible.

Also the PA increases the complexity of the scattering data. For the latter task we will start with a software project while implementing PA on the spectrometer TOPAS. For the former we propose a concerted effort by all the chopper spectrometer instrument groups, the detector development groups and the data management center.

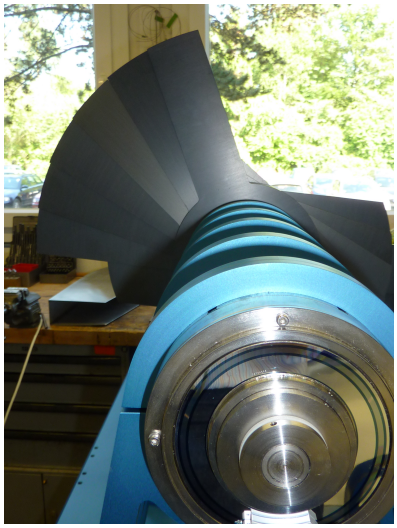

Figure 20: Left: Image of the Fan chopper prototype with removed housing.

1.3 Technical maturity

Aiming to be a world-class chopper spectrometer, it is clear that many components today do not meet the requirements of T-REX or have not been built before. Here we identify the critical components.

1.3.1 Chopper system

The requirements on the P chopper disk pairs represent state-of-the-art chopper technology. In section 1.2.5 we present the resolution and flux figures, which can be reached with the present chopper technology, i.e. the chopper frequencies do not exceed 336 Hz. It should be noted that a progress in technology will immediately increase the opportunities to reach even finer energy resolution. Using carbon fiber disks with imprinted ^{10}B sheets provides a high absorption for thermal and cold neutrons. The choppers will be operated at 110 m and 165 m distance from the moderator without direct view onto the moderator. The reduced solid angle will lead to a significant reduction of the radiation level at the position of the chopper disks. Behind the P chopper the tremendous thermal and cold neutrons flux is reduced as the P chopper limits the spectral range of each pulse. Choppers with magnetic bearings developed by FZJ feature extremely little maintenance requirements. It should be noted that all the choppers are placed far from the moderator, out of the currently foreseen common shielding area. It is a real advantage especially during the commissioning, when a frequent access might be needed. The foreseen increase in the chopper diameter is gentle. Solutions must be found which confirm the reliability of the chopper diagnostics in harsh radiation environment. The same is true for the band-width choppers, which are installed closer to the neutron source. As the chopper frequency is only 14Hz, we think that a robust design can be realized. For the newly developed Fan chopper we have already constructed a prototype, shown

in Fig. 20. Long term and performance tests will be made to assure a reliable operation of the device in 2019/2020. This includes also tests in a neutron environment to collect information about the effect of the radiation field. As the axle of the device is at a distance of 0.5 m from the neutron beam and the neutron beam has a narrow spectral width, we expect only a weak neutron field. There is however no limitation to equip the device with magnetic bearings to avoid possible problems with the lubrication.

1.3.2 Detector

This is the most critical component. The projected detection area is nearly 21 m^2. The following detector concepts have been considered:

- ^{3}He detector tubes: present day technology with the problem of ^{3}He isotope availability,
- Wavelength Shifting Fibers: large area coverage possible for diffractometers (POWGEN at SNS), but problem of after-glow. Therefore excluded for inelastic instruments,
- ^{10}B coated thin film technology: ESS type tested for cold neutrons at ILL Jalousie type from CDT tested for POWTEX (MLZ).

As the latter is rapidly evolving, we have based our cost estimate on this promising detector concept. Furthermore the ESS detector group investigated the case of a ^{10}B thin film detector specifically for a bispectral instrument, which we enclose to this proposal [57].

1.3.3 Neutron guide and shielding

The removable extraction system presented in this proposal is based on the established technique of solid state benders. As it is installed outside the monolith the environment conditions are acceptable for a reliable and enduring operation.

Up to now 165 m long elliptic neutron guides have not been built, hence the excellent transfer estimated in the simulations is not granted. However, simulations on guide imperfections and alignment errors confirm that within the accuracy reached on guides at present the flux is only affected in the percent level.

1.3.4 Polarization Analysis

We have started the commissioning of the wide angle PA at the TOPAS spectrometer, based on the improved PASTIS setup. The magnetic field calculations show that gradients decrease, when the dimensions of the coils are increased. Until start of the operation of T-REX we will gain experience to realize the analyzer. The stages of the polarizers are operated at different JCNS instruments, hence the risk assigned to this component is low due to the specific know-how of the proposers.

2 Costing

The estimate of costing includes the four phases of the instrument construction process, in agreement with the ESS baseline: engineering design and planning (1-2 years), final design (1 year), procurement and installation (2 years) and beam testing and cold commissioning (2 years). The components have been costed on the basis of experience gained at JCNS in various instrument projects, recommendations from the ESS experts, quotations. The costs are divided into the different hardware categories.

Guides are costed on the basis of updated quotations for the supermirror index m, taking into account the total coated area. This price includes installation and mounting, while guide housing and vacuum system costs are specified.

The *shielding* along the guide is estimated to 2.5 m^3/m of guide heavy concrete, costed at 5 k€/m^3. The common shielding for the long instruments sector up to 30m is not taken into account.

Detectors (^{10}B multi-grid technology) are costed as a single unit at 3.1 M€, including the electronics. Here we used the target cost estimate for these detectors of 100 k€/m^2 communicated by the ESS detector group.

While the *sample environment* is important for the mission of T-REX, the costing includes so far only standard components. The actual sample environment dedicated for T-REX will depends on the SE pool to be established at the ESS and on the scientific requirements, which might develop not only until the finalization of the instrument, but also during the operation.

The human resources devoted to the instrument are estimated to 144 person months for scientists, 120 person months for engineers and 144 person months for technicians. The manpower is costed at 10 k€per month in average.

Table 5: Costing table.

Item	Subitem	Cost [k€]
Shutters	heavy shutter	600
	Instrument shutter	100
	IPPS	150
Neutron guide system	Neutron guide	2000
	Bi-spectral extraction bender	200
	vacuum housing	200
	vacuum system	75
	shielding	1800
Choppers	Bandwidth pair	200
	T0	200
	P pair	400
	M pair	400
	Fan	150
Additional optical components	slit system	30
	monitors	55
Polarization and Analysis	SEOP polarizer	50
	Magic PASTIS	80
	guide changer	50
	SM polarizing bender	200
	^{3}He	150
	^{3}He recovery	40
	guide fields	50
	vacuum housing	50
Sample Environment	only standard sample environment assumed	200
Instrument cabin		30
Cabling		150
Secondary Spectrometer	Multigrid ^{10}B detectors including electronics, mechanics	3100
	Vessel	800
	Vacuum system	200
	shielding	500
Consumables		1000
TOTAL HARDWARE		**13210**
20% contingency		2642
Human resources		4080
GRAND TOTAL		**19932**

3 List of abbreviations

- PA: Polarization Analysis
- RIXS: resonant Inelastic X-Rays Scattering
- RRM: Repetition Rate Multiplication
- E_i: Energy of neutrons incident to the sample
- $E = \hbar\omega$: Neutron energy transfer during the scattering process
- $\lambda_{i,f}$: Initial and final neutron wavelength, respectively
- P and M choppers: Pulse shaping and Monochromating choppers, respectively

References

[1] Enclosure: 'users.pdf'

[2] M. Loire *et al.*, *Parity-broken chiral spin dynamics in* $Ba_3NbFe_3Si_2O_{14}$, Phys. Rev. Lett. 106, 207201 (2011)

[3] C. Zhang *et al.*, *Magnetic anisotropy in hole-doped superconducting* $Ba_{0.67}K_{0.33}Fe_2As_2$ *probed by polarized inelastic neutron scattering*, Phys. Rev. B 87, 081101(R) (2013)

[4] J. M. Tranquada *et al.*, *Quantum magnetic excitations from stripes in copper oxide superconductors*, Nature 429, 534 (2004)

[5] L.-J. Chang *et al.*, *Higgs transition from a magnetic Coulomb liquid to a ferromagnet in* $Yb_2Ti_2O_7$, Nat. Commun. 3, 992 (2012)

[6] M. L. Baker *et al.*, *Spin dynamics of molecular nanomagnets unravelled at atomic scale by four-dimensional inelastic neutron scattering*, Nature Physics 8, 906 (2012)

[7] Y. Drees *et al.*, *Hour-glass magnetic spectrum in a stripeless insulating transition metal oxide*, Nat. Commun. 4, 2449 (2013)

[8] W. Paulus *et al.*, *Lattice dynamics to trigger low temperature oxygen mobility in solid oxide ion conductors*, JACS 130, 16080 (2008)

[9] J. L. C. Rowsell *et al.*, *Characterization of* H_2 *binding sites in prototypical metalorganic frameworks by inelastic neutron scattering*, JACS 127, 14904 (2005)

[10] A. M. Stadler *et al.*, *Cytoplasmic water and hydration layer dynamics in human red blood cells*, JACS 130, 16852 (2008)

[11] K. Henzler-Wildman *et al.*, *Dynamic personalities of proteins*, Nature 450, 964 (2007)

[12] M. Schumacher *et al.*, *Ion channels: an open and shut case*, Nature 417, 501 (2002)

[13] M. Perutz *et al.*, *The stereochemical mechanism of the cooperative effects in hemoglobin revisited*, Annu. Rev. Biophys. Biomol. Struct. 27, 1 (1998)

[14] S. J. Benkovic *et al.*, *A perspective on enzyme catalysis*, Science 301, 1196 (2003)

[15] I. A. Balabin *et al.*, *Dynamically controlled protein tunneling paths in photosynthetic reaction centers*, Science 290, 114 (2000)

[16] D. A. Turton *et al.*, *Terahertz underdamped vibrational motion governs protein-ligand binding in solution*, Nat. Comm. 5, 3999 (2014)

[17] M. T. Cicerone *et al.*, *β-Relaxation governs protein stability in sugar-glass matrices*, Soft Matter 8, 2983 (2012)

[18] P. Kumar *et al.*, *The Boson peak in supercooled water*, Nature Sci. Rep. 3, 1980 (2013)

[19] G. Acbas *et al.*, *Optical measurements of long-range protein vibrations*, Nat. Comm. 5, 3076 (2014)

[20] L. van Eijck *et al.*, *Direct Determination of the Base-Pair Force Constant of DNA from the Acoustic Phonon Dispersion of the Double Helix*, Phys. Rev. Lett. 107, 088102 (2011)

[21] M. C. Rheinstadter *et al.*,*Collective dynamics of lipid membranes studied by inelastic neutron scattering*, Phys. Rev. Lett. 93, 108107 (2004)

[22] M. Longo *et al.*, *Terahertz Dynamics in Human Cells and Their Chromatin*, J. Phys. Chem. Lett. 5, 2177 (2014)

[23] A. W. Perriman *et al.*, *Reversible dioxygen binding in solvent-free liquid myoglobin*, Nature Chemistry, 2, 622 (2010)

[24] F.-X. Gallat *et al.*, *A polymer surfactant corona dynamically replaces water in solvent-free protein liquids and ensures macromolecular flexibility and activity*, JACS, 134, 13168 (2012)

[25] Enclosure: 'B-REX.pdf'

[26] L. Orsingher *et al.*, *High-frequency dynamics of vitreous* $GeSe_2$, Phys. Rev. B **82**, 115201 (2010).

[27] S. Hosokawa, M. Inui, Y. Kajihara, K. Matsuda, T. Ichitsubo, W.C. Pilgrim, H. Sinn, L.E. González, D.J. González, S. Tsutsui, and A.Q.R. Baron, Phys. Rev. Lett. **102**, 105502 (2009).

[28] V.M. Giordano and G. Monaco, Proc. Natl. Acad. Sci. U.S.A. **107**, 2198521989 (2010).

[29] M. Zanatta *et al.*, *Collective ion dynamics in liquid zinc: Evidence for complex dynamics in a non-free electron liquid metal*, Phys. Rev. Lett., accepted.

[30] M. Zanatta *et al.*, *Inelastic Neutron Scattering investigation in glassy* $SiSe_2$*: complex dynamics at the atomic scale*, J. Phys. Chem. Lett. 4, 1143 (2013)

[31] K. Niss *et al.*, *Influence of pressure on the Boson Peak: stronger than elastic medium transformation*, Phys. Rev. Lett. 99, 055502 (2007)

[32] G. Baldi *et al.*, *Connection between Boson Peak and elastic properties in silicate glasses*, Phys. Rev. Lett. 102, 195502 (2009)

[33] B. Rufflé *et al.*, *Scaling the temperature-dependent Boson Peak of vitreous silica with the high-frequency bulk modulus derived from Brillouin Scattering data*, Phys. Rev. Lett. 104, 067402 (2010)

[34] ERC Project CHRONOS – A geochemical clock to measure timescales of volcanic eruptions, URL: http://pvrg.unipg.it/research-projects/

[35] J. Voigt *et al.*, *Chopper layout for spectrometers at long pulse neutron sources*, Nucl. Instr. and Meth. in Phys. Res. A 741, 26 (2014)

[36] Jones T.J.L., Davidson I, Boland B.C., Bowden Z.A., Taylor A.D., Proceedings of the 9th Meeting of the International Collaboration on Advanced Neutron Sources, Swiss Institute for Nuclear Research 1987, p.529 (ISBN3-907998-01-4)

[37] McQueeney R.J. and Robinson R.A. 2003 Neutron News 14 36

[38] Itoh S, Yokoo T, Satoh S, Yano S, Kawana D, Suzuki J and Sato T 2011 Nucl. Instr. and Meth. in Phys. Res. A 631 9097

[39] Itoh S, Ueno K, Ohkubo R, Sagehashi H, Funahashi Y and Yokoo T 2012 Nucl. Instr. and Meth. in Phys. Res. A 661 86-92

[40] Enclosure: 'cp_Fermi_disc.pdf'

[41] Enclosure: 'Funnel.pdf'

[42] Enclosure: 'T-REX_transport_system.pdf'

[43] Enclosure: 'T0choppers.pdf'

[44] K.H. Andersen, personal communication

[45] L. D. Cussen, *Advanced conic section guide design for ESSEX*, Oral contribution at ESS simulators meeting 15.08.2012, (2012) URL: http://www.essworkshop.org/Meetings/20120815_Lund/NewGuideForLund1.ppt

[46] C. Zendler *et al.*, *An improved elliptic guide concept for a homogeneous neutron beam without direct line of sight*, Nucl. Instr. and Meth. in Phys. Res. A 746, 39 (2014)

[47] E. Babcock *et al.*, *Considerations on quality factors from super mirrors and ^{3}He spin filters for polarization analyzers on wide Q-range instrumentation*, J. Phys. Soc. Jpn. 82 SA030 (2013)

[48] E. Babcock *et al.*, *In-situ SEOP polarizer and initial tests on a high flux neutron beam*, Physica B: Condensed Matter 404, 2655 (2009)

[49] J. Voigt *et al.*, *Polarization analysis for the thermal chopper spectrometer TOPAS*, accepted for publication EPJ Web of Conferences

[50] N. Violini *et al.*, *A method to compute the covariance matrix of wavevector-energy transfer for neutron time-of-flight spectrometers*, Nucl. Instr. and Met. in Phys. Res. A 736, 31 (2014)

[51] A. Vickery *et al.*, *A Monte Carlo simulation of neutron instrument resolution functions*, J. Phys. Soc. Jpn. 82, SA037 (2013)

[52] R. I. Bewley *et al.*, *LET, a cold neutron multi-disk chopper spectrometer at ISIS*, Nucl. Instr. and Met. in Phys. Res. A 637, 128 (2011)

[53] J. Ollivier *et al.*, *IN5 cold neutron time-of-flight spectrometer, prepared to tackle single crystal spectroscopy*, J. Phys. Soc. Jpn. 80, SB003 (2011)

[54] G. Ehlers *et al.*, *The new cold neutron chopper spectrometer at the Spallation Neutron Source: Design and performance*, Rev. of Sci. Instr. 82, 085108 (2011)

[55] K. Nakajima *et al.*, *AMATERAS: a cold-neutron disk chopper spectrometer*, J. Phys. Soc. Jpn. 80 SB028 (2011)

[56] R. Kajimoto *et al.*, *The Fermi chopper spectrometer 4SEASONS at J-PARC*, J. Phys. Soc. Jpn. 80, SB025 (2011)

[57] Enclosure: A. Khaplanov, *On detectors for the chopper spectrometer proposal T-REX*, 'trex_detector.pdf'

Summary of main changes applied to the version from 15^{th} January 2015

- STAP
  - *The only area of the science case which appeared weak was that concerning disordered materials and liquids; specifically the suggestion to introduce collimators to transform T-REX into a Brillouin spectrometer appears ill thought out, and it is unlikely that the 3m sample-detector distance on TREX would be compatible with Brillouin scattering requirements.*

    We revised the section. While this is not the central application for T-REX it shows now, which challenges as of today can be addressed excellently by T-REX. We requested the chairman of the STAP to further clarify the point and following this discussion we decided to add an enclosure to further detail the instrumental requirements: minimum angle, collimation, Q and energy resolution and a comparison between the performance of T-REX and BRISP that should help to clarify what science can not now be done on BRISP, but which could be done on T-REX. From this analysis it results that the option of a collimator (0.5°) can be useful to perform Brillouin neutron scattering in optimal conditions using T-REX, while even without it the core of this scientific applications can be covered.
  - *The only minor criticism the panel has is with regard to the calculated energy resolution at higher neutron energies. To achieve a reasonable resolution (which the STAP estimates should be no larger than 5% of Ei) T-REX uses a second opening in the M chopper which is smaller than the guide opening resulting in a big hit in neutron flux. The proposal team do present an intermediate solution where the full opening of the M chopper is kept and one reduces the moderator component with the P chopper to improve the resolution, particularly away from the elastic line. However the panel feels that it is important to optimise the flux at high energies with a reasonable resolution. To this end, the panel recommends the T-REX proposal team compare their current instrument with an optimised 'splitter' option and also again with a Fermi chopper option. Perhaps both a Fermi and disk chopper are needed, with the Fermi moving into position for the high-resolution applications.*

    The first point we addressed by investigating different means to improve the energy resolution in the thermal energy range. The solution presented in the former version of the proposal with a 2.5° chopper window provides the required energy energy resolution $< 5\%$ also with the reduced chopper speed (336 Hz) even for the highest neutron energy. The disc chopper window covers 60% of the neutron guide, resulting in an additional flux penalty on top of quadratic scaling due to the finer energy resolution. This penalty is reduced for the highest energies, where the center of guide is better illuminated than the borders.

Additionally we investigate the solution by replacing the final M-chopper pair by a Fermi chopper and a disc chopper. The disc chopper is only needed to avoid any transmission, when the curved Fermi chopper is in 180° position. Additionally the P-chopper discs require three equally distributed windows to match the repetition rate of the Fermi chopper.

As a third alternative we study a funnel solution, i.e. we replace the final section of the neutron guide. The solution is different from the LET funnel, as the long focusing guide does not allow the symmetric focusing/defocusing with respct to the center of the funnel. In order to avoid strong correlations between the divergence and the position, the window width is only 7 mm, while the center of the two windows are displaced by ≈ 14 mm. The resulting energy resolution is excellent, but the flux is lower as expected from the transmission of the funnel. The carefull investigation of this issue revealed, that the intensity distribution in front of the chopper is not homogeneous but increases towards the inner guide wall. As the counter rotating choppers open from the center of the individual neutron windows this leads to an additional flux reduction. More flexibility might be added to this solution by re-considering the entire focusing section of the neutron guide, a task, which we could envisage for the phase 1 of construction.

– *The panel did feel that 406 Hz choppers with 70 cm diameter were a big risk. The fastest 70 cm choppers running at present are 336 Hz choppers at J-Parc. They had intended to build 400 Hz choppers but failed. With the current design if the choppers don't reach 406 Hz, which is quite likely, then the resolution at higher energies would be even worse. This emphasises the above point that they should look very hard at other possible options.*

  We completely agree with the STAP on the latter and have therefore re-run the virtual experiments with a maximum chopper frequency of 336 Hz. Accordingly fig. 16 has been updated and re-formatted and the numbers in table 4 have been changed accordingly for the settings, which are affected by this change.

- **Ken Andersen: internal review of T-REX**

  NOTE: the page and line numbers are referred to the January version, therefore in the present version a mismatch is expected.

  – *Executive Summary page ii, Figure caption: this is usually known as a time-distance diagram, not pathtime- of-flight.*

    The suggested correction has been applied.

  – *page 19, bullet point 2: a detector cell size of 25x25mm2 is given. Such an area is usually interpreted as the lateral dimensions. The lateral dimensions do not influence the energy resolution (to a first approximation). The radial dimension does. Rephrase.*

The *cell size* is replaced by voxel (volumetric pixel), which gives 22 mm radial position uncertainty (FWHM).

– *page 21, paragraph below bullet points, line 6-7: reference is made to the spatial resolution of the detector affecting the energy resolution. The spatial resolution usually refers to the lateral directions (perpendicular to the beam). Same issue as the point above.*

Spatial resolution is replaced by *radial resolution*.

– *page 22, table 2: My first reading of the table gives the impression that each line corresponds to a single chopper disk. The P1 and P2 lines therefore describe a pair of counter-rotating choppers. Later in the text (page 23) it becomes a bit more confusing, and it is no longer clear to me that perhaps P1 might be a counter-rotating chopper pair and P2 might be another pair. It would be very helpful to make a clear statement in the caption of the table that each line corresponds to a single disk (or not, if that is the case).*

We have added an explanation to the table caption: The P1 disc and the P2 disc have one high resolution pair of windows (22 deg) and one pair of high flux windows (36 deg). The M1 and the M2 discs have a high resolution window (2.5 deg) and a high flux window (4.3 deg.).

– *page 22, bullet point below table 2: it is not clear to me that the T0 chopper is actually needed. Some argumentation about the need for it would be appropriate.*

The request is addressed in that a justification for the use of T0 chopper is provided: it is a common practice and the test on HRC at J-Parc is convincingly showing a reduction of noise for thermal neutrons. Respective references are added.

– *page 22, first paragraph of section 1.2.1.1: the driver given for choosing the positions of the P and M chopper is given as their frequencies (equation 1). It should also be stated that the resulting position of the P chopper is an important consideration for maintenance access. These are very high speed choppers, which need regular access for both planned and unplanned maintenance. If at all possible, they should be placed outside direct line-of-sight (LOS) of the guide entrance, to enable access when the proton beam is on. If they cannot be placed out of LOS, then it may be necessary to add a heavy shutter upstream to enable such access. The T0 chopper does not allow this, as it cannot be a radiation safety device.*

The light shutter has been replaced by a heavy shutter in the costing table.

– *page 25, section 1.2.2.1, lines 9-12: It is not clear from the description if the (polarising or non-polarising) bender will be designed to transmit thermal neutrons and thus act as a bispectral switch. It is implied from the energy ranges that it does not need to be transparent to allow neutrons from the thermal source to pass through, but this is never explicitly stated. It sounds*

like it the Si wafers might be coated with Gd on top of the supermirrors. Please clarify.

The bender (polarising and non-polarising) is not designed to transmit thermal neutrons, and it is confirmed that the transmission is low, as it is now shown in figure 10 b), which has been modified. In the simulations the substrate is Si. A statement is added at that position to clarify the issue. Currently the details of construction are under consideration, therefore it might well be that the final realization will foresee Gd coating on top of the s.m. .

– *page 26, bullet points 1 and 2: the first bullet point describes a kink in the guide at the P-chopper position which is at 110 m. The second bullet point describes an alternative guide with an increased kink angle, but says the kink should be at 30 m from the moderator. That position is inconsistent with the description in the first bullet point. It also states that the T0 chopper is at 30 m, while table 2 places it at 99 m. Clarify.*

The situation is better clarified in figure 1.a) in the enclosure 'T-REX transport system', thus the reference to the document is added before the bullet points. The bullet points are changed to better clarify that in the second layout the kink is at the same position, but the kink angle is increased such that the LOS is broken at 30 m. Therefore the T0 chopper might have been placed upstream that position. By combining kink and T0 the LOS is broken and the prompt pulse is suppressed such that the background level can be lowered significantly.

– *page 27, line 1: it is stated that the curved guide reaches high values of brilliance transfer (BT) at 100 meV. From Fig. 11b it is shown that the BT for this guide configuration is above 70% for all energies up to about 200 meV (not easy to tell from the logarithmic x-axis). I think 70% is already pretty good.*

The comment is appreciated and the sentence is modified according to the observation in order to stress that the BT is 70% already at 200 meV.

– *page 27, section 1.2.3.1, line 2: it is stated that 1% elastic energy resolution can be achieved with the 3 m sample-detector distance, assuming that the total flight path uncertainty is less than 20 mm. Is that a good assumption? Does the total flight path uncertainty include the flight path uncertainty starting from the moderator or only from the sample? A little bit of explanation is needed here.*

Something was missing here: the statement has been changed to clarify that 20mm is the detector contribution. Anyhow we take the occasion to point out that in reference [49] the energy resolution is derived in first order ap-

proximation

$$\sigma^2_{\hbar\omega} = m^2 \left\{ \left(A_e + B_e \frac{\hat{L}_{MS}}{\hat{L}_{PM}} \right)^2 \tau_P^2 + B_e^2 \tau_D^2 + \left[\left(A_e + B_e \frac{\hat{L}_{MS}}{\hat{L}_{PM}} \right)^2 + B_e^2 \right] \tau_M^2 + \right.$$
$$\left. + \frac{1}{\hat{v}} \left(A_e + B_e \frac{\hat{L}_{MS}}{\hat{L}_{PM}} \right)^2 \sigma^2_{L_{PM}} + \left(\frac{B_e}{\hat{v}} \right)^2 \sigma^2_{L_{MS}} + \left(\frac{B_e}{\hat{v}'} \right)^2 \sigma^2_{L_{SD}} \right\}, \tag{5}$$

where we used the definitions $A_e = \hat{v}^3/\hat{L}_{PM}$ and $B_e = \hat{v}'^3/\hat{L}_{SD}$. The **moderator contribution** is accounted for in $\sigma^2_{L_{PM}}$. It turns out that, for elastic scattering ($v = v'$) it is weighted with a fraction $(L_{SD} + L_{MS})/L_{PM}$ of the sample and detector contributions. Since for T-REX $L_{PM} = 55m$, $L_{SD} = 3m$ and $L_{MS} = 1.3m$, it can be neglected.

– *page 28, line 1: the asymmetric detector layout does not really give access to larger Q or Qz (Qz needs to be defined, by the way). That is determined by the maximum scattering angles (in and out of plane), rather than the fact that the detector layout is asymmetric. The asymmetry of the detector is good for maximising the Q-range for a given detector area. Rephrase.*

  The sentence is changed according to the suggested rephrasing. Q_z was deleted for sake of simplicity.

– *page 30, section 1.2.4, line 4: a statement is made about the narrow bandwidth. When using thermal neutrons, the bandwidth is far from narrow.*

  The sentence has been corrected: the band in this case is in wavelength. It is specified and should not be misleading in the present way.

– *page 30, section 1.2.4.1, paragraph 2, line 4: it is stated that a continuously-pumped 3He cell will be installed downstream of the P chopper. It is essential that this polariser is accessible when the proton beam is on. It therefore needs to be either outside LOS with a secondary shutter in front of it, or have a primary shutter installed upstream. This needs to be stated. It will require regular access, both planned and unplanned.*

  We have changed 'downstream the P chopper' to 'just upstream the M chopper' and added a sentence to express that this position has access, when the proton beam is on.

– *page 31, fig. 13 left: the polarisation level in the cold-neutron range is about 93%. It could probably be improved to 96-97% without too much difficulty.*

– *page 31, section 1.2.4.2, paragraph 2, lines 1-2: wide-angle PA is also being developed at the ILL.*

  The ILL is added to the list.

- *page 34, section 1.2.5.2, lines 5-6 from bottom: different energy transfer ranges are proposed to be covered for cold and thermal neutrons: thermal: energy transfer < 0.80xEi cold: energy transfer < 0.56xEi why the difference? I understand the 0.80xEi is about right in order to cover a good inelastic range. Why change the criterion for cold neutrons? Please explain.*

  Both criteria are common practise at continuous neutron sources for thermal and cold neutrons, the 'thermal' criterion is used, when the energy region of interest is large energy transfer, while the 'cold' criterion is used when mainly the quasielastic scattering is addressed. We added some explanatory sentences.

- *page 36, table 4: impressive - both the result and the level of effort which must have gone into making flux calculations of all these instruments.*

  We are thankful to KA for the comment.

- *page 36, paragraph 1: the basic issues are that chopper spectrometers are extremely versatile instruments in which energy, flux and resolution can be quite freely tuned. On a long-pulse source, such as the ESS, making the instrument long is a way of maximizing that flexibility.*

  The sentence is added (page 35).

- *Section 1.2.5.3: A good, balanced consideration of the ESS (low-resolution) spectroscopy suite.*

  We are thankful to KA for the comment.

- *page 38, paragraph 1, last sentence: it is stated that the thermal energy range is indispensable for density of states measurements. That is not very apparent in the science case section. If this is an important point, it should be given more prominence in the science case.*

  The section 1.1.6 has been reviewed to make clear, how this field will benefit from T-REX and in particular from the performance in the thermal energy range. While this field is not the main focus of the T-REX science, at this time T-REX will be the only instrument at the ESS to study phonon spectra well above 50 meV.

- *page 40, paragraph 1: there is a good consideration of maintenance issues related to choppers. It is important to involve the ESS chopper group in these considerations.*

  We are thankful to KA for the comment. We are sure that there will be occasion for discussion of this topic in future.

- *page 45: all references after number 33 are missing.*

  The version of the proposal in the indico page of spectroscopy STAP contains the references. It might have been a problem with visualization.

- Arno Hiess, Scientific Activities Division

- *The study functional materials in the phonon range outside of single crystal research (there are other instruments at ESS AND it will be hard to do frequent sample changes if the sample area is as complicated as the proposal sounds). Sample environment ideas:*
- *Want standard sample environment seems like a cryostat to mK range is part of the package.*
- *Magnet to 14T necessary for the proposed experiments, but not included in the budget*
- *10GPa pressure with Paris-Edinburgh cell and here the cell could be part of the standard sample environment allocation and additional costs (such as pressure generator) might be part of a shared pool system*
- *Illumination of sample by laser light not calculated, might also require larger cooling capacity than standard cryostat*
- *Gas loading (under pressure???) not considered in sample environment (gas handling cell?)*
- *Instrument will rarely use general lab space for sample preparation or possibly sample treatment.*

We added a remark about the completeness of the SE budget to the 'Costing' section.

- Jonathan Taylor, DMSC
  - *400Hz disc is a big risk and the thermal component of the science case relies on it to get reasonable resolution. i.e. if it doesn't run the high energy configuration will have poor resolution.*

    In the current version of the proposal the max frequency considered is 336Hz, nowadays it is possible at existing facilities.
  - *Removable bender looks complex, PA is a key aspect of the proposal which is good to see but the costing and complexity i think are under estimated. The v polariser configuration gives a longrun 120m to transport polarisation.*

    The long guide field seems to be not too complicated as the field strength for the guide field keeping the cold neutron polarization is comparably low. The inclusion of a third stage on the lift does not seem to be an additional complication of the device for the cold beam extraction. We agree, that the operation in the harsh conditions close to the monolith is challenging for any device, but we don't consider it more difficult than the operation of pulse shaping choppers at this position.

    We would like to emphasize that the realization of multispectral instruments such as VOR and TREX offer unprecedented opportunities for neutron spectroscopy. This can be seen by the trend to increase the energy range of cold TAS instruments towards high energies. TREX offers an optimized thermal

performance, but also the cold performance is reduced only by 30 to 20 % compared to a fully optimized cold instrument. For the case of cold polarized neutrons, TREX closes also this gap.

- Anton Khaplanov, Richard Hall-Wilton, Detectors
  - *It should be noted that information on the detector solution using Multi-Grid and comparison to He3 and a dedicated optimisation (to the parameters provided by the proposers) was provided to the proposers, however, none of this information was included in the proposal. This information is attached to this review. Information addressing efficiency, gamma rejection requirements was available but was not used in the proposal.*

    We enclose the report, which has been provided by the ESS detector group and refer to it in the 'Technical maturity' section.
  - *70% efficiency at 1 Åexpectation is stated, however this is not realistic with any of the proposed technologies (50-55% is). This was described in the information sent to the proposers. 70% may be the efficiency in the centre of a He3 tube filled with an unaffordable amount of He3, but does not represent a realistic situation (round tubes, dead areas, etc).*

    The figures in the report differ from the figures that our design for the TOPAS spectrometer reach: our 10 bar tubes have 0.5 mm thickness, we have 1 mm spacing between the tubes and 2mm between tubes at different detector boxes, which combine 16 tubes. If these figures are used for the calculation in the report, the overall efficiency of 70 % at 1 Å is reached.
  - *End of 1.2.3.1: discussion on background suppression via depth of interaction is conceptually incorrect. Depth profiles may be used for analysing energy distribution of neutrons. This may be compared with expectation for consistency, however it is impossible to discriminate bad events from good.*

    It is true, that it is not possible to discriminate good from bad events. But if you compare the patterns, one should find an exponential decreasing probability on a straight line. Scattering from the sample and the close environment should fall onto a radial line, while scattering from a position sufficiently distinct from the sample position should result in a pattern on a non-radial line. We have changed the sentence to clarify that we are not distinguishing individual absorption events but analyze the pattern resulting from the direction and the wavelength of the scattered neutron beam.
  - *More details on shielding and background requirements would be helpful. These are key issues for the instrument.*

    This is a task that we intend to work out in phase 1.
  - *Beam Monitors not included in costs.*

    Monitors are costed 55 k€ in the item 'Additional optical components'.

- Choppers group
  - *The level of performance required for the monochromating choppers (406Hz @ 700mm) is at the cutting edge of available equipment. The complexity of the system outlined in the base proposal is high. The FAN chopper is currently at the proof of concept phase and requires further development to demonstrate long-term operability.*

    As in the previous comment: in the current version of the proposal we report the performance for a maximum frequency of 336Hz, which is state of the art. As a result, we increase the flux of the instrument on the cost of the best energy resolution reachable. The new version contains also solutions to reach better resolution with state-of-the-art technology. In section 1.3.1. we rephrase the paragraph to clarify that an excellent performance of the instrument is reached using the chopper speed available today. Furthermore we add a figure and a table to section 1.2.5 showing the resolution available for different options using chopper technology available today.
  - *Significant instrument specific development is required especially with regards to improving the serviceability, availability and long-term operability of the prototype FAN chopper. Development maybe required to ensure the long term reliability of the 406Hz monochromating choppers.*

    We will continue the development of the Fan chopper with long term operation tests and test at neutron facilities. By the time of installation we expect to have a very good understanding of the operation characteristics of the device. These tests are mentioned in section 1.3.1
  - *The fan chopper system is not currently compatible with the serviceability requirements of ESS. An alternative to the FAN chopper could be the use of disk choppers, albeit with a slight loss of operational flexibility, as employed on another instrument proposal.*

Instrument requirements for the measurement of collective excitations in disordered systems

April 2015

Disordered systems and liquids support the propagation of isotropic elastic waves in the macroscopic regime, i.e. when the wavelength is much larger than the typical interatomic spacing. In this limit, network details can be neglected and disordered materials behave similarly to powder crystals. On the contrary, when the wavelength scale is reduced to a few nanometers, the continuum approximation breaks down and sound waves evolve toward a more complex pattern of vibrations, characterized by strongly-damped phonon-like modes. The study of these collective excitations requires measurements of the $S(Q,\omega)$ at energy transfers up to some tens of meV and at low exchanged wavevectors (from about 1.5 Å^{-}1 down to 0.1 Å^{-}1). Such conditions can be technically achieved by the simultaneous use of incident thermal energies and small-angle detection (down to $\sim 1°$), which requires a bi-dimensional collimation of the incident beam not larger than 0.5° on both horizontal and vertical directions. Besides some inelastic X-ray scattering instruments at major synchrotron facilities, very few neutron spectrometers worldwide can efficiently access the necessary (Q,ω) region. Examples are BRISP at ILL and HRC at J-PARC, whereas a similar inverse spectrometer has been recently proposed for TS1 at SNS [1].

Thanks to the available thermal energies and the good detector coverage in the forward scattering region, T-REX is well suited for accessing the dynamical range of interest. In addition, the example highlighted in the main text of the proposal [2] shows that the implementation of RRM on T-REX can mark an important advancement with respect to existing spectrometers, because it provides a more efficient and easier-to-use tool to map the complex patterns of collective excitations in disordered systems.

In fact the energy resolution of T-REX is fairly comparable to the one of BRISP at the same incident energy: for instance BRISP has 2.9% elastic energy resolution at 83.6 meV, while T-REX can be tuned to an elastic energy resolution of 3.3% at 81.9 meV. At the latter incident energy, the divergence transported by the neutron guide system of T-REX provides Q-resolution and minimum scattering angle already adequate to reach Q-values down to nearly 0.1 Å^{-1} (see Figs. 1 and 2). It is important to stress here that the primary beam divergence largely dominates the Q-resolution. Indeed the chosen detector pixel size and sample-detector distance bring only minor contributions to the Q-resolution.

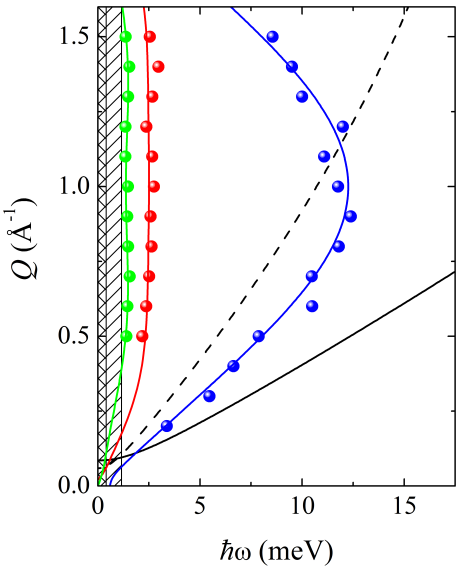

Figure 1: Kinematic range of T-REX at 1 Å (black solid line) and 2 Å (black dashed line). The elastic energy resolution (FWHM) is represented by the shadowed areas. The dispersion curves measured for $SiSe_2$ are also shown, to highlight that the required dynamical range, in particular the low-Q inelastic region, is actually accessible.

At longer wavelengths, the divergence provided by the guide gets larger and larger (1.5° at 2 Å), causing a broader image of the direct beam at the detector, thus a narrower incident beam divergence is required to reach angles down to 1° and extend the lowest accessible Q down to 0.1 $Å^{-1}$ (see Figure2). This can be achieved by employing a collimation system, when needed by the users. We stress that the optional use of collimators does not compromise the performance or any of the instrument capabilities for which T-REX is optimized.

By improving the collimation in the vertical and horizontal directions, the intensity decreases quadratically. Considering the simulated flux at the sample of T-REX, without collimation a gain factor from 20 to 50 with respect to BRISP is expected for a single E_i (on BRISP the flux at the sample is 1.2 10^4 and 0.8 10^4 n/s/cm^2 at 1 Å and 2 Å , respectively, with nearly 3% energy resolution). Therefore, despite the insertion of collimators, T-REX will still outperform BRISP by at least one order of magnitude in flux per wavelength. RRM operation will further improve the gain factor.

As the $S(Q)$ of disordered systems is intrinsically very small in the low-Q region of interest, the scattering signal from collective modes is always very weak. As a consequence, even on dedicated instruments like BRISP, measuring times usually fall in scale of days for a single thermodynamic point. This definitely hampers the study of collective excitations in many systems where a survey of

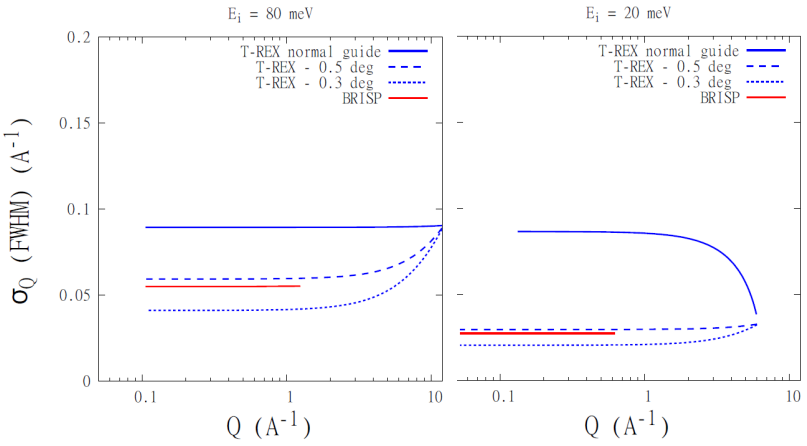

Figure 2: Q resolution (FWHM) calculated in elastic scattering condition for T-REX and BRISP. The improved collimation enables to reach lower detection angles and Q values. With a collimation of 0.5° the performance of BRISP is matched.

their behaviour on a large portion of the phase diagram is of great interest. A typical longstanding example is liquid Rb, where the high temperatures and pressures necessary to keep the liquid metal in the thermodynamic conditions of interest are technically incompatible with long acquisition times. The intensity gain factor promised by T-REX will therefore allow important steps forward.

In conclusion, although collective modes in disordered systems will probably not be its primary scientific target, T-REX has the potential to provide unprecedented insights in this field.

References

[1] J. K. Zhao et al., IBIS: an inverse geometry Brillouin inelastic neutron spectrometer for the SNS, Rev. Sci. Instrum. **84**, 025113 (2013).

[2] M. Zanatta et al., Inelastic Neutron Scattering investigation in glassy $SiSe_2$: complex dynamics at the atomic scale, J. Phys. Chem. Lett. **4**, 1143 (2013)

Report on simulation of the LET funnel system

N. Violini, J. Voigt

August 28, 2013

The present report is devoted to describe the investigation of the performance of the LET guide concept, with a specific focus on the funnel system. We received the model of the LET spectrometer from Rob Bewley. It is a McStas instrument file, that we translated into a Vitess pipeline. The Fig.(1) is taken from NIMA 637 (2011) 128-134. It shows the guide layout. Three reference points are considered along the neutron guide that are important for the following considerations and for understanding of our results. The point A is in front of the moderator behind the beam-port, B is at the end of the straight guide, behind the funnel and the point C is at the sample position. In order to investigate the performance of the guide itself, the simulated model does not include the choppers.

We used two different figures of merit. The first is the transmission. It is evaluated placing identical wavelength sensitive monitors at the positions A, B and C. The ratio between the intensities is shown in Fig.(2). The straight section of the neutron transports larger divergence with increasing wavelength. The divergence at position A is by far larger than the divergence that can be digested at the sample position. Moreover the transmission at the point C is evaluated with respect to the point B. Reasonable agreement is found between the McStas and the Vitess model, thus showing that the model is well reproduced in Vitess. The deviations are due to a slightly different representation of the reflectivity curves of super-mirrors in the two packages. The transmission decreases increasing the wavelength. As the calculation takes as reference the intensity in B, this behaviour is due to the trend of the transmission in B evaluated with respect to A. Increasing the wavelength the straight section transmits a larger divergence that requires higher wavevector transfer, thus the reflections occur with a lower reflectivity.

The second figure of merit we used is the brilliance transfer within a phase space region of interest defined at the sample. The brilliance monitors measure the integral intensity within user-defined limits in position and divergence as a function of neutron wavelength (or other variables). It is basically a wavelength sensitive monitor with the addition of limits both in position and divergence, thus it restricts the measurement of intensity to the desired phase space region. We stress that in the case the brilliance is evaluated at the point A in a homogeneously illuminated region, it is a direct measurement of the phase space density provided by the moderator. Therefore the evaluation of this quantity at differ-

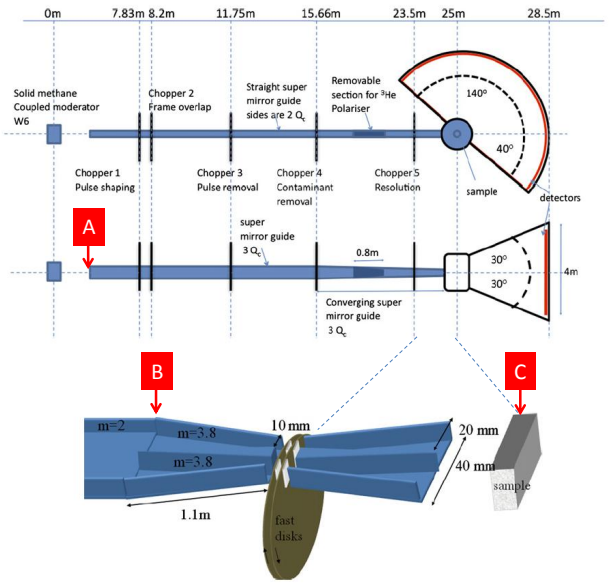

Figure 1: LET guide layout taken from NIMA 637 (2011) 128134. In the simulations monitors placed at the positions A, B and C are used to calculate the brilliance transfer and the transmission.

ent positions along the guide must fulfill the Liouville's theorem. We evaluated the brilliance transfer at the position C with respect to A and B and at the position B with respect to A. The limits of integration are -2cm to +2cm both in vertical and horizontal direction and -0.25° to +0.25° horizontal divergence, -0.5° to +0.5° vertical divergence. Fig.s(3, 4) show 2D position and divergence monitors placed at the positions A, B and C within a $\Delta\lambda = 0.1\mathring{A}$ around $1\mathring{A}$ and $8\mathring{A}$ respectively. It is seen that a full illumination of the box is guaranteed at A, thus allowing to take this point as a reference for the computation of the brilliance transfer. The results are shown in Fig.(2).

The different behaviour of the brilliance transfer in comparison to the transmission can be understood from the 2D acceptance diagrams taken at the sample position. They are shown in Fig.s(5,6,7). Indeed the 2D position and divergence monitors, in Fig.(5) and Fig.(6) respectively, reveal an almost homogeneous distribution within the region of interest, which is shown in the figures as a white box. The Fig.(7) shows the correlation between horizontal position and horizontal divergence. It is seen that the region of interest is not completely illuminated for the wavelengths below 4.6Å. A strong wavelength-dependent effect is also visible. The brilliance transfer measured is consistent with these observations.

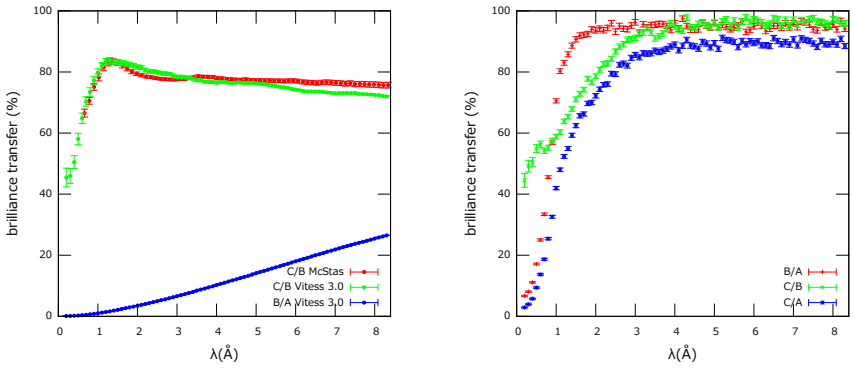

Figure 2: LEFT: Relative transmission relating the intensity at positions A, B, C along the neutron guide. The transmission evaluated in B with respect to A increases with the wavelength. Only a fraction of the divergence entering the straight guide segment can be transported. The transmission evaluated in C with respect to B using the McStas (red points) and the Vitess (green points) model is in fair agreement. RIGHT: The brilliance transfer is evaluated within -/+2cm , -/+0.25° horizontal and -/+0.5° vertical divergence. Brilliance transfer evaluated at B with respect to A (red points), at C with respect to B (green) and at C with respect to A (blue).

It should be noted, that the phase space regions defined to calculate the brilliance are rather small. From Fig. 7 it is clear, that the brilliance calculated using larger regions would be reduced due to the inhomogeneous illumination in the outer part of the acceptance diagrams.

1 Conclusions

The transmission through the funnel, which is evaluated at point C with respect to point B, is affected by the performance of the straight section: at longer wavelength the divergence distribution becomes broader leading to trajectories with more bounces along the funnel. As the high coating has a reduced reflectivity, this could explain the slightly reduced transmission for longer wavelength.

The two figures of merit used say that the funnel is able to transmit more than 80% of the thermal neutrons close to 1Å(see Fig.(2)) that it receives from the straight guide. At 1 Å the accepted phase space region is significantly smaller than the user defined region of interest. As the intensity is normalized by the 'area' of the region of interest, this leads to a reduced brilliance transfer of about 60 % at 1 Å, if one relates position B and C. For longer wavelength, the

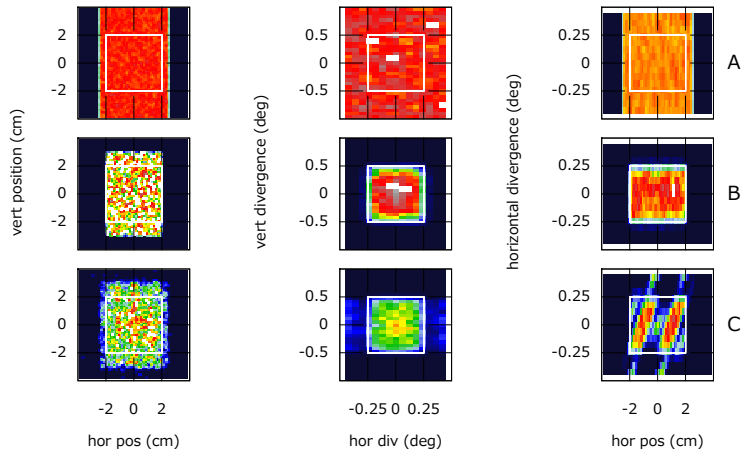

Figure 3: 2D snapshots in a 0.1Å large bandwidth around 1Å at the positions A, B and C. The white box represents the integration limits used to calculate the brilliance transfer. The intensity in the diagrams at point A are normalized to guarantee the visibility of the plot, B and C plots are on the same scale.

region of interest is more or less homogeneously illuminated. The reduction of the brilliance comes than only from the reflectivity being smaller than one. The straight section transfers at wavelength 1 Å nearly the 80 % brilliance, i.e. the phase space density is reduced to 80 % in the region of interest (see the red curve in Fig.(2)), as the coating is not sufficient to transport the divergence within the region of interest completely at this neutron wavelength. As a consequence the overall guide system is able to transfer at the sample nearly the 50% of the desired phase space at 1Å. As divergences in the region of interest exclude trajectories with several bounces, the brilliance transfer saturates for neutron wavelength above 3Å.

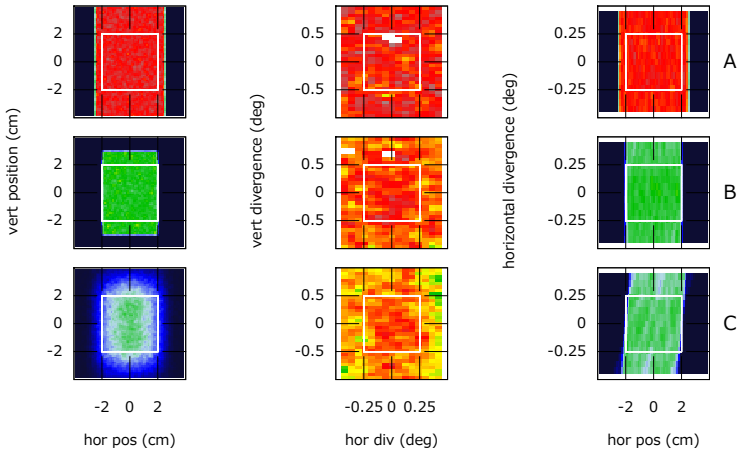

Figure 4: 2D position snapshots in a 0.1Å large bandwidth around 8Å at the positions A, B and C. The white box represents the integration limits used to calculate the brilliance transfer. Plots at A, B and C on the same scale.

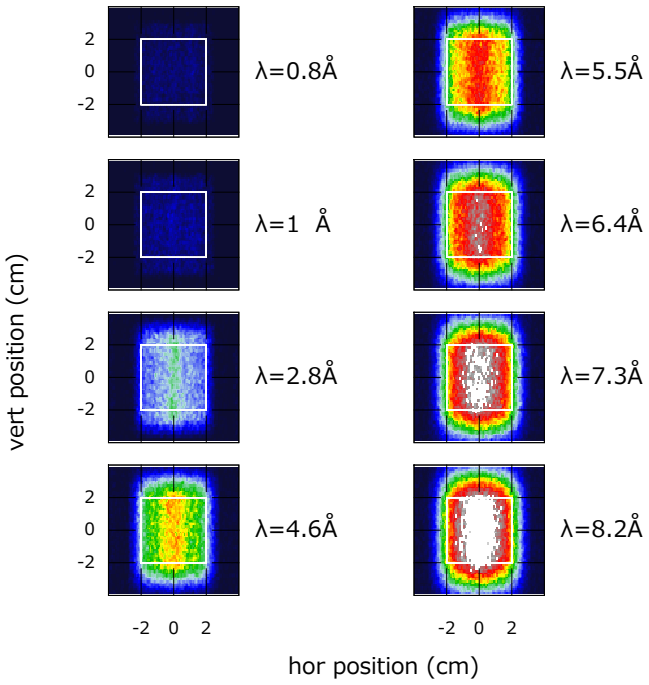

Figure 5: 2D position snapshots in a 0.1Å large bandwidth around different wavelengths from 0.8 to 8.2Å at position C. The white box represents the integration limits used to calculate the brilliance transfer.

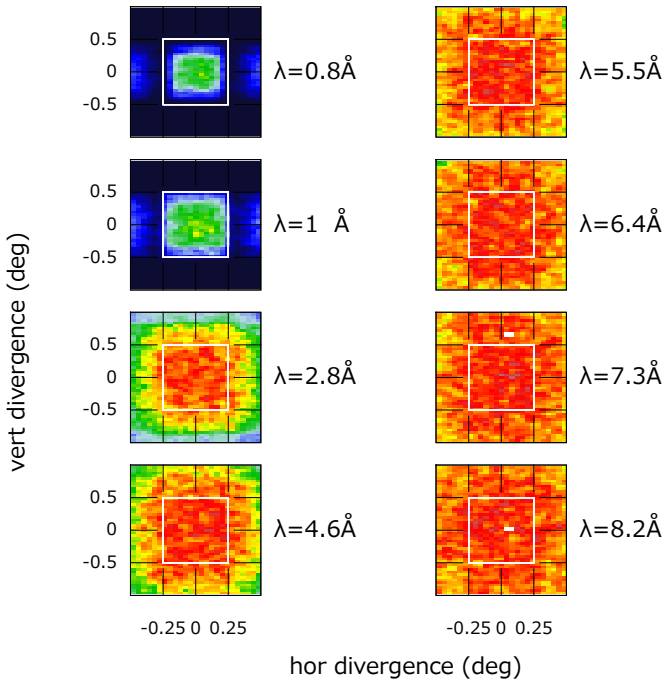

Figure 6: 2D divergence snapshots in a 0.1Å large bandwidth around different wavelengths from 0.8 to 8.2Å at position C. The white box represents the integration limits used to calculate the brilliance transfer.

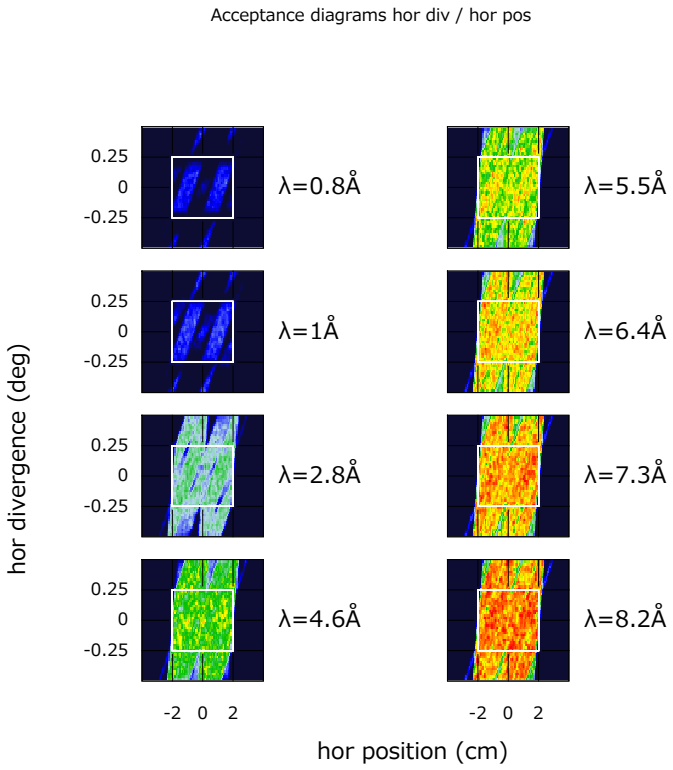

Figure 7: 2D acceptance diagrams (horizontal position/horizontal divergence) in a 0.1Å large bandwidth around different wavelengths from 0.8 to 8.2Å at position C. The white box represents the integration limits used to calculate the brilliance transfer.

Disc choppers vs. Fermi choppers for T-REX

Jörg Voigt, Nicolo Violini

December 13, 2014

1 Introduction

T-REX is a chopper spectrometer for thermal and cold energies ranging from 2 meV up to 160 meV. Direct geometry time-of-flight spectrometers operated today employ Fermi choppers and disc choppers to create a short neutron burst. In the following I will consider only ToF-ToF instruments, i.e. the time of flight is used for the initial energy determination and for the final energy analysis. At reactor sources this principle is realized at a number of instruments, e. g. IN 5, TofTof, NEAT, and DCS. These instruments use the cold spectrum and employ all counter rotating disc chopper pairs. The secondary time of flight typically exceeds 2 ms at $\lambda = 3$ Å, hence a 20 μs pulse gives a time resolution of 2% or better for longer wavelength. Reducing the angular window of the chopper also shorter pulse length are possible and lead to development of the funnel concept now in use at LET and planned for the new NEAT. Time-of-flight only instruments exist today at the short pulse spallation sources ISIS, SNS and J-Parc. They use Fermi choppers with frequencies up to 600 Hz to reach burst times below 10 μs. The instrument cover a dynamical range up to several 100 meV, even up to 2 eV. The requirements of T-REX will be in between these cases, as the spectral range between 160 and 20 meV is particularly emphasized in the instrument design.

2 Fermi chopper issues

Fermi choppers are in use at most of the ToF spectrometers using thermal and epithermal energies. As the diameter of the rotating body is much smaller, they can spin at higher frequencies to provide very short pulses in the μs range. The choppers employed today at short pulse spallation sources can usually spin the frequencies up to 600 Hz. As Fermi choppers cut basically within the divergence domain they affect the position variable of the phase space only in second order. In particular the use as a M chopper requires only modest absorber thicknesses and hence has only negligible front face losses. The usage in time-focusing hybrid ToF spectrometers will not be discussed here.

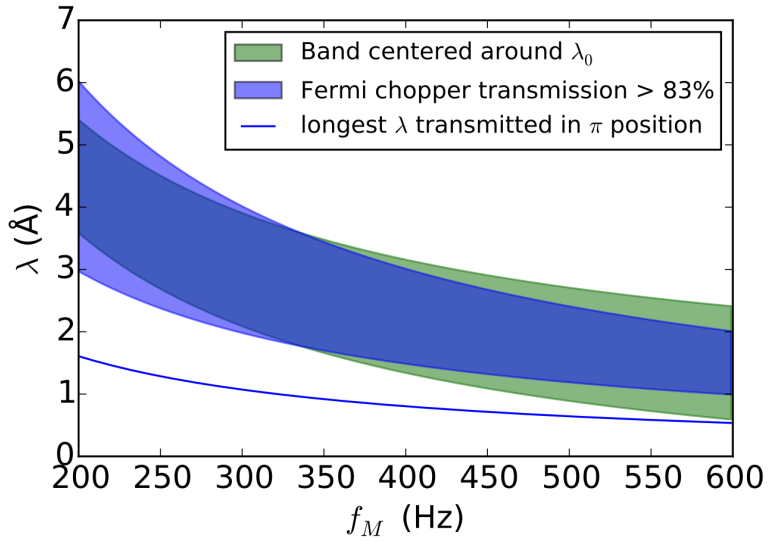

Figure 1: Bandwidth for a 155 m long instrument transmitted band of a curved Fermi chopper, $L = 54$ mm, $R = 350$ mm, $d = 1.4$ mm.

The main issue for the use of Fermi choppers is the wavelength depending transmission due to the finite time-of-flight within the collimating channel. We can define a critical wavelength from the geometrical parameters of the chopper, the channel length L and the channel width d:

$$\lambda_c = \frac{h}{m_n}\frac{4d}{\omega L^2} \tag{1}$$

For a straight chopper the transmission can be expressed as a function of the ratio $x = \frac{\lambda}{\lambda_c}$ by the following empirical formula [1]

$$T(x) = \begin{cases} 1 - \frac{8}{3}x^2 & , \text{if} x < 0.25 \quad (2) \\ \frac{16}{3}\sqrt{x} - 8x + \frac{8}{3}x^2 & , \text{if} x \leq 1 \quad (3) \\ 0 & , \text{if} x > 1. \quad (4) \end{cases}$$

So the straight Fermi chopper acts as a high pass and is fully opaque above the critical wavelength of the chopper. Curving the chopper channels with radius R such that the transmission is optimized (at a given rotation frequency ω) for the wavelength $\lambda_0 = \frac{h}{m_n}(2\omega R)^{-1}$ turns the Fermi chopper into a band pass with transmission in the range

$$\lambda_0 - \lambda_c < \lambda < \lambda_0 + \lambda_c \tag{5}$$

So the band that should be passed through the Fermi chopper puts severe constraints on the chopper design, especially if the bandwidth becomes large.

In Fig. 1 we compare the transmitted band of a Fermi chopper at the M-chopper position with the natural bandwidth of a 155 m long spectrometer. The radius of

curvature is 350 mm, the channel length 54 mm and the channel width 1.4 mm. The blue area is given by the condition $x = 0.25$. For a chopper frequency $\omega < 350$ Hz, the whole band falls into the high transmission region of the chopper. But also at 600 Hz, the transmission at the band limits is larger than 65%.

The straight Fermi chopper has a repetition rate twice of its frequency as it opens, when the collimator is parallel to the beam direction and when it is in π position. For the curved chopper the transmission is different and becomes zero (assuming a perfect absorber), when the curved channel has no direct line-of-sight. To avoid the additional pulses with low intensity one can choose the geometry in a way, that the neutron cannot pass the Fermi chopper, when it is in π position. In π position the transmitted band is limited by the condition

$$\lambda < -\lambda_0 + \lambda_c. \tag{6}$$

If the bandwidth choppers assure that no neutrons below this limit are present, the respective pulses are suppressed and the repetition rate is identical to the chopper frequency. Fig. 1 includes also the limit of the transmission in π position. The geometry of the chopper had be choosen such that at 600 Hz, which is the maximum frequency used today, the chopper transmits only in one position.

3 Comparative simulations of a disc chopper and a Fermi chopper setup for T-REX

To decide, which chopper concept fits better the requirements of the science case, we have setup simulations using a CCR disc chopper pair or a Fermi chopper at the M-chopper position. In both cases the P-chopper is realized as counter rotating chopper pair. The frequency of this chopper is determined by the M-chopper repetition rate. The choppers are placed to $l_M = 165$ m and $l_p = 110$ m from the source, requesting the ratio $\frac{f_P}{f_M} - \frac{3}{2}$ between the repetition rates f_P, f_M, respectively.

When the M-chopper is a disc chopper pair, we limit the chopper frequency to 406 Hz, the radius of the chopper disc is $R = 350$ mm and each discs has two windows, a 4.3° wide window at the 0° and a 2.5° wide window at 90°. The former is slightly wider than the neutron guide cross section, while the later reduces the transmitted beam size. To match the condition for the repetition rate, the P-chopper discs have two equivalent chopper windows at 0° and 180° (22° wide) and at 90° and 270° (36° wide) and spin at a maximum frequency of 304.5 Hz.

For the case of the Fermi chopper used as M-chopper, we keep the P-chopper window pattern. As the Fermi choppers can spin at a higher frequency, the repetition rate is now limited by the highest frequency of the P-choppers, 406 Hz, yielding the maximum M-chopper frequency $\nu_M = 532$ Hz. Two different sets of collimating channels are used for high flux or high energy resolution, 2.5° and 1.6°.

It should be noted, that the burst time for the CCR disc depends only on the angular width of the chopper windows. For the Fermi chopper it depends as well on the chopper collimation and the width of the divergence distribution at the position of the chopper, which varies between 0.5° at $\lambda = 0.7$ Åand 2° at $\lambda > 2$ Å.

We performed the simulations for two bands, the thermal band 16 meV $< E <$ 160 meV and a cold band, 2.5 meV $< E <$ 5 meV. The number of pulses at T-REX will be controlled by the Fan chopper, which suppresses pulses, if the time frame is not sufficient to meet a user defined criterion. Here we require for the thermal band, that neutrons, which lost 80% of their energy, reach the detector before the next pulse arrives at the sample. For the cold neutrons the final wavelength $\lambda' = 1.5\lambda$ should be detected before the next pulse reaches the sample. The chopper frequencies and windows are given in table 1. To determine the instrumental resolution we place a cylindrical pure elastic scatterer with 20 mm diameter at the sample position and take the width of an energy monitor with 20 mm thickness at a sample-to-detector distance $l_{SD} = 3$ m.

Configuration	f_P (Hz)	β_P(°)	f_M (Hz)	β_M(°) Window or collimation
HR thermal, FC	406	22	532	1.6
HF thermal, FC	406	36	532	2.5
HR thermal, DC	304.5	22	406	2.5
HF thermal, DC	304.5	36	406	4.3
Opt4loss thermal	304.5	22	406	4.3
HR cold, FC	304.5	36	406	2.5
HF cold, FC	105	36	140	2.5
HR cold, DC	304.5	36	406	4.3
HF cold, DC	105	36	140	4.3

Table 1: Chopper settings for the different configurations shown in Fig. 2

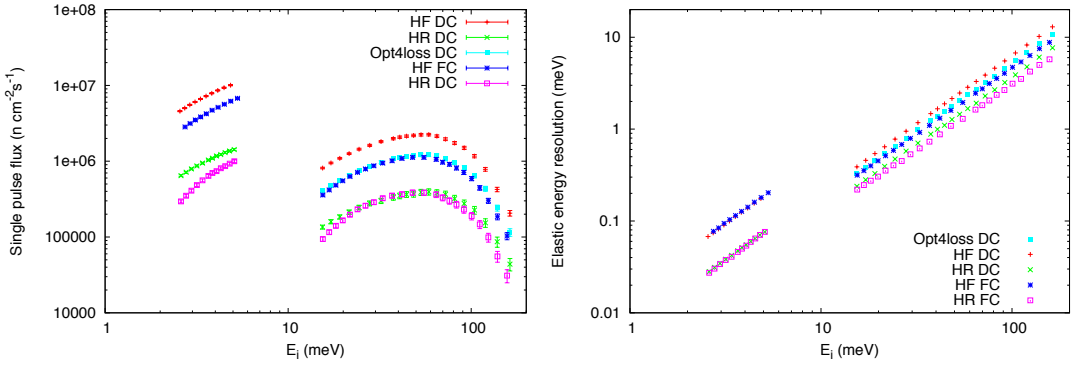

Figure 2: Left: Single pulse flux for the thermal and a cold band for different chopper settings as explained in the text. Right: Elastic energy resolution for the individual pulses for the different settings.

The results of the simulations are summarized in Fig. 2. First we realize that despite the significantly higher frequency of the Fermi chopper setup the number of pulses as dictated by the criteria given above varies only from 23 to 21. Even with the nar-

row bandwidth of T-REX the timeframes become long enough to be matched by the repetition rate of the disc chopper for most of the pulses.

In the cold spectral range, the Fermi and disc chopper configurations do not differ. The disc chopper allows even with the large angular window an elastic resolution $\frac{\Delta\hbar\omega}{E} \approx 1\%$ with a flux, which is still high enough to allow polarization analysis, e.g. for clean measurements of the atomic diffusion of elements with a spin incoherent scattering cross section. The resolution $\Delta\hbar\omega < 30$ meV can be realized for $\lambda < 6$ Å. Hence it is possible to have a decent overlap between the dynamic range of reactor based backscattering instruments and direct geometry ToF spectrometers in the same Q-range.

In the thermal range a high energy resolution of 3% for $E = 100$ meV can be reached only by high resolution Fermi chopper configuration. It should however be noted, that typically neutron energy loss processes are studied with high initial energy E. If you balance the time uncertainty contributions from the P and the M chopper one can therefore increase the burst time of the M chopper and reduce the burst time of the P chopper. While the elastic resolution is only modestly enhanced, the performance is now optimized for the resolution of energy loss processes.

4 Conclusion

We compare the performance of a chopper system build up by either counter rotating disc chopper pairs or a combination of a disc chopper pair at the P position and a Fermi chopper at the M position. We show, that for the narrow wavelength of T-REX both options are viable solutions, but that we are favoring the pure disc chopper configuration for their better transmission properties.

References

[1] P. A. Egelstaff. Technical Report 1131, AERE N/R, 1953.

Investigation of timing and positioning of T_0 choppers at long pulse neutron sources

N. Violini, J. Voigt and T. Brückel

Jülich Centre for Neutron Science, JCNS, Forschungszentrum Jülich GmbH, Leo Brandt Strasse, D-52425 Jülich, Germany

E-mail: n.violini@fz-juelich.de

Abstract. We examine the prerequisites for the operation of T_0 choppers at a long pulse spallation source using the parameters of the European Spallation Source (ESS). We discuss the constraints imposed to the chopper position and the operation parameters by the long pulse nature and the low repetition rate of the ESS. For an instrument having a moderator-to-detector distance $L_D = 155$ m with a double elliptic neutron guide shape we analyze possible solutions for chopper rotational frequencies of 7 and 28 Hz, that are acceptable for a cold instrument, while for a bi-spectral or a thermal instrument the lower frequency requires the chopper to be placed at a large distance from the moderator.

1. Introduction

At spallation neutron sources a proton beam is injected into the neutron production target causing the emission of high-energy particles that can hardly be shielded, as the energy, e.g. for fast neutrons, is limited by the proton beam energy to several GeV. The high-energy particles, which can leave the monolith shielding, are potentially scattered and/or moderated within the instruments beam-lines. This source of background has to be kept as low as possible, since the key figure describing the performance of any neutron instrument is the signal to noise ratio. Several measures are currently in use at existing facilities and various options exist to assure that the experimental area is out of the direct line-of-sight of the neutron source. Geometrically the line-of-sight can be avoided by curved neutron guides[1] also including more involved design such as the *Selene* concept [2]. In time the use of T_0 choppers mitigates the intensity of high energy neutrons by blocking off the beam-line around the time of neutron production. It consists of a rotor with blades that block the beam-line and the rotor is synchronized with the injection of the proton beam and therefore with the emission of the prompt neutron pulse. The use of T_0 choppers is a common practice at spallation sources [3, 4]. T_0 choppers rotating at comparably high frequencies of 100 Hz are in use at the Japan Proton Accelerator Research Complex (J-PARC), where the tests performed on High Resolution Chopper Spectrometer (HRC) [5] show a reduction of two orders of magnitude in the background noise detected for monochromatic beams of energy above 100 meV [6].

The long pulse of the ESS requires different design parameters and also further technical development. The crucial difference between short and long pulse spallation sources is the interaction time of the proton beam with the target: the short pulse requires a fully opaque

chopper only for μs, while in the long pulse this time amount to several ms, which is a substantial fraction of the periodicity of the source.

Here we describe how the long pulse nature and the low repetition rate (14 Hz) of the ESS affect the layout of T_0 choppers, but we do not cover any aspects of the engineering design of a T_0 chopper and we especially keep the search for appropriate materials and thickness open. Our considerations apply to the different layouts that are used today, with a rotation axis parallel to the main neutron flight direction. We assume that the choppers are symmetric with respect to the rotation axis, i.e. they close the neutron beam twice during a full revolution.

2. Timing and positioning

We describe in figure 1 the absorption of a T_0 chopper as a function of time with respect to the pulse structure at the ESS, assuming that the chopper is placed at a distance L_{ST_0} from the moderator surface. First, the T_0 chopper has to confirm that the neutron beam is fully closed when high-energy particles are produced. We assume that this time range is given by the ESS neutron pulse length of τ_s =2.86 ms plus an additional arbitrary time after the pulse τ_{ag}, referred to as after glow, therefore having $T_0 = \tau_s + \tau_{ag}$. Furthermore the chopper reduces

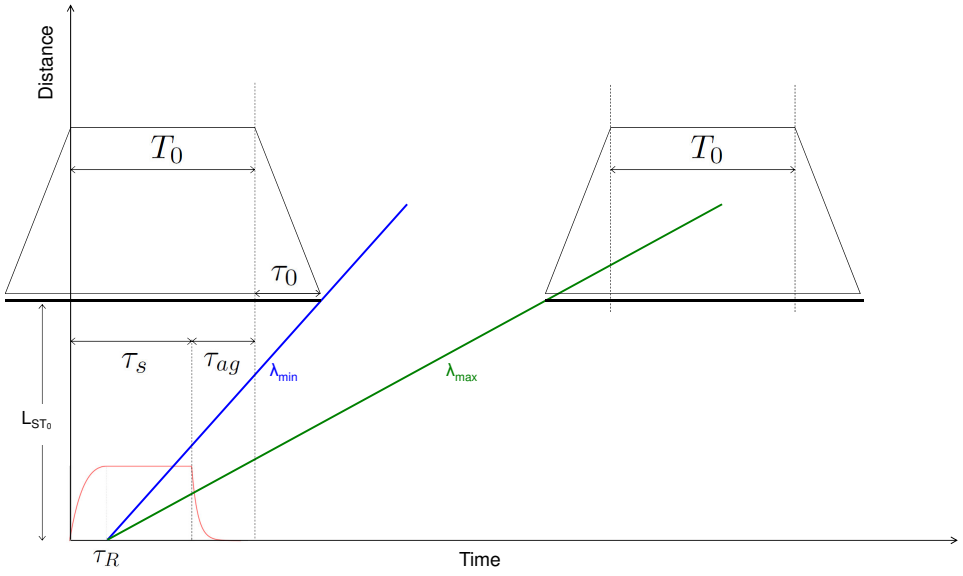

Figure 1. Schematic representation of the T_0 chopper time operation within a tof-diagram snapshot taken from the moderator to the chopper position L_{ST_0}. τ_0 is the opening and closing time, T_0 is the time interval in which the chopper is fully closed. Thus the horizontal black lines represent the chopper closing. The ESS pulse shape as a function of time is also represented (red curve). The blue and the green lines represent neutrons starting from the moderator at the rise time τ_R, with the desired minimal and maximal wavelength $\lambda_{\min}$ and $\lambda_{\max}$ respectively.

the transmission during the additional time necessary for the hammer to be removed from the neutron guide cross section

$$\tau_0 = \frac{2\arctan\frac{w}{2R}}{2\pi f} = \frac{\alpha}{2\pi f}, \tag{1}$$

where f is the chopper rotational frequency, w is the guide width and α the angular width of the neutron guide at the chopper position. The latter depends basically on the radius of the chopper blade and the guide cross section at the position of the chopper. The radius R in equation (1) is taken from the bottom of the neutron window to the axle of the chopper. The width of the chopper hammer has to be larger than the guide width in order to allow complete closing. Therefore the reduced transmission might be relevant for complex guide designs with variable cross section along the neutron flight path.

As a consequence of the long neutron pulse structure, the total angular width of the hammer, which is given by

$$\beta = T_0 \times 2\pi f + \alpha, \tag{2}$$

increases linearly with the frequency, as can be seen from table 1.

As it is seen in figure 1, fixing the position of the T_0 chopper reduces the transmission for any wavelength shorter than

$$\lambda_{\min} = \frac{h}{m_n} \frac{T_0 + \tau_0 - \tau_R}{L_{ST_0}}, \tag{3}$$

which depends on the starting time at the moderator of the neutrons reaching the chopper when it is fully open. When the chopper closes again, it determines the upper limit of the wavelength band, which is transmitted without gaps due to the chopper operation,

$$\lambda_{\max} = \frac{h}{m_n} \frac{(2f)^{-1} - \tau_0 - \tau_R}{L_{ST_0}}, \tag{4}$$

where it is assumed that the chopper closes the beam twice during a full revolution. However, the repetition rate of the T_0 chopper has to fulfill the more relaxed condition to be an integer multiple of the source frequency to block the background from every source pulse. The resolution defining chopper system selects the neutrons released during a portion of the pulse, whose length depends on the required energy resolution. For a chopper system as proposed in [7] the effective extraction time $\tau_R \pm \tau_{\text{eff}}/2$ can be centered at any time during the neutron pulse, independent of the incoming wavelength. In particular it can be moved towards the end of the pulse to maximize $\lambda_{\min}$ giving $\tau_R = \tau_s - \tau_{\text{eff}}/2$. The requested effective pulse length τ_{eff} constraints the position of the T_0 chopper L_{ST_0}, depending on the minimum wavelength required,

$$L_{ST_0}^{\min} = \frac{h}{m_n} \frac{T_0 + \tau_0 - (\tau_s - \tau_{\text{eff}})}{\lambda_{min}}, \tag{5}$$

while the upper limit for the position depends also on the requested bandwidth $\Delta\lambda$:

$$L_{ST_0}^{\max} = \frac{h}{m_n} \frac{(2f)^{-1} - \tau_0 - (\tau_R + \tau_{\text{eff}})}{\lambda_{\min} + \Delta\lambda}. \tag{6}$$

In figure 2 we present potential positions for the T_0 chopper to transmit at least the natural bandwidth ($\Delta\lambda = 1.88$Å) of a 155 m long instrument, which is a typical length for the long ESS

Table 1. Hammer width of the T_0 chopper calculated from equation (2) for different rotational frequencies commensurate with the ESS source frequency. The neutron guide cross section used for the calculation is $8.5 \times 8.5\text{cm}^2$.

Frequency (Hz)	7	14	28	56
β (deg.)	29.57	36.78	51.19	80.02

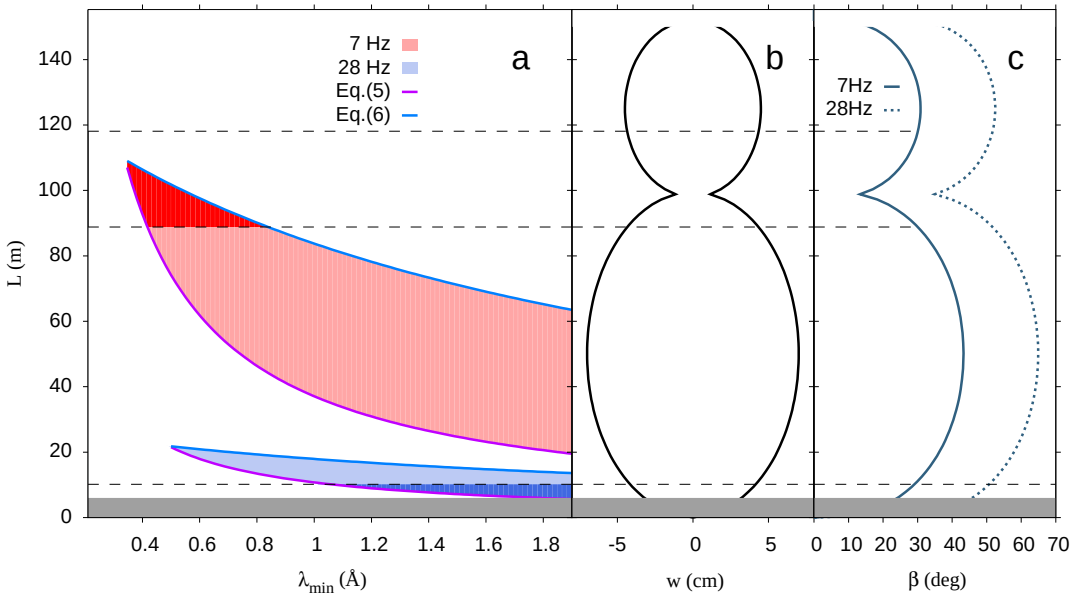

Figure 2. Possible positions for different frequencies of the T_0 chopper if the usable wavelength band starts at $\lambda_{\min}$ and extends over the natural bandwidth (here 1.88 Å for a total instrument length of 155m). The lower limit is defined by equation (5), the upper limit is set by the equation (6). The dark red and dark blue areas represent the regions where the guide width is smaller than 8.5cm. The pulse can be used for an effective pulse length $\tau_{\text{eff}} = 500\mu$s from the end of the pulse for the lower limit and from the beginning of the plateau at the upper limit, respectively. The grey area represents the inaccessible area within the monolith.

instruments, as a function of the lowest wavelength λ_{min} to be transmitted for different chopper frequencies. The panel *b*) represents the neutron guide width assumed for the calculation of the hammer size according to equation (2) that is shown in panel *c*). The double elliptic shape results in a smaller guide width close to the focal points of the ellipses than compared to the width in the ellipse center, which is manifest in the T_0 chopper hammer width shown in panel *c)*. In order to limit the size of the hammer to a reasonable value, we emphasized with darker color the regions where the guide is smaller than 8.5cm, a value that is similar to the one assumed in [6]. Therefore two working conditions for the chopper are identified: it can be operated in the region across the connection of the two ellipses with a rotational frequency of 7 Hz or close to the start of the first ellipse for $f = 28$ Hz. The latter is valid for an instrument using neutrons with $\lambda > 1.1$ Å, which is sufficient for any cold instrument, while any instrument using thermal to epithermal neutrons needs a larger distance to make use of short wavelength neutrons. One could envision a T_0 chopper at this position as the second line-of-sight breaker, once the line-of-sight is first broken by a curved or kinked guide section upstream the chopper position. In this case the T_0 chopper has to block the fast particles emitted from the first impact point, therefore its thickness might be reduced as compared to a chopper in the primary fast particle spectrum.

Making use of acceptance diagrams in figure 3, the transmission properties of the T_0 chopper are analyzed for the two situations, assuming the position of the chopper is close to the upper limit expressed by equation 6:

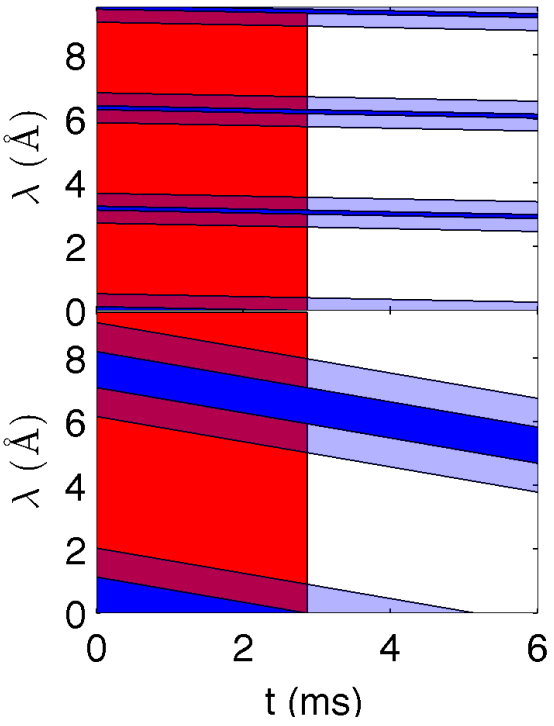

Figure 3. Acceptance diagrams for T_0 choppers spinning at different frequencies (top: 7 Hz, bottom: 28 Hz) and placed at different positions (top: $L_{ST_0} = 90$ m, bottom: $L_{ST_0} = 10$ m). The red areas indicates when the T_0 chopper transmits the neutrons originating from the source pulse, neglecting the after glow. The light blue area indicates regions where the chopper is opening and closing, in the dark blue regions the chopper is completely opaque. The T_0 chopper is fully closed for 2.86 ms. The chopper hammer size is calculated according to table 1. The repetition rate is twice the chopper frequency.

- When the chopper is placed close to the moderator, as shown in the bottom panel, the lower bandwidth limit is quite high and a higher frequency is needed to keep τ_0 short or alternatively one might employ a set of two counter-rotating T_0 choppers in series [7]. On the other hand the transmitted bandwidth is twice wider than the natural bandwidth of an instrument with total length $L_D = 155$ m. An increase of the bandwidth by skipping a pulse can always be realized for this layout.
- Placing the chopper at a larger distance, as shown in the top panel, the lower wavelength limit is reduced for a lower frequency, despite the longer τ_0. The natural bandwidth starting from a lower limit of 0.7 Å is transmitted continuously, while higher order bands are separated by a wavelength gap that depends on the chopper position and speed. The gap in the spectrum is narrower, but the transmitted bandwidth is also reduced. Hence the choice of the T_0 chopper position can limit the opportunities for pulse skipping.

3. Conclusions

We discussed analytic considerations related to the use of T_0 choppers at a long pulse spallation source using ESS parameters. Due to the long pulse structure the T_0 chopper constraints the lower limit of the neutron wavelength spectrum. As the T_0 chopper and the source pulse act also as a band filter, the transmitted band must be at least as wide as the requested instrument band. We discussed in detail possible solutions for chopper frequencies of 7 and 28 Hz. Depending on the neutron wavelength band of interest these options are both acceptable for a cold instrument. For a bi-spectral or a thermal instrument, which uses neutron wavelengths down to 0.7Å the lower frequency requires the chopper to be placed at a large distance from the moderator. Considering the constraints and uncertainties attached to the T_0 chopper layout, additional means to prevent the effect on the instrument performance must be pursuit. Here we mention to avoid the direct line-of-sight sufficiently by the neutron guide layout, possibly for rather long instruments, or having the instrument so compact that the neutrons are always analyzed before the next source pulse begins. Our results show that the T_0 chopper design for a long pulse

spallation source is a complex task and has severe implications for the instrument operation, not to mention the complexity of the engineering and radiological design. In particular the wavelength limits and gaps in the spectrum have to be considered to retain a large flexibility in terms of usable neutron wavelength. We hope that the present contribution can be of use for instrument designers, which need to use T_0 choppers in their instrument.

3.1. Acknowledgments
Authors acknowledge funding by BMBF (Bundesministerium für Bildung und Forschung) through the collaborative project 05E10CJ1.

4. References

[1] Maier-Leibnitz H and Springer T 1963 *Reactor Sci. Technol.* **17** 217.
[2] Stahn J, Panzner T, Filges U, Marcelot C and Böni P 2011 *Nucl. Instr. and Meth. in Phys. Res.* A **634** S12-S16
[3] Jones T.J.L., Davidson I, Boland B.C., Bowden Z.A., Taylor A.D., *Proceedings of the 9th Meeting of the International Collaboration on Advanced Neutron Sources, Swiss Institute for Nuclear Research* 1987, p.529 (ISBN3-907998-01-4)
[4] McQueeney R.J. and Robinson R.A. 2003 *Neutron News* **14** 36
[5] Itoh S, Yokoo T, Satoh S, Yano S, Kawana D, Suzuki J and Sato T 2011 *Nucl. Instr. and Meth. in Phys. Res.* A **631** 9097
[6] Itoh S, Ueno K, Ohkubo R, Sagehashi H, Funahashi Y and Yokoo T 2012 *Nucl. Instr. and Meth. in Phys. Res.* A **661** 86-92
[7] Voigt J, Violini N and Brückel T 2014 *Nucl. Instr. and Meth. in Phys. Res.* A **741** 26-32

On detectors for the chopper spectrometer proposal T-REX

March 25, 2015

1 Efficiency requirement

Efficiency of a neutron detector is directly related to the neutron capture cross section for the converter isotope. For the neutron energies of interest and for all relevant isotopes, including ^{3}He and ^{10}B, this cross section is inversely proportional to the velocity of the neutron. Due to this, the efficiency of a detector increases rapidly with wavelength until it saturates when all neutrons are absorbed by the available converter. It has been shown in the document produced by the ESS detector group [1], that this dependence is similar for both ^{3}He and ^{10}B. Furthermore, several different optimisations of the layer thicknesses used in the ^{10}B detector are shown.

In order to address the primary neutron energy range of interest for the T-REX instrument of 10 to 100 meV, an optimisation for 1 $\mathring{A}$ was performed, see figures 1 and 2. This calculation can be directly compared to the efficiency of a ^{3}He tube averaged over its diameter where the loss in the metal has been taken into account as in [1]. We can see that 40-50% efficiency can be reached using 30-50 boron layers for 1 $\mathring{A}$, approximately equal to the efficiency of ^{3}He tubes at 5 bar, assuming round He-tubes, reasonable tube wall thickness and tube spacing.

Averaged over the full wavelength range, 1 to 20 $\mathring{A}$, efficiency will be significantly higher than the minimum at the lower end, around 60 to 70% with variation of at most 35% from maximum to 1 $\mathring{A}$. Therefore the effect of the efficiency curve of the detector will have a minimal effect on the error bars in the measurements. Further contributions to the error bars are due to the source spectrum, transmission of the guide system (see proposal document), scattering intensity. The latter, of course, varies over many orders of magnitude for the features measured and will tend to dominate the error bars of a measurement.

We can note that the efficiency curve of the detector has a similar shape to the guide transmission curve, with both curves dropping off for wavelength approaching 1 $\mathring{A}$. For purely elastic scattering this would be an obvious disadvantage, as a 35% drop in efficiency and 55% drop in transmission (based on fig 1.7) would translate into a 70% drop overall. For inelastic measurements, such as on a chopper spectrometer, the overall efficiency curve is more complex, since a neutron that passed a guide at one energy is detected at another. For measurements of large energy transfers of up to 150 meV, a neutron would have to be transmitted at high, or low end of the spectrum and detected at

the opposite end, depending on whether energy was transferred to or from the neutron. In such a scenario, the drop in efficiency and transmission for low wavelength do not combine with each other, but instead individually contribute to a falloff at the extreme ends of the range.

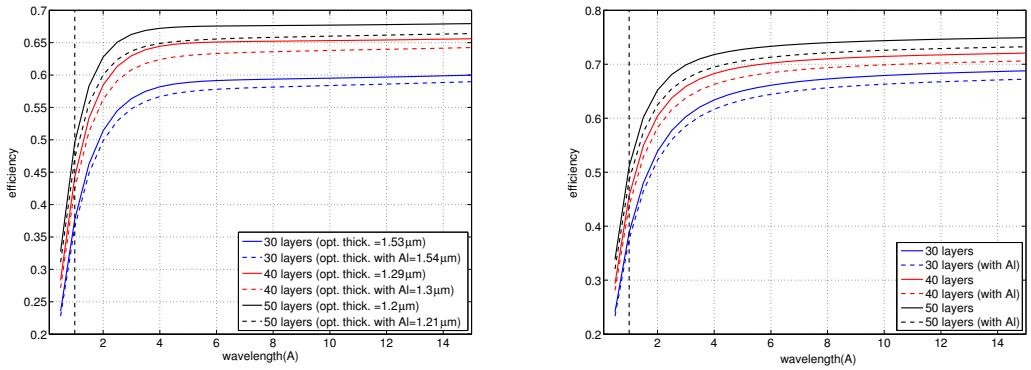

Figure 1: Efficiency curve for the boron layer detector with the optimisation where all weight has been given to 1 $\mathring{A}$ (with efficiencies at other wavelengths a product of this optimisation). Efficiency above $\sim 2\mathring{A}$ can be increased by giving weight also to higher energies in the optimisation. **Left:** fixed layer thickness **right:** variable layer thickness. **Note:** plots for a wider range of optimisations are available in [1]

2 Design considerations with Multi-Grid

A suggested design for the detector array is based on the current Multi-Grid demonstrator [2, 3, 4, 5]. This is a 3 m by 80 cm module that has been modelled on the modules of the IN5 spectrometer. In this detector, the fraction of sensitive area is 85%. This parameter is dependent on the pressure difference between the detector and the ambient environment, since the thickness of the walls between detector elements needs to be chosen accordingly. Recent tests indicate that the B10 detector can be operated at pressures of only a few tens of mbar, therefore the thickness of these walls can be reduced in the future. It should be noted that the detectors of this size should be designed together with the instrument vessel – this would allow for structural savings in the overall design and minimise the dead area.

The boron carbide layers have been developed [6], and a facility for production of $^{10}B_4C$ layers that meets that capacity necessary for the ESS instruments with large-area detectors has already been setup. The thickness of boron layers would be close to 1.0 μm (optionally varying from the front to the back of the detector). In order to make a specific choice, it is necessary to know where in the wavelength range the statistics are the lowest in order to prioritise that region in the optimisation. The thickness could be gradually increased to 3.0 μm at the back of the detector to achieve the highest average

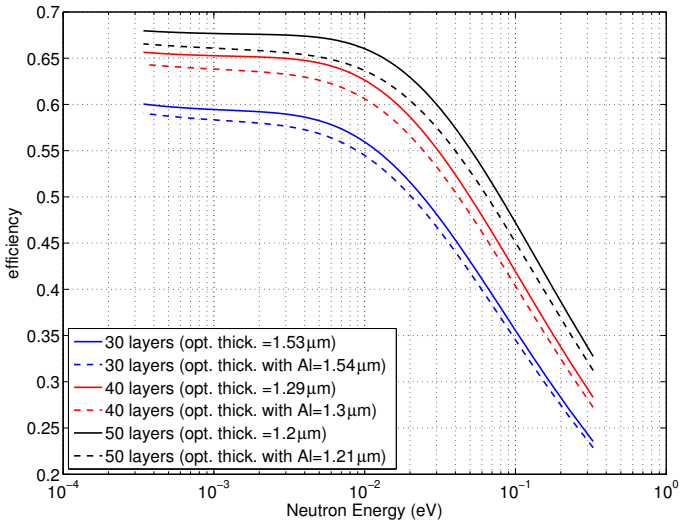

Figure 2: Efficiency curve for the boron layer detector with the optimisation purely for $1\AA$ – same as figure 1 (Left) but plotted as a function of energy.

efficiency.

The number of layers depends primarily on the emphasis on the efficiency at and below $1\mathring{A}$. With 15 double layers a reasonable balance between efficiency over entire wavelength range and complexity is reached. Further increase in the number of layers will add 5-10% to efficiency in the region 1-1.5$\AA$. Further increase in efficiency (primarily for longer wavelengths) can be reached by using a variable $^{10}B_4C$-layer thickness over the depth of the detector, see figure 1 (right).

The background of the B10 detectors have been investigated thoroughly. Gamma-ray background investigation has been published and shows that the position-sensitive Multi-Grid detector matches He3 background [7]. Background due to naturally-occurring α-emitters can be an issue in either B10 or He3 detectors when using aluminium parts, however, aluminium with high enough purity is commercially available and solves this issue.

References

[1] M. Echegaray *et al.*, *ESS Strategy for Detectors for the Direct Geometry Instrument Class: Schedule and Prospects for Bispectral instruments* ESS report (2014)

[2] A. Khaplanov *et al.*, *Multi-Grid Boron-10 detector for large area applications in neutron scattering science*, *arXiv:1209.0566* (2012).

[3] J. Correa *et al.*, *10B4C Multi-Grid as an Alternative to 3He for Large Area Neutron Detectors*, *Trans. Nucl. Sc.* (2013) DOI: 10.1109/TNS.2012.2227798.

[4] B. Guerard *et al.*, *10B multi-grid proportional gas counters for large area thermal neutron detectors*, *Nucl. Instr. Meth. A* (2012) http://dx.doi.org/10.1016/j.nima.2012.12.021.

[5] J Birch *et al.*, *In-beam test of the Boron-10 Multi-Grid neutron detector at the IN6 time-of-flight spectrometer at the ILL* J. Phys.: Conf. Ser. (2014) 528 012040 doi:10.1088/1742-6596/528/1/012040

[6] C. Höglund, *et al.*, B_4C *thin films for neutron detection*, *J. Appl. Phys.* **111(104908)** (2012).

[7] A. Khaplanov et al., *Investigation of gamma-ray sensitivity of neutron detectors based on thin converter films J. Inst.* (2013) 1748-0221 8 P10025 doi:10.1088/1748-0221/8/10/P10025

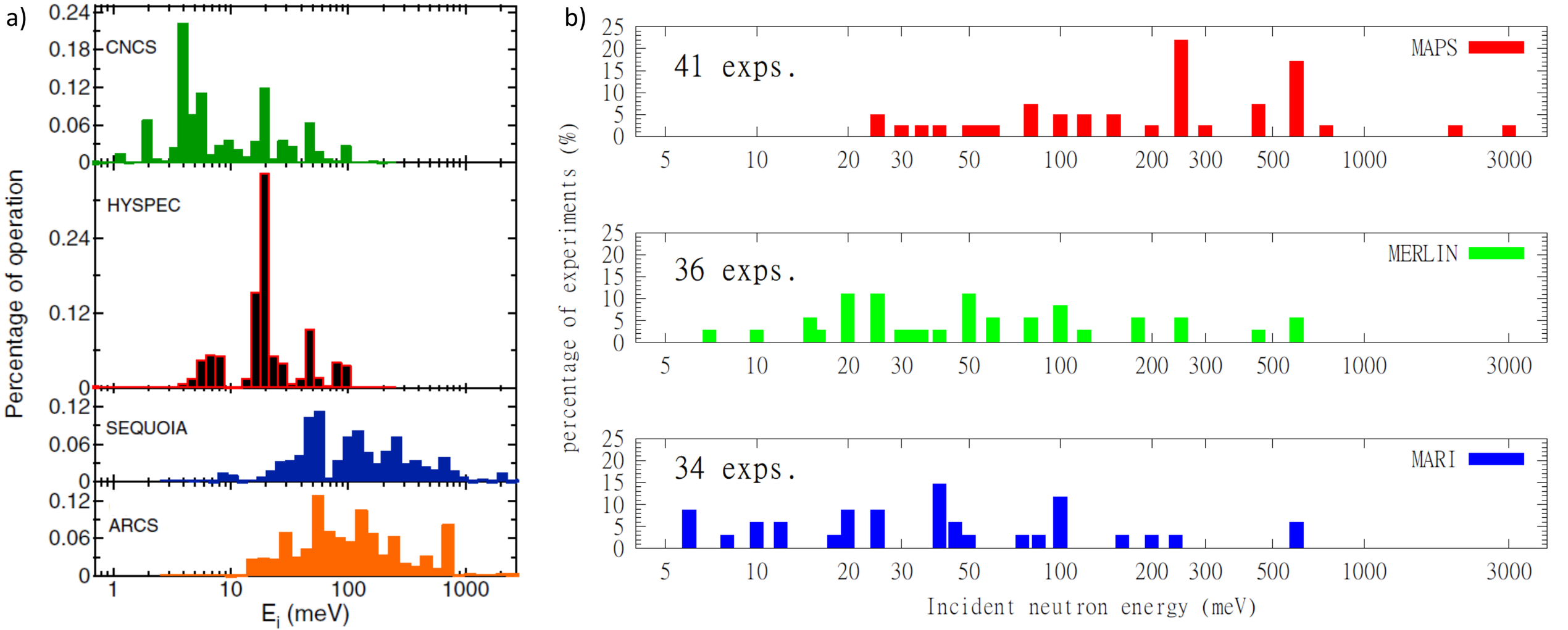
a)
CNCS
HYSPEC
SEQUOIA
ARCS
Percentage of operation
E_i (meV)
b)
41 exps.
MAPS
36 exps.
MERLIN
34 exps.
MARI
percentage of experiments (%)
Incident neutron energy (meV)

Investigation of neutron transport systems for T-REX

N. Violini

December 2014

1 Introduction

The T-REX spectrometer layout envisages the Pulse Shaping (P) choppers at 110 m and the Monochromating choppers (M) at 165 m distance from the source. Due to the requirements of short burst times and optimized transmission of the choppers the guide cross section is limited at the position of the choppers. This lead to the double elliptic guide layout, which features very good brilliance transfer and also a homogeneous beam and divergence profile at the sample position. The problem of this layout is the direct view into the moderator, which potentially prevents the excellent background condition necessarry for a well performing spectrometer. It can be modified by including a horizontal kink at the connection of the two ellipses at the cost of 10-20% of the flux in the thermal energy range. We will refer to this geometry as EKE (Ellipse Kink Ellipse). It fulfills the request of avoiding the line-of-sight (LoS) once.

While keeping the ellipse for the vertical shape, another concept was investigated that consists of a curve, followed by a straight and an elliptic section (CSE geometry). As the requested horizontal phase space on the sample is $1\text{cm} \times \frac{2\pi}{\lambda} 1^\circ$, this alternative layout accepts a narrow divergence from a large area moderator that is subsequently focused into the phase space volume of interest. For low divergence also a thermal guide can be curved out of the direct line of sight with a good brilliance transfer.

The new concept aims for breaking the line of sight at a reasonably far distance from the sample to have a sufficient distance to transfer the wide collimated beam into a narrow beam with a divergence meeting the flux and Q-resolution requirements of T-REX. As a second mean to prevent high energy particles from reaching the sample area we foresee a $T0$ chopper downstream the direct line of sight to block particles emitted by impact of the prompt pulse. As a consequence not only the $T0$ chopper, but all optical components downstream are not placed in the fast neutron field from the prompt pulse.

The CSE layout shows higher performance than the EKE in a large lambda range and provides brilliance transfer, within +/- 0.25°, of nearly the 75% at 100 meV neutron energy (see fig1).

In order to fulfill its scientific mission, T-REX has to make use of both thermal and cold neutrons, therefore a bender for the extraction of cold neutron is envisaged outside the monolith wall. It can be removed when not using cold neutrons, without compromise of the instrument performance in the thermal energy range, as the main instrument axis faces directly the thermal moderator.

In 2014 the team has contributed to the optimization of the moderators desing by means of investigation of the T-REX performance, when placed at *pancake* moderators and optimised thermal (OT) moderators. Detailed written reports were provided to the ESS. Here we summarize the main conclusions:

- *pancake* moderators: reducing the moderator height, from 12 cm to 3 cm, the guide performance decreases, because the guide is not fed with a large enough phase space, even starting with the vertical walls at 2 m from the moderator. The intrinsic brilliance gain, nevertheless, compensates the performance reduction enabling a gain of 1.5 in average in terms of flux at the sample in the thermal energy range.

- OT moderators: reducing the moderators width from 12cm to 6 cm reduces the horizontal offset between the center of thermal and cold moderators, therefore a benefit is offered for extraction of cold neutrons. In the OT layout the efficiency of the bender is found to be 85% in average (see Section 3 for more details). The intrinsic brilliance gain together with the new CSE guide layout enables a gain of slightly more than 2 in average in terms of flux at the sample in the thermal energy range.

2 Neutron guide optimization

The simulations described in the present document were performed in Vitess 3.2. The following parameters describe the elliptic geometry: width and height of guide entrance and exit, distance from the guide exit to the focal point of the ellipse. The elliptic shape is approximated with linear segments, whose length and number is given. Four reflectivity curves can be given for any wall in any given guide segment. The reflectivity curves used in the simulations match the performace of recent SwissNeutronics supermirrors (see fig. 1). Waviness and misalignments are neglected.

We assumed a reference moderator emitting a normalized brilliance of 1 $n/s/cm^2/\text{Å}/sr$. The figure of merit used is the brilliance transfer, i.e. the integral intensity measured within the desired phase space region. We stress that in case the brilliance is evaluated in front of the moderator in a homogeneously illuminated region, it is a direct measurement of the phase space density provided by the moderator. Therefore the evaluation of this quantity at different positions along the guide must fulfill Liouville's theorem.

2.1 The envisaged guide layout

The proposed guide follows a double elliptic shape in the *vertical* plane to provide reasonably small apertures at the position of the P and M choppers. The system features

a progressive distribution of the super mirror index m that enables the reflection for neutrons flying through the first focal point and hitting the central position of the single guide segment. In order to obtain such an optimized geometry, we performed an investigation of the guide performance, varying the long and small axis.

Several shapes have been investigated for the *horizontal* direction to avoid that the experimental area has the direct LoS of the moderator. Here we compare three solutions, which are described in fig.1a):

- a EKE shape with a kink across the P-chopper position, following the concept proposed in Ref.s [1, 2], where the LoS is broken once,
- the same EKE shape with the kink angle increased in order to break the LoS at 30 m from the moderator, where the T0 chopper can be placed,
- a CSE shape, that breaks the line of sight before a distance of 100 m from the moderator. A subsequent straight section should homogenize the divergence distribution and the focusing section tailors the phase space to the requirements of the intstrument.

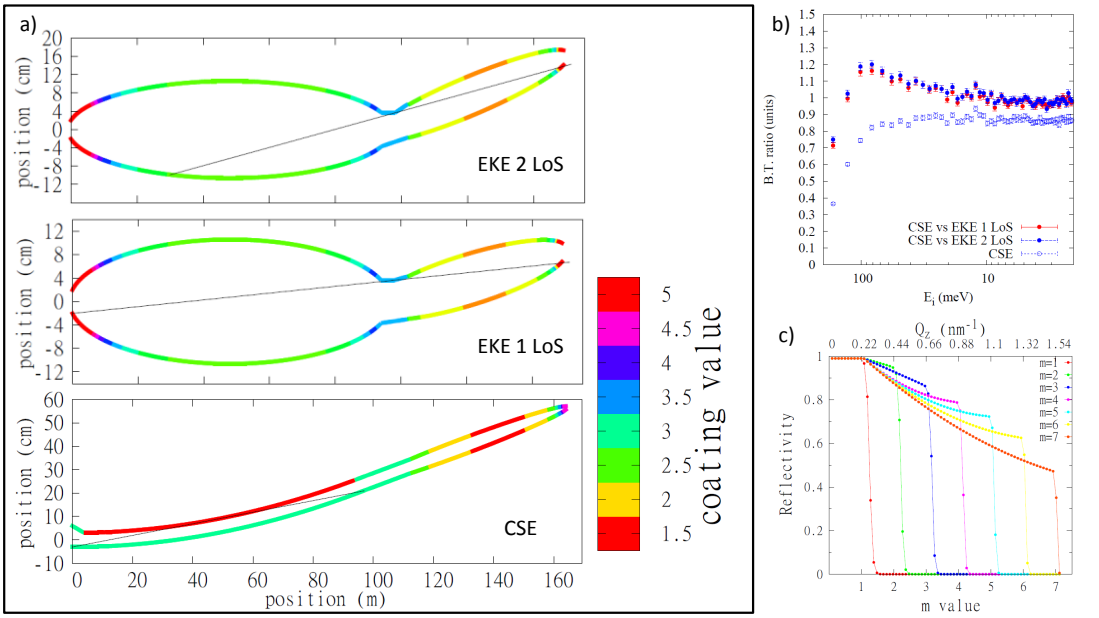

Figure 1: a) Schematic rendering of the three horizontal shapes taken into consideration for the guide of T-REX. The value of the supermirror m index is represented in colour scale and the respectives reflectivity curves are shown in c). b) The brilliance transfer at the sample after the curved shape (empty circles) is compared to the one from the double ellipse connected with the kink.

The three options shown in fig.1a) result from the individual optimization. The optimization process of the EKE shapes has involved: the long and small axes, the length

of the two ellipses, the length and height of the straight section and the lenght and dimensions of the kink. The optimization of the CSE shape involved the width of the guide: for each width we firstly calculated the radius of curvature necessary to break the LoS at the same distance from the entrance, upstream the P-chopper, then an individual optimization involved the length of the straight section and the shape of the ellipse. We have also investigated whether a collimating, i.e. with widening cross section, segment before the curved segment improves the brilliance transfer. The effect of such a segment was neglible. Therefore we start the guide immediately with the curved section.

In fig.1b) we compare the brilliance transfer at the sample for the three options within the region of interest identified in a sample size 1x3cm^2 within a divergence of +/-0.25°. This rather narrow divergence range is considered most important for the high energies used at T-REX. The curved solution performs better than the others, with a maximum gain of 20% and it reaches high values of the brilliance transfer already at around 100 meV. Therefore it is the proper choice to put emphasis on the use of thermal neutron energies. The requested beam cross section confirms homogeneous illumination of the sample, e.g. if single crystals are rotated for mapping of excitations or for large area thin liquid samples. The divergence window provides reasonable good Q resolution for the high energy applications.

2.2 Beam characteristics at the sample

In fig.2 we report results from simulations of the T-REX layout. The intensity distribution at the sample positions is shown as a function of the horizontal and vertical position and is obtained from integration in a 1mm-thin slice. The divergence distributions are instead obtained from integration in a 0.1°-thin slice. The fig.2 also shows 2D monitors taken at the sample position in a narrow energy band around the selected values:

- 2D pos: horizontal position along x axis, vertical position along y axis,
- 2D div: horizontal divergence along x axis, vertical divergence along y axis,
- hor pos/div: horizontal position along x axis, horizontal divergence along y axis,
- vert pos/div: vertical position along x axis, vertical divergence along y axis.

The color scale represents the intensity normalized to unity. It can be seen that the guide system is optimized to transport a different divergence for the different energies in order to fulfill the requirements for Q resolution. Therefore fig.3 shows the comparison between the brilliance transfer to the sample position in the region of interest identified by a sample area of 1x3cm^2 and a divergence of +/-0.25°, +/-0.5° and +/-1° along the vertical and the horizontal directions. The limits of the three integration areas are over-imposed to the 2D plots of fig.2 at the respective energy of interest.

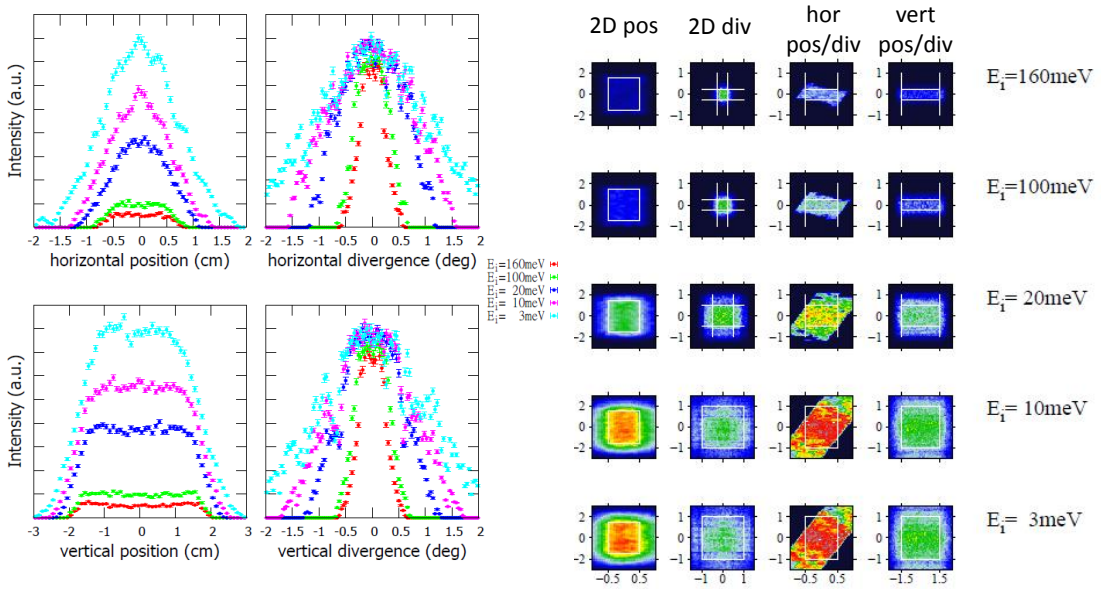

Figure 2: *Left*: Intensity distribution at the sample position as a function of horizontal and vertical position and divergence, for a set of neutron energies. *Right*: 2D-position and 2D-divergence monitors taken at the sample position. The white boxes represent the area of integration assumed to calculate the brilliance transfer shown in the fig1b)

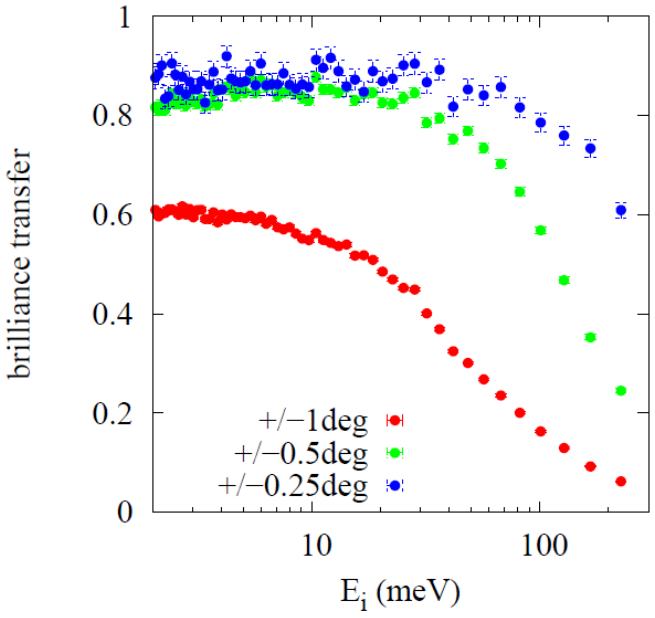

Figure 3: The brilliance transfer at the sample within the region of interest identified by a sample area of 1x3cm^2 and a divergence of +/-0.25°, +/-0.5° and +/-1° along the vertical and the horizontal direction.

3 Extraction system for cold neutrons

During the design phase of T-REX we considered several solutions for the extraction of neutrons from the cold moderator, while keeping the instrument axis in direct view of the thermal moderator. As first proposed by Mezei and Russina [3] the extraction system can be realized with a flat super mirror, several meters long, permanently installed inside the monolith of target station. This system is already implemented at the EXED [4] beam line at HZB and is shown to work well with straight guides. The system is able to reflect neutrons originating with long wavelengths from the cold moderator. Neutrons originating from the thermal moderator with short wavelength are able to pass through the mirror, thanks to their large wavevector and the low absorption probability of the mirror. Therefore the mirror acts like a switch between the two moderators as the wavelength increases. Recent simulation work has been performed to understand, whether the bispectral extraction works equally well when combined with elliptic guides[5] and also in combination with a focusing feeder[6]. For an instrument as long as T-REX, the cost in terms of flux is the 50% for neutrons with wavelength larger than 3Å. This can be considered a proper solution for a shorter instrument, because (i) the extraction efficiency reaches 70% and (ii) the measurements use a band ranging from cold to thermal wavelengths. Conversely the T-REX total length defines a *natural* band of nearly 1.7Å. Therefore measurements using the thermal energy range from 20 to 160 meV can be distinct from measurements using cold neutrons. Therefore the instrument needs a device that can be put in place and removed, offering a larger flexibility and avoiding to compromise in vain the thermal neutron flux. We investigated the performance of two alternative solutions for a removable device to be placed outside the monolith wall at 6 m distance from the moderator surface:

- A bender that consists of Si wafers long L with a radius of curvature $R = L/\alpha$, where α is the angular offset of the cold moderator with respect to the thermal axis. The thickness of the wafers and the m index were free parameters for the optimization.

- A stack of flat Si wafers. The thickness of the wafers, the length, the orientation (α) and the m index were free parameters for the optimization.

In both cases the Si wafers are coated on one side with a supermirror. The optimal parameters depend on the moderator layout and are summarized in table 1. The results for the TDR moderator (12x12cm^2) are also valid for the *pancake* layout (3x12cm^2), as only the horizontal offset between the thermal and cold moderator has an effect on the geometrical parameters and on the performance. The OT moderator dimensions are assumed to be 6x6cm^2. We performed simulations of both systems in combination with the EKE and CSE shapes. As shown in fig.4 b) the bender is found to perform better than the stack in the region of interest for cold neutrons, which is defined in a sample area of 1x3cm^2, within a divergence of +/-1°. When comparing the bender to the stack the EKE shape is much more favorable than the CSE, because the first ellipse needs to be fed with a larger divergence than the curved guide. Nevertheless the performance

	OT moderator		TDR/*pancake* moderator	
	bender	stack	bender	stack
Length (cm)	5	10	5	5
Radius of curvature (m)	3.7		3	
supermirror index m	2	2.5	2	2.5
thickness of Si wafers (μm)	150	75	300	70
α (°)	0.7	0.4	1	0.7

Table 1: Geometrical parameters of the best performing layout obtained from the simulations.

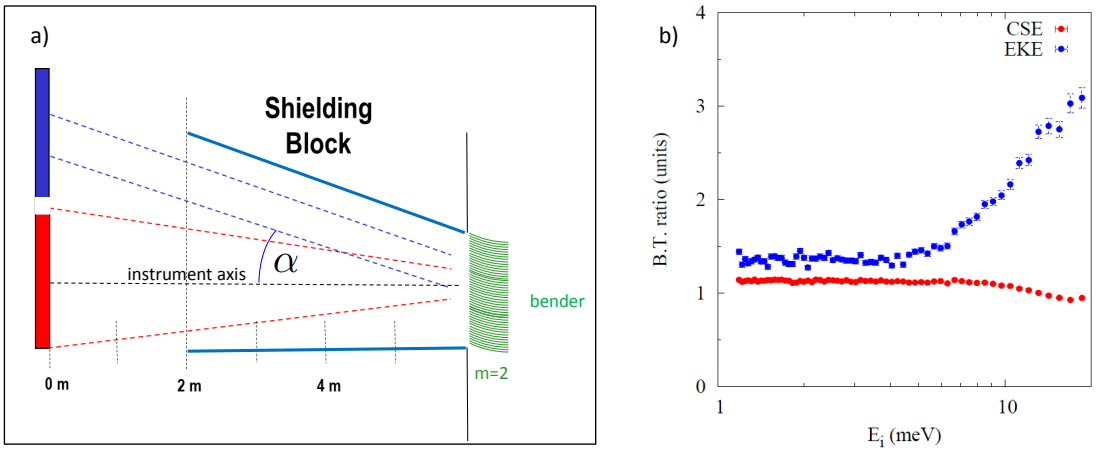

Figure 4: a) Sketch of the extraction system outside the target monolith. b) The efficiency of the bender is compared to the stack of mirrors when used in combination with the double ellipse with the kink (EKE) and the curved guide followed by a straight section and an ellipse (CSE).

of the bender is also superior for the CSE case, because of the quite large divergence accepted for the cold neutrons.

References

[1] L. Cussen et al., (2013) in press

[2] C. Zendler et al., NIMA 746 (2014), 39-46

[3] F. Mezei, M. Russina, Neutron-optical component array for the specific spectral shaping of neutron beams or pulses, Patent US 7030397 (2006) B2

[4] K. Lieutenant et al., J. of Neu. Res. 14 (2) (2006) 14

[5] H. Jacobsen et al. NIMA 717 (2013) 69–76

[6] C. Zendler et al. NIMA 704 (2013) 68–75

Centro de Física de Materiales
Materials Physics Center

Prof. Arantxa Arbe
(+34) 943.01.8802
a.arbe@ehu.es

Letter of Interest for the T-REX Project at ESS

Dear members of the Advisory Committee of the ESS:

With this letter I want to express my strong support for the construction of the bispectral chopper spectrometer T-REX at the ESS.

In my opinion, in order to open new possibilities in the investigation of soft matter there are two key ingredients to consider in the design of a ToF instrument: (i) separation of coh/inc contributions with polarization analysis (ii) extension of the available Q-range to lower Qs (at least Q ≈ 0.1Å-1) with reasonable energy resolution. These capabilities would facilitate the interpretation of results in partially deuterated samples and allow exploiting also the information provided by coherent scattering (collective dynamics). In particular, it would be possible to properly access the dynamic structure factor of labelled objects (e.g. the single chain dynamic structure factor in a polymeric complex material) that is nowadays accessible by NSE at long times. In this way, ToF could complement NSE by providing the faster regime (early stages) of the dynamic structure factor. Of course, in addition, increasing the dynamic window and the intensity of the instrument are always a must. T-REX fulfills all these requirements and I feel that this instrument could be of utmost importance for future research in the soft matter field.

San Sebastián, March 12, 2014

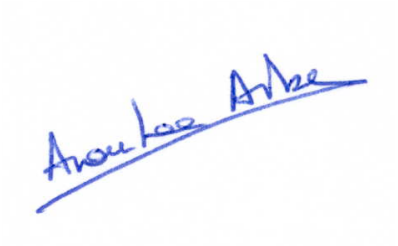

IOP | Institute of Physics
Juno Champion

THE UNIVERSITY OF WARWICK

Prof. Dr. Thomas Brückel
Forschungszentrum Jülich GmbH
52425 Jülich, Germany

21st March 2014

Dear Thomas,

We are very interested to hear of the progress made by you and collaborators in discussions regarding the building of a bispectral chopper spectrometer for the ESS. We are pleased at the outcome of these discussions and read with interest your proposal for the instrument T-REX: Time of Flight Reciprocal Space Explorer.

Our research work within the Superconductivity and Magnetism Group at Warwick makes extensive use of both neutrons and muons at various central facilities. While our strengths are in the production of high quality crystals for such studies combined with extensive physical properties measurements at low temperatures in our own laboratories, these studies always lead on to neutron scattering experiments at European facilities such as ISIS, ILL, PSI, JCNS, and HZB, to arrive at a unified picture of the properties of the materials of interest. Our work in recent years has included investigations of frustrated magnets (spin ice type materials, Shastry-Sutherland lattices, etc.), low-dimensional magnetic materials, novel transition metal oxide materials, and exotic superconductors. All the members of our Group (see below) have a successful track record of obtaining beam time for experiments at the facilities named above.

We use a wide range of techniques for our work including both elastic and inelastic neutron scattering methods. We make use of conventional triple axis spectrometers, as well as time-of-flight instruments such as LET and IN5. We have also made use of polarized neutrons on diffractometers such as D7 and DNS. We believe that the new inelastic neutron scattering instrument with polarization analysis, as proposed at the ESS, will greatly enhance the scope of the studies that we will be able to perform.

In addition to our own research, we work with a wide circle of collaborators, sometimes to perform complementary measurements, but also by providing high quality crystals for their neutron experiments (this is funded through our EPSRC programme "Single Crystal Growth at Warwick"). Our participation in experiments at T-REX will therefore be through both our own programmes and those of our collaborators.

In summary, we would like to express our very strong support for your proposal for T-REX at the ESS. We wish you every success when you present your case to the Scientific Advisory Committee of the ESS, and hope to hear of a positive outcome from this committee in due course.

With best wishes,

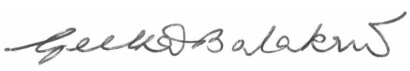

On behalf of: Geetha Balakrishnan, Don Paul, Martin Lees and Oleg Petrenko.

Professor Geetha Balakrishnan
Department of Physics
University of Warwick
Coventry CV4 7AL
United Kingdom
Tel.: +44 (0)24 76528409/150897
E mail: g.balakrishnan@warwick.ac.uk

Dr. Rafik Ballou
Directeur de Recherche - CNRS

Prof. Dr. Thomas Brückel
Direktor des Peter Grünberg Instituts
Direktor des Jülich Centre for Neutron Sciences
Forchungszentrum Jülich GmbH
PGI-4, JCNS-2
52425 Jülich, Deutschland

Grenoble, March 21st, 2014

Dear Prof. Brückel

I would like to express hereby my strong support for the project of the instrument T-REX, the Time-of-flight Reciprocal space Explorer, for the European Spallation Source.

A number of the research activities developed at the Institut Néel concerns the structural, electronic, magnetic and superconducting properties of new materials, which often resort to neutron experiments. As for the studies led in my team, we are interested to experimentally access the dynamical susceptibility of materials showing geometric frustration, chiral magnetism, magnetoelectric phenomena, quantum frustration or hierarchal correlations. The widest range in energy transfer and momentum transfer is generally requested. We learn, for instance from frustrated magnets, that dynamical correlations may lead to unexpected scattering functions, the crucial details of which might escape observation when the reciprocal space-time is not probed in a systematic way. The T-REX spectrometer will obviously offer the opportunity to conduct such experiments in extremely efficient ways. It goes without saying that the polarization analysis option will be invaluable. The neutron flux will allow considering compounds of which it is extremely hard to grow large size single crystals or compounds with low amplitude magnetic density. I have in mind here a whole series of topological insulators or organo-metallic materials.

As a scientist intensively using neutron scattering for his research works, I believe the T-REX project is extremely important and I hope that such an instrument will be operational as soon as possible to boost a whole field of scientific research. I wish success of the T-REX proposal.

Sincerely,

Rafik Ballou

Institut NEEL/CNRS-UJF - 25, rue des Martyrs - Bâtiment - BP 166 -
38042 Grenoble cedex 9 - France
+33 (0)4 76 88 79 18 - +33 (0)4 76 88 11 91
rafik.ballou@neel.cnrs.fr

JÜLICH
FORSCHUNGSZENTRUM

Jülich Centre for Neutron Science
JCNS-2: Streumethoden

Direktor des Instituts:
Prof. Dr. Thomas Brückel

Forschungszentrum Jülich GmbH · JCNS-2 · 52425 Jülich

Ihr Zeichen:
Ihre Nachricht vom:
Unser Zeichen: RH / köp
Unsere Nachricht vom:

Ansprechpartner: Raphaël Hermann

Telefon: +49 2461 61-4786
Telefax: +49 2461 61-2610

E-Mail: r.hermann@fz-juelich.de

Jülich, 13.03.2014

To whom it may concern,

It is with great pleasure that I express my strongest support for inclusion of the proposed bispectral T-REX neutron spectrometer for the European Spallation Source instrument suite. The features of the instrument are such that they will prove particularly useful for general lattice dynamics investigations on materials science problems as carried out in my group, notably on the topics of thermoelectric materials, magnetocalorics, and battery or fuel cell materials. Specifically, this instrument provides the features that I have commonly seen requested for vibrational spectroscopy as a referee for ILL college 7 research proposals, namely both excellent resolution near the elastic line and access to large energy transfer range. Such proposals nowadays typically require the combined use of two instruments, but the availability of a multipurpose instrument such as T-REX will add tremendous flexibility to the research by enabling simultaneous access to quasi elastic scattering and inelastic scattering in order to provide direct insight in the transformation from localized dynamics to diffusive phenomena through activation mechanisms. Nowadays painstaking parametric studies or operando experiments are promised a bright future on this instrument. As added benefits, both the day-0 polarization analysis capability and the large reciprocal space volume accessed in one setting will prove of particular importance not only for magnetic systems but also for energy related materials science problems in which diffuse scattering signal is often swamped by incoherent scattering contribution from constituents that are intrinsically part of the investigated problem. The improved capabilities are a direct reply to the required adaptation of the neutron instrumentation to the practical problem instead of the reverse approach.

Sincerely,

Raphael Hermann, Prof. Dr.

Jülich Centre for Neutron Science JCNS and Peter Grünberg Institut PGI, JCNS-2, PGI-4: Scattering methods, Forschungszentrum Juelich GmbH, D-52425 Juelich &Invited Professor at the Faculty of Sciences, Dept Chimie - Bat B6, Universite de Liege, B-4000 LIEGE

Prof. Dr. Thomas Brückel
Forschungszentrum Jülich GmbH
PGI-4, JCNS-2
52425 Jülich

Jun.-Prof. Dr. Dmytro Inosov
Institute for Solid State Physics
Technische Universität Dresden
Zellescher Weg 16
D-01067 Dresden
☎ +49 (351) 463-34731
+49 (351) 463-37734
Dmytro.Inosov@tu-dresden.de

March 10, 2014

Letter of support for the construction of the T-REX instrument

Dear Prof. Brückel,
dear members of the Scientific Advisory Committee of the ESS,

In reply to your letter from 06.03.2014, I confirm that our neutron spectroscopy group at the TU Dresden will be very interested in using the T-REX instrument at the ESS, once it is constructed. Our current research to a large extent relies on the cold-neutron time-of-flight spectrometers, such as IN5 (ILL), CNCS (SNS) and LET (ISIS). In recent years, we already performed several experiments at these instruments, and a number of new research proposals have already been submitted by our group this year. The materials of interest include $Ce^{11}B_6$, $Ce_{1-x}La_x{}^{11}B_6$, $Ce_3Pd_{20}Si_6$ and potentially other heavy-fermion compounds with low-energy spin dynamics. The characteristic energy transfer in the range of only $0.25-0.5$ meV (as in the case of CeB_6) makes the high energy resolution offered by these cold-neutron spectrometers (and, in future, by the T-REX) indispensable. Furthermore, boride compounds are characterized by high absorption cross sections, which significantly reduces the observable magnetic signal even in samples with the highest level of isotopic ^{11}B enrichment. This renders the intensity of the neutron beam a very crucial parameter for the successful outcome of an INS experiment.

According to the summary of the main instrument parameters, estimated for T-REX, its performance will exceed that of currently available instruments (IN5, CNCS or LET) by about an order of magnitude, on average. At the same time, it will offer a similar or better energy resolution and a broader range of incident energies. This flexibility will be especially important for studying new materials, where the energy range of magnetic excitations is *a priori* unknown, or to measure features in the spin-excitation spectrum that cover a broad range of energies. For instance, measurements of the complete spin-wave dispersion in the "thermal" energy range can be combined with measurements of the minute spin gaps of the order of 0.1 meV in the same experiment. Moreover, the tenfold improvement in the measurement time will enable parametric studies as a function of an applied magnetic field or temperature. With current instruments that typically require a few days for a complete high-statistics coverage of the 4-dimensional energy-momentum space, only a few values of external parameters can be measured within a single experiment, which makes continuous field or temperature scans impractical. The new T-REX instrument, on the other hand, will overcome this limitation by offering the possibility to acquire > 10 complete energy-momentum-space maps per day, hence a nearly continuous dataset as a function of an external parameter can be obtained in a single experiment. Without doubt, all of our current projects would hugely benefit from the existence of a high-performance instrument such as T-REX.

Yours faithfully,

Prof. Dmytro Inosov.

HZB Helmholtz Zentrum Berlin

Helmholtz-Zentrum Berlin für Materialien und Energie GmbH | Hahn-Meitner-Platz 1 | 14109 Berlin

European
Spallation Source

Bella Lake
Department of Quantum
Phenomena in Novel Materials
Hahn-Meitner-Platz 1
14109 Berlin
Tel +49 30 8062-42058

bella.lake@helmholtz-berlin.de

Berlin, 07.03.2014

Proposed T-REX spectrometer for ESS

Dear Members of ESS,

I am writing this letter in support of the T-REX spectrometer being proposed by members of Forschungszentrum Jülich. What makes this instrument particularly interesting is its wide spectral range (0.5-100meV) which combined with repetition rate multplication will allow the complete spectrum of magnetic and phononic excitations (of most materials) to be measured. In addition the possibility of polarization analysis add a completely new dimension which to date is almost unexplored in time-of-flight instruments, particularly those in the thermal energy range. The possibility to map the entire spectrum as a function of energy, wavevector and also polarization opens up a new way of measuring data and the insights this will bring will undoubtedly be profound and far-reaching.

Personally I can see this spectrometer as very important for my own research fields (magnetism and superconductivity) but I am glad to see that it promises to serve other research areas including soft matter and energy research.

Yours sincerely

Bella Lake

Bella Lake

Dr Jacques OLLIVIER
Institut Laue-Langevin
6 rue J. Horowitz, BP156
38042 GRENOBLE Cedex
Email : ollivier@ill.eu
Tel.: 04.76.20.75.67

To Whom It May Concern

Grenoble, Monday 24 March 2014

As a scientist working in solid state physics and with time-of-flight spectrometry I think that the bi-spectral time-of-flight instrument called T-REX meets the goals for allowing facing the challenges of the inelastic neutron scattering in the future.

First of all it spans on a large dynamical range, around 4 order of magnitudes in energy, covering most of the physical phenomena appearing in solid state physics such as in magnetic materials, superconductors or thermoelectric materials. The design of the instrument permits a large set-up flexibility with in particular the original design of a fan chopper to tune accurately the repetition rate multiplication acquisition mode. The implementation of polarisation analysis is considered from the beginning, such an "option" becoming unavoidable on future instruments.

For these reasons and others, the T-REX instrument is a spectrometer I would certainly like to use in the future.

Sincerely yours,

Jacques Ollivier

Physicist,
Responsible of the IN5 time-of-flight instrument,
Institut Laue-Langevin

UNIWERSYTET IM. ADAMA MICKIEWICZA W POZNANIU
Wydział Fizyki

Dr hab. A. Pajzderska
Faculty of Physics
A. Mickiewicz University
Poznan, Poland

Poznan, 25 March 2014

Dear Prof. Brückel,

On behalf of Dean of Faculty of Physics, A. Mickiewicz University in Poznan (Poland) and employees of the Faculty involved in neutron scattering experiment it is my pleasure to write a letter in support of the proposal for the instrument T-REX (the Time-of-flight Reciprocal space Explorer).

We have analyzed in detail the project as well as the main instrument parameters and we have considered this instrument as very useful in our future research. The proposed instrument, due to its properties, will enable unique experiments in condensed matter systems, soft matter, life sciences, nanomagnetic systems and different kinds of functional materials. Therefore, the proposed spectrometer is highly relevant and well in line with the research focus of our Faculty.

In conclusion, we fully support this project.

Sincerely yours,

Aleksandra Pajzderska

Aleksandra Pajzderska

ul. Umultowska 85, Collegium Physicum, 61-614 Poznań
NIP 777 00 06 350, REGON 000001293
tel. +48 61 829 51 50, +48 61 829 52 02, fax. +48 61 829 51 55
dziekfiz@amu.edu.pl

www.fizyka.amu.edu.pl

Commissariat à l'Energie Atomique
Centre National de la Recherche Scientifique

Dr Sylvain Petit

Ph : +33.1.69.08.60.39
Fax : +33.1.69.08.82.61
Email : sylvain.petit@cea.fr

Saclay, March 19th, 2013

To whom it may concern.

Subject: T-REX time of flight spectrometer at ESS.

With this letter I would like to express my strong interest in the T-REX instrumental project, which will provide the research community at ESS with a state of the art neutron time of flight spectrometer.

This new time of flight instrument will push the time of flight technique to its best. The significant increase in flux will become a major asset for my research projects, which require a comprehensive survey of the reciprocal space, with in some cases polarization analysis, to separate magnetic and nuclear contributions.

I am currently working in the field of multiferroics, a rich class of magnets where ferroelectricity and magnetism are intimately coupled, opening the route to new technological applications. More generally speaking, magnetism is a field of condensed matter research whose scientific outcome has invaded our everyday life. It regularly provides novel physics as well as fundamental concepts, which enrich the human scientific knowledge and can be used to develop novel technologies. Amongst major current issues in magnetism are, for instance, the study of highly frustrated magnets, spin liquids or spin ices, the coupling of the magnetic degrees of freedom (spin, orbit) with others, like the charge or the lattice, in potential multifunctional materials, the study of strongly correlated electron systems and of low dimensional magnets. By providing a direct access to the spectrum of excited states, inelastic neutron scattering offers a unique possibility for researchers to explore a whole spectrum of physical phenomena occurring in condensed matter.

There is no doubt that the T-REX instrument will be a major actor in the investigation of these different issues. I therefore would like to emphasize the importance of including the T-REX in the ESS instrument suite.

Dr S. Petit

HELMHOLTZ ZENTRUM BERLIN
für Materialien und Energie

Helmholtz-Zentrum Berlin für Materialien und Energie GmbH | Hahn-Meitner-Platz 1 | 14109 Berlin

Prof. Dr. T. Brückel

Forschungszentrum Jülich GmbH

52425 JÜLICH

Margarita Russina
F-ISFM
Hahn-Meitner-Platz 1
14109 Berlin

Tel +49 (0)30 | 8062-4 3159

Margarita.Russina@helmholtz-berlin.de

Berlin, 24.03.2014

Betreff: Letter of support for T-REX time-of flight chopper spectrometer

Dear Prof. Dr. Brückel,

It is my pleasure to write a letter in support of the proposal for the construction of the time-of flight spectrometer T-REX being submitted to the European Spallation Source.

Working many years in the field of neutron spectroscopy I could see that inelastic neutron scattering is in particular a powerful tool in the growing field of exploration of nanomaterials. Excellence in this area is an important strategic goal for all neutron scattering centres and for first rate material science research with neutron scattering. The energy range required for nanomaterial studies is extremely broad and spreads from the meV range (thermal excitations) down to the µeV range. Parametric studies in this energy range can best be covered by a direct TOF-type spectrometer. The high intensity of the proposed spectrometer will open up new possibilities for studying size-dependent magnetic properties and spin dynamic behavior of nanoparticles, nanocomposites and filled or partially filled nanoporous matter such as carbon nanotubes (CNTs). The physical constraints resulting from the size of nanostructures in these materials lead to new properties and functionality. In meso- and nanoporous matter the structural properties of the matrix are combined with those of the dispersed nanoparticles or adsorbed species. Mobility of dispersed species is a central issue of those systems that can best be addressed by quasielastic neutron scattering QENS. T-REX will be highly beneficial for

studies and design of novel hydrogen storage systems. Inelastic and quasielastic neutron scattering is ideally suited for these materials as it provides direct information on the nature of the interaction of hydrogen with host matter. Future studies on the proposed instrument can shed light on the mechanisms of reaction, dehydrogenation and rehydrogenation, tailoring the operating regimes of such materials.

The instrument will take full benefit of the high flux delivered by ESS and will at the same time couple it with large flexibility usually provided by reactor based instruments. The operation using Repetition Rate Multiplication will allow speeding up and substantially improving data collection. On the one hand, it will allow us to broaden the (Q,E) range simultaneously covered. The combination of the information from various experimental settings and resolutions at different wavelengths will allow for dynamics analysis with “zoom in” and “zoom out” capabilities usually obtained by means of several experiments at different spectrometers. On the other hand, the settings with several wavelengths will allow improving substantially the consistency and reliability of the data correction and treatment (for instance multiple scattering, multi-phonons and etc.) and will open up herewith new scales or dynamic range for the dynamics analysis which were before inaccessible. The high luminosity of the instrument will allow for many applications currently limited due to insufficient intensity. The polarization and high field capabilities of the proposed TOF spectrometer will strongly enhance its effectiveness in exploration of complex materials.

In conclusion, I fully support the efforts of the Forschungszentrum Jülich as they propose to build the T-REX time-of-flight spectrometer at ESS. The high performance of the proposed instrument will make it an outstanding experimental tool in the rapidly evolving and highly topical field of nanomaterials research and also most broadly benefit the entire neutron scattering community at large.

Sincerely

Margarita Russina